NASA Contractor Report 185299

Creep and Fracture of Dispersion-Strengthened Materials

Sai V. Raj
Cleveland State University
Cleveland, Ohio

June 1991

Prepared for
Lewis Research Center
Under Cooperative Agreement NCC3-72

National Aeronautics and
Space Administration

CREEP AND FRACTURE OF DISPERSION-STRENGTHENED MATERIALS*

Sai V. Raj**
Cleveland State University
Department of Chemical Engineering
Cleveland, Ohio 44106

SUMMARY

The creep and fracture of dispersion-strengthened materials is reviewed. A compilation of creep data on several alloys showed that the reported values of the stress exponent for creep varied between 3.5 and 100. The activation energy for creep exceeded that for lattice self-diffusion in the matrix in the case of some materials and a threshold stress behavior was generally reported in these instances. The threshold stress is shown to be dependent on the interparticle spacing and it is significantly affected by the initial microstructure. The effect of particle size and the nature of the dispersoid on the threshold stress is not well understood at the present time. In general, most investigations indicate that the microstructure after creep is similar to that before testing and very few dislocations are usually observed.

It is shown that the stress acting on a dispersoid due to a rapidly moving dislocation can exceed the particle yield strength of $G_p/1000$, where G_p is the shear modulus of the dispersoid. The case when the particle deforms is examined and it is suggested that the dislocation creep threshold stress of the alloy is equal to the yield strength of the dispersoid under these conditions. These results indicate the possibility that the dislocation creep threshold stress is determined by either the particle yield strength or the stress required to detach a dislocation from the dispersoid-matrix interface. The conditions under which the threshold stress is influenced by one or the other mechanism are discussed and it is shown that the particle yield strength is important until the extent of dislocation core relaxation at the dispersoid-matrix interface exceeds about 25 percent depending on the nature of the particle-matrix combination.

Finally, the effect of grain boundaries and grain morphology on the creep and fracture behavior of dispersion-strengthened alloys is examined.

1.0 INTRODUCTION

It is now well recognized that the introduction of small amounts of fine dispersoid particles in a crystalline matrix generally results in a considerably stronger alloy. In contrast to precipitate-hardened alloys, which may undergo microstructural changes when exposed to elevated temperatures during the normal life time of a structural component, an ideal dispersion-strengthened alloy exhibits microstructural stability even at temperatures

---

*This work will also be a chapter in the Handbook of Metallic Composites, S. Ochiai, editor; Marcell Dekker, New York, New York.

**NASA Resident Research Associate at Lewis Research Center.

close to the melting point of the matrix material. These two features, namely high temperature strength and microstructural stability, have been the primary impetus in the development of numerous dispersion-strengthened alloys (see Morral, 1977, for a review of the literature till 1977).

As a result of considerable amount of work done during the last four decades, the factors which influence dispersion strengthening are better understood today. These include the type of dispersoids used, particle size, d_p, particle spacing,[1] λ, grain size, d, grain aspect ratio, GAR, and processing techniques. In an earlier review, Grant (1966) outlined the desired properties required of the dispersoid to ensure good dispersion strengthening. These are a high melting point, high elastic moduli, and good chemical, crystallographic, and microstructural stability in the matrix material. In general, the properties of many oxides (e.g., Al_2O_3, SiO_2, ThO_2, and Y_2O_3) fulfill these requirements, and a considerable amount of work has been done on oxide dispersion-strengthened (ODS) alloys owing to their potential importance in engineering applications (e.g., Hansen, 1967; Ault and Burte, 1968; and Hansen, 1969).

The objective of the present paper is to review the creep and stress rupture behavior of dispersion-strengthened alloys. A table of compiled creep data on a wide variety of materials is also included as a source of ready reference. It is intended that the present paper serve to compliment earlier reviews (Guard, 1962; Ansell, 1968; Gibeling and Nix, 1980; Sellars and Petkovic-Luton, 1980; Čadek, 1981; Bilde-Sorensen, 1983; and Blum and Reppich, 1985) on particle-strengthened materials by updating the information in some areas while providing new insights in others.

The basic approach adopted in this paper is to examine the creep characteristics of dispersion-strengthened alloys against the background of known behavior of pure metals and solid solution alloys. Therefore, a summary of the creep behavior of single phase materials in presented in Sec. 2.0. Next, the creep behavior of single crystalline and coarse-grained dispersion-strengthened materials are reviewed and discussed in Secs. 3.0 and 4.0. This is followed by a consideration of the role of grain boundaries on the creep and fracture behavior of these alloys in Sec. 5.0, while the areas requiring further research are identified in Sec. 6.0.

2.0 CREEP BEHAVIOR OF SINGLE PHASE MATERIALS

The creep behavior of pure metals and solid solution alloys has been reviewed extensively by a number of investigators (Sherby, 1962; McLean, 1966; Sherby and Burke, 1967; Weertman, 1968; Mukherjee, Bird, and Dorn, 1969; Bird, Mukherjee, and Dorn, 1969; Takeuchi and Argon, 1976; Blum, 1977; Nix and Ilschner, 1980; Langdon, 1981, 1983; and Bendersky, Rosen, and Mukherjee, 1985). Therefore, only the salient features of the creep of single phase materials are summarized in this section.

---

[1] In this paper, λ, refers to the particle center-to-center distance, whereas λ_m represents the particle edge-to-edge distance.

2.1 Power-law creep

The steady-state creep rate, $\dot{\varepsilon}$, of single phase materials at low and intermediate stresses is generally well-represented by a power-law relation:

$$\dot{\varepsilon} = A_1(DGb/kT)(b/d)^p(\sigma/G)^n \tag{1}$$

here D is the appropriate diffusion coefficient, G is the shear modulus, b is the Burgers vector, T is the absolute temperature, k is Boltzmann's constant, σ is the applied stress, and A_1, p, and n are dimensionless constants. Table I lists the characteristics of several creep mechanisms which are known to occur in metals and solid solution alloys, but it is noted that while these serve as useful guidelines in understanding the creep behavior of many materials, they may not always be applicable. For example, values of $Q_c > Q_l$ have been reported in some h.c.p. metals at very high temperatures (Vagarali and Langdon, 1981), where Q_c is the true activation energy for creep and Q_l is the activation energy for lattice self-diffusion.

For a pure metal tested at intermediate stresses (typically, $5\times10^{-6} \lesssim \sigma/G \lesssim 5\times10^{-4}$), $n \approx 4.5$, $p = 0$, and $D = D_l$, where D_l is the lattice self-diffusion coefficient (i.e., $D_l = D_{ol} \exp(-Q_l/RT)$, where D_{ol} is the frequency factor, and R is the universal gas constant). Under these conditions, dislocation climb is the rate-controlling mechanism sometimes referred to as high temperature (H.T.) climb. This type of creep response is now termed as metal type or class M behavior. It has also been observed in many solid solution alloys when dislocation climb is slower than the viscous glide motion of dislocations caused by the presence of a solute atmosphere. However, under certain conditions, the creep behavior of some solid solution alloys is dominated by viscous glide when the latter is slower than climb. This is called alloy-type or class A behavior and it is characterized by values of $n = 3$, $p = 0$, and $D = \tilde{D}_g$ in equation (1), where $\tilde{D}_g$ is the diffusion coefficient for viscous glide-controlled behavior (Fuentes-Samaniego and Nix, 1981).

At low stresses (typically, $\sigma/G < 5\times10^{-6}$), the rate-controlling mechanisms are generally governed by the stress-directed flow of vacancies, either through the lattice or along the grain boundaries, from grain boundaries under relative tensile stresses to those under relative compression. These processes collectively are termed diffusion creep, and they are characterized by $n = 1$, $p = 2$ or 3, and $D = D_l$ or D_{gb} in equation (1), where D_{gb} is for the grain boundary diffusion coefficient. The importance of these mechanisms in dispersion-strengthened materials has been reviewed recently by Whittenberger (1992), and the present review will not cover this area of creep.

TABLE I. - CHARACTERISTICS OF CLASS A, CLASS M, DIFFUSION AND EXPONENTIAL CREEP BEHAVIOR IN METALS AND SOLID SOLUTION ALLOYS

Low ← σ/G → High				
Property	Diffusion creep	Class M	Class A	Exponential creep
$\dot{\varepsilon} - \sigma$ relation	Power-law; $n \approx 1.0$; $p \approx 2$ or 3	Power-law; $n \approx 4.5$; $p = 0$	Power-law; $n \approx 3.0$; $p = 0$	Exponential; $\exp(B\,\sigma/G)$; $p = ?$
Activation energy for creep	Q_l or Q_{gb}	Q_l (or $\tilde{Q}_{c1}$ for alloys)*	$\tilde{Q}_g$**	Less than Q_l and may be stresss dependent
Primary creep curve	Normal	Normal	Short normal; linear; sigmoidal; or inverse	Normal
Substructure	Essentially similar to the initial microstructure	Well-formed, equiaxed subgrains; dislocation networks	Essentially random dislocations; subgrain formation possible	Elongated subgrains; cells; dislocation tangles
Transients after a stress increase	---	Normal	Inverse	Normal
Dominant mechanism	Vacancy diffusion	Dislocation climb	Viscous glide	Probably dislocation intersection

*$\tilde{Q}_{c1}$ is the activation energy in the equation $\tilde{D}_c = \tilde{D}_{oc} \exp(-\tilde{Q}_{c1}/RT)$, here $\tilde{D}_c$ is the complex diffusion coefficient for a class M alloy and $\tilde{D}_{oc}$ is a frequency factor.

**$\tilde{Q}_g$ is the activation energy in the equation $\tilde{D}_g = \tilde{D}_{og} \exp(-\tilde{Q}_g/RT)$, where $\tilde{D}_g$ is the complex diffusion coefficient for a class A alloy and $\tilde{D}_{og}$ is a frequency factor.

2.2 Exponential Creep

At high stresses, the power-law relation given by equation (1) breaks down, and the data are better represented by an exponential relation:

$$\dot{\varepsilon} = A_2(\sigma)\exp(-Q_c/RT)\exp(B\sigma/G) \tag{2}$$

where $A_2(\sigma)$ is a parameter which incorporates the stress dependence of the dislocation density, and B is a dimensionless constant. The mechanisms governing deformation in this region is not well-understood, although recent work on copper (Raj and Langdon, 1989, 1991(a) and (b)) suggests that the rate-controlling process is nondiffusional in nature and involves the intersection of immobile "forest" dislocations as the probable dominant mechanism.

2.3 The Transition From Power-Law To Exponential Creep For Class M Behavior

A point that is not often recognized in the creep literature is the importance of the $\dot{\varepsilon} - \sigma$ relation used in the analysis of creep data. Despite their somewhat empirical nature, the formulations represented by equations (1) and (2) indicate the dominance of different rate-controlling mechanisms. Although the power-law relation with a stress exponent of $n > 4.5$ for class M behavior may often fit creep data quite well, such representations may be physically meaningless if the mechanism governing creep is nondiffusional in nature. Values of $n > 4.5$ have been reported in the literature for pure metals (Bird, Mukherjee, and Dorn, 1969), and these have been variously attributed to a number of factors: the importance of dislocation core mechanisms (Robinson and Sherby, 1969; and Frost and Ashby, 1982); the effect of stacking fault energy (Bird, Mukherjee, and Dorn, 1969); statistical scatter (Mukherjee, Bird, and Porn, 1969); the influence of internal stresses (Davies *et al.*, 1973; Parker and Wilshire, 1975, 1978; and Nelmes and Wilshire, 1976); and the advent of exponential creep (Blum and Reppich, 1969; and Raj, 1986).

Unfortunately, owing to the scatter in the experimental data, it is difficult to verify unambiguously whether the stress exponent for dislocation climb-controlled power-law creep has a unique value. Despite this, certain general comments can be made which indicate that some of the factors discussed earlier may not be universally applicable. First, models involving dislocation core diffusion are often inconsistent with the experimental data on pure metals (Spingarn, Barnett, and Nix, 1979; and Raj and Langdon, 1989). Second, values of n are remarkably constant and equal about 4.0 to 4.5 for several single phase materials despite large differences in the stacking fault energy (Blum and Reppich, 1969; Raj, 1986; and Raj and Pharr, 1989). Third, the values of $n > 4.5$ are much too large to be entirely accounted for by statistical scatter. Fourth, rationalizations based on the internal stress approach may not be physically valid (Lin and Sherby, 1981).

An attractive interpretation of values of $n > 4.5$ is to attribute these to the increasing dominance of exponential creep. The data compiled by Blum and Reppich (1969) suggests that this may indeed be the case, since n was

observed to increase from $n = 4.0$ to much higher values with an increase in the magnitude of σ/T. A more recent analysis of the creep data on pure f.c.c. metals also supports this viewpoint (Fig. 1) (Raj, 1986). In this case, it was demonstrated that the normalized creep rates, $(\dot{\varepsilon}kT/D_1Gb)_{PLB}$, at which the power-law relation breaks down decreased by about three orders of magnitude for a decrease in Γ/Gb by about an order of magnitude, where Γ is the stacking fault energy (Raj and Langdon, 1991(b)). Interestingly, the breakdown in the power-law relation with $n \approx 4.5$ was observed to occur at an average value of about $(\sigma/G)_{PLB} \approx 5x10^{-4}$, where $(\sigma/G)_{PLB}$ is the normalized value of stress at which the power law breaks down. These results can be rationalized on the basis that a decrease in the normalized stacking fault energy results in a corresponding decrease in the rate of recovery by dislocation climb, so that nondiffusional mechanisms dominant in the exponential creep regime would tend to dominate at lower values of normalized creep rates above $(\dot{\varepsilon}kT/D_1Gb)_{PLB}$ as Γ/Gb decreases and lead to the observance of $n > 4.5$ when $\sigma/G > (\sigma/G)_{PLB}$.

2.4 The Effect of Microstructure on The Creep Rate

Although stress, temperature and grain size play an important role in determining the nature of the dominant mechanism and its contribution to the total creep rate, other factors can also influence the creep process (e.g., pressure, porosity, types of defects, and microstructural parameters other than grain size). In most engineering applications involving metals and alloys, the creep properties are significantly influenced by the substructure since the constant, A_1, in equation (1) is a function of microstructural parameters. However, owing to the inherent difficulties associated with a complete quantification of the different microstructural parameters (e.g., the subgrain size, d_s, and the dislocation density, ρ), as well as the complexities which may arise because of the interdependent nature of some of these variables, relatively few quantitative formulations exist in the literature which specifically attempt to incorporate these parameters in the creep rate equation.

Barrett and Sherby (1965) and Mohamed and Langdon (1974a), observed that $A_1 \propto \Gamma^{3.5}$ or $(\Gamma/Gb)^3$, respectively. Sherby *et al.* (Robinson and Sherby, 1969; and Sherby, Klundt, and Miller, 1977) suggested that the creep rate at a constant microstructure is dependent on the subgrain size through[2]

$$\dot{\varepsilon} = A_3(DGb/kT)(d_s/b)^3(\sigma/G)^8 \qquad (3)$$

where A_3 is a dimensionless constant. Equation (3) predicts that subgrain refinement can lead to substantial strengthening at high temperatures provided a stable subgrain size can be achieved.

[2]The form of the original equation has been modified in order to be consistent with equation (1).

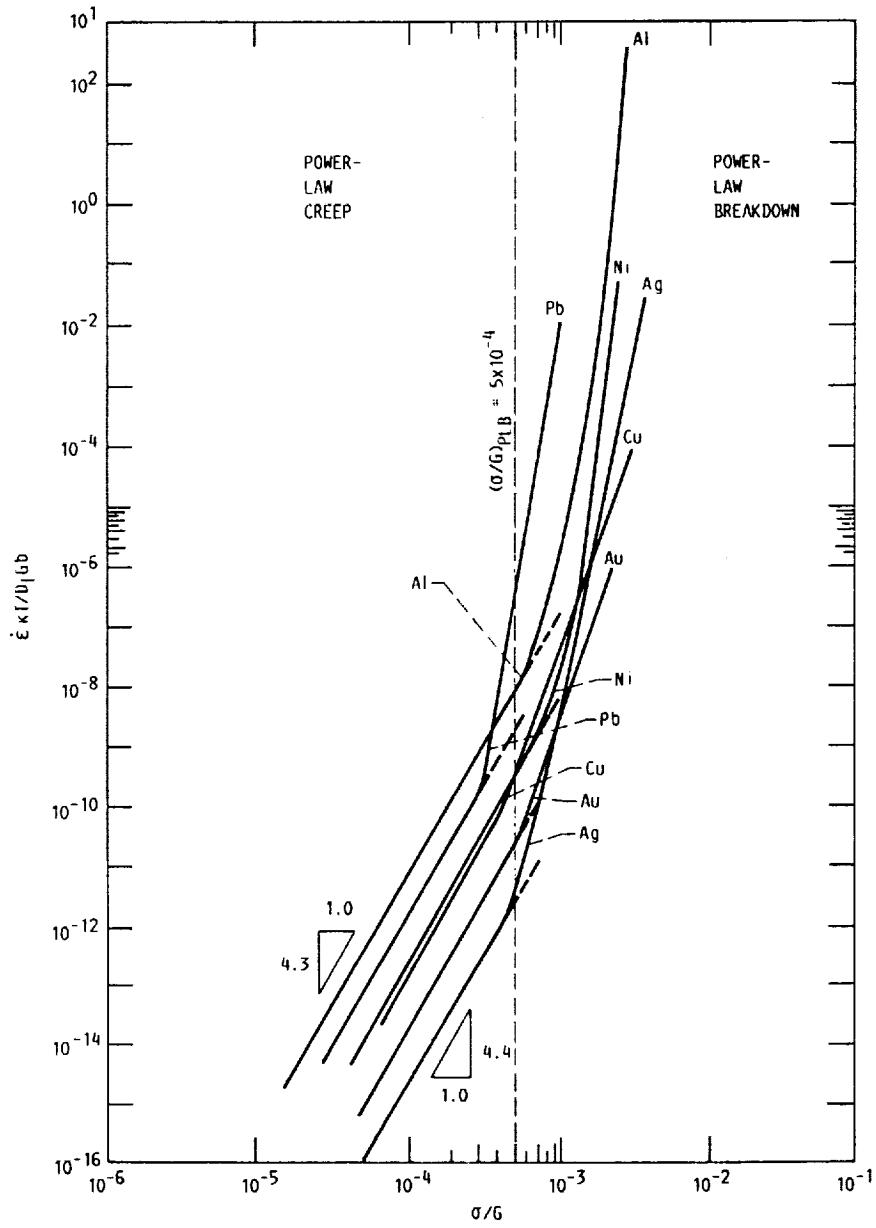

FIGURE 1. - PLOT OF $\dot{\varepsilon}kT/D_1Gb$ AGAINST σ/G FOR SEVERAL f.c.c. METALS SHOWING THAT THE POWER-LAW CREEP RELATION BREAKS DOWN AT ABOUT A VALUE OF $(\sigma/G)_{PLB} \approx 5\times10^{-4}$ (RAJ, 1986) (REPRINTED WITH PERMISSION, PERGAMON JOURNALS LTD.).

Although such direct relations between the creep rate and the microstructural parameters are useful, some elements of the substructure are also related to the applied stress. For example, the equilibrium subgrain size depends on the applied stress through

$$(d_s/b) = K(G/\sigma)^m \tag{4}$$

where K and m are dimensionless constants which are inversely dependent on each other (Raj and Pharr, 1986). Thus, for a value of $m = 1$, K assumes a value of 23. Similarly, available evidence indicates that $\rho \propto \sigma^2$ (Mukherjee, Bird, and Dorn, 1969; Bird, Mukherjee, and Dorn, 1969; and Takeuchi and Argon, 1976).

3.0 DISLOCATION CREEP OF DISPERSION-STRENGTHENED MATERIALS

The creep of dispersion-strengthened alloys is often influenced by intra- and intergranular mechanisms. Owing to the complex nature of these processes, it is often simpler to study the two types of mechanisms separately. Therefore, in the present section it will be assumed that the role of grain boundaries is negligible. This assumption is expected to be applicable for single crystals or for materials with a very elongated, coarse-grained microstructure in the testing direction.

3.1 The Shape of the Transient Curves

Most high temperature experimental data on dispersion-strengthened materials have been obtained either under constant stress (or load) or constant strain rate (or crosshead velocity) conditions. The data obtained from both types of tests are often compared with each other and it is useful to document the nature of the creep curves or the constant strain rate stress-strain plots typically observed in most investigations. The types of experimental curves reported in the literature fall broadly into one of the categories shown schematically in Fig. 2. It is emphasized that these serve only as guidelines and other variations might have been reported in some investigations.

Figure 2(a) shows three types of creep curves (N, R, T) obtained by plotting strain, ε, against time, t. Curve N, which is similar to that usually observed in class M materials, consists of an instantaneous strain, a primary stage in which the creep rate decreases with time, a secondary stage with an approximately constant creep rate, and a tertiary region where the creep rate increases continuously leading to fracture with the total fracture strain being typically less than 3 percent. Curve R differs from curve N in that the ε - t plot exhibits a number of primary stages separated by instantaneous jumps in creep strain with no single and well-defined secondary creep region. In extreme cases, no measurable creep may occur for long periods between two consecutive primary regions (Ansell and Weertman, 1959). Curve T and curve N differ primarily in the nature of the tertiary stage that is observed. In contrast to curve N, where the advent of tertiary creep is relatively gradual, curve T exhibits a sharp transition from the secondary to the tertiary stage with the latter being almost parallel to the

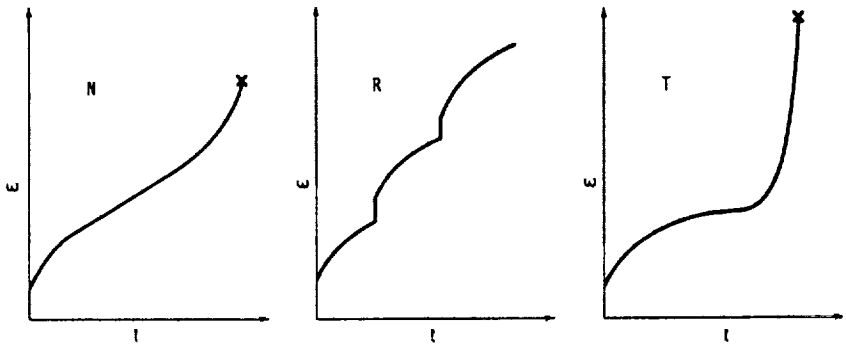

(a) CREEP CURVES.

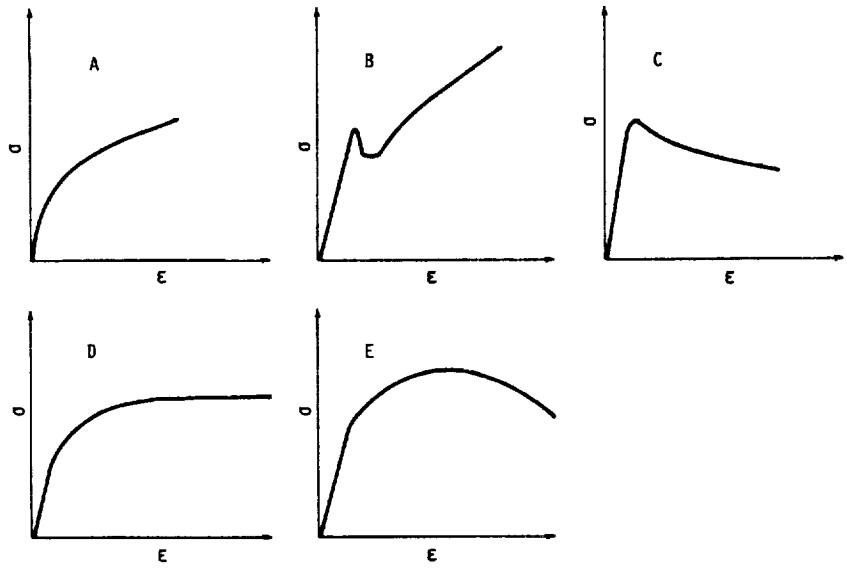

(b) STRESS - STRAIN CURVES.

FIGURE 2. - SCHEMATIC REPRESENTATION OF THE TYPES OF TYPICAL (a) CREEP AND (b) STRESS STRAIN CURVES OBSERVED FOR DISPERSION-STRENGTHENED MATERIALS.

strain axis. In this case, the total fracture strain is usually about 5 to 20 times greater than the strain to the onset of tertiary creep. Therefore, a considerable amount of strain accumulates before fracture in a relatively short time, although the total strain before the commencement of the tertiary stage can often be less than 1 percent. In practical situations, this behavior can lead to unforeseen and potentially disastrous failures of engineering structures. Although curves N and T are more commonly reported, other types of creep curves are sometimes observed. For example, dispersion-strengthened Al-5% Mg-0.3% Fe alloys exhibit inverse, linear and sigmoidal creep curves (Horita, 1983).

Several different stress-strain curves are observed when dispersion-strengthened alloys are tested under constant strain rate conditions, and these are shown in Fig. 2(b). Curve A represents the normal type of continuous hardening behavior exhibited by many pure metals, whereas curve B shows a yield drop followed by extensive strain hardening. Curve C shows a tendency towards softening after the yield point, whereas curve D shows little or no strain hardening effects after yielding followed by continued flow at approximately a constant stress. Curve E shows some work hardening before the material undergoes necking.

Although it is difficult to correlate the constant stress and the constant strain rate plots directly in any detailed manner, it is possible to make certain general comparisons between the two results. Thus, for example, the primary stage of curve N (Fig. 2(a)) and the strain hardening behavior shown in curve A (Fig. 2(b)) can be attributed to changes in the substructure. Similarly, sigmoidal and inverse primary creep curves may be compared with curves B and C, respectively, since the basic features of these plots can be generally attributed to an increase in the density of mobile dislocations.

3.2 The Stress Dependence of the Creep Rate

In general, the addition of small amounts of dispersoids to single phase and precipitate-hardened materials decreases the creep rate considerably. For example, considering the creep data for Al and Al-2 (vol. %) Al_2O_3 shown in Fig. 3 (Oliver and Nix, 1982), it is seen that the creep rates for the dispersion-strengthened alloy are lower than those for the pure metal by several orders of magnitude. More importantly, the creep rates for the alloy fall steeply when the stress decreases by small amounts below $\sigma/E \approx 10^{-3}$, where E is the Young's modulus. Presumably, this indicates the existence of a threshold stress, σ_{th}, below which the creep rate is zero or immeasurably small in practice.[3] This observation has great technological implications

[3]The definition of σ_{th} used in this paper follows that of Gibeling and Nix (1980), who have discussed the differences in terminology and the physical origins of the terms "back stress," "friction stress," "internal stress," and "threshold stress." Accordingly, in the present paper, σ_{th} is identified with the stress below which no creep occurs.

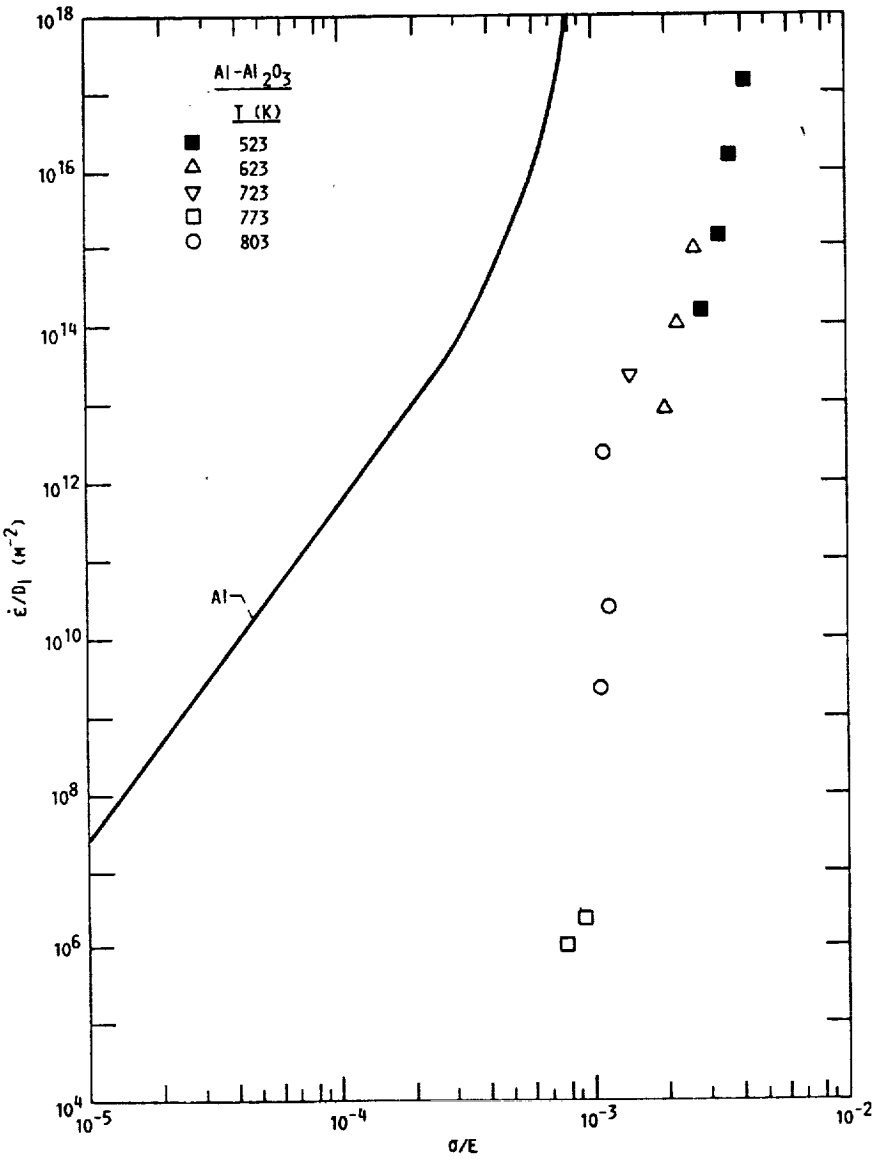

FIGURE 3. - VARIATION OF $\dot{\epsilon}kT/D_lGb$ AGAINST σ/G FOR PURE ALUMINUM AND Al-Al_2O_3 SHOWING A SHARP DECREASE IN THE NORMALIZED CREEP RATE FOR THE ALLOY WHEN $\sigma/E < 2x10^{-3}$ (OLIVER AND NIX, 1982) (REPRINTED WITH PERMISSION, PERGAMON JOURNALS LTD.).

since σ_{th} defines the maximum design stress that an engineering component can be subjected to without appreciable creep when the desired lifetime is required to be very long.

Creep data obtained on dispersion-strengthened alloys can be represented either by a power-law or an exponential creep relation. In most instances, the former correlation has been the preferred form of representing the $\dot{\varepsilon} - \sigma$ data, and in these cases, the magnitude of n has been found to vary between 3.5 (Durber and Davies, 1974) and 100 (Whittenberger, 1979). The values of n reported for several materials are tabulated in Table A.1 in the Appendix. In addition, the table includes information on the experimental conditions used in each investigation and other reported results.

Referring to Table A.1, some general observations may be made regarding the stress dependence of the secondary creep rate. First, values of n between 4.0 and 4.5 have been reported for several dispersion-strengthened materials. Typically, this group consists of pure metals and solid solution alloys as the matrix material which have been heat treated to give an equiaxed recrystallized microstructure. Second, constant values of n, usually between 6.0 and 8.0, have been observed for some alloys. Third, values of $n > 8$ have been reported for a large number of dispersion-strengthened alloys, where n generally increases with decreasing stress and increasing temperature. In this case, a threshold stress is often observed in these materials. A number of factors appear to influence this type of creep behavior: processing techniques, grain size, grain aspect ratio, volume fraction, V_f, of the dispersoids, interparticle spacing, and the range of test stresses and temperatures. It is therefore clear that the addition of dispersoids to a metallic matrix does not necessarily lead to threshold stress behavior. Instead, as shown in Table A.1, only some matrix-dispersoid combinations, coupled with variations in the microstructure and processing techniques, result in this type of stress dependency of the creep rate.

Unfortunately, in many instances the analysis of elevated temperature data reported in the literature assumes the applicability of the power-law creep relationship and no attempt is generally made to verify that the exponential creep relation is actually unsuitable. Indeed the power-law relation may not always be valid. For example, Fig. 4 shows that the creep data obtained on an Al-4 wt. % Al_2O_3 alloy are well-represented by an exponential relation (Milička, Čadek, Ryš, 1970). In practice, the nature of the stress dependence can vary with the processing technique used and the volume fraction of the dispersoid. This is shown in Fig. 5 for dispersion-strengthened lead, where it is observed that the data for the as-extruded material appears to exhibit an exponential creep behavior while that for the recrystallized alloy follows a power-law creep relation when $\sigma < 16$ MPa. Interestingly, the as-extruded material is weaker than the recrystallized alloy despite the fact that it contains a larger volume fraction of dispersoids. This may be due to the fact that the extruded material had a smaller grain size (Table A.1) so that grain boundary sliding could have influenced the creep rate significantly.

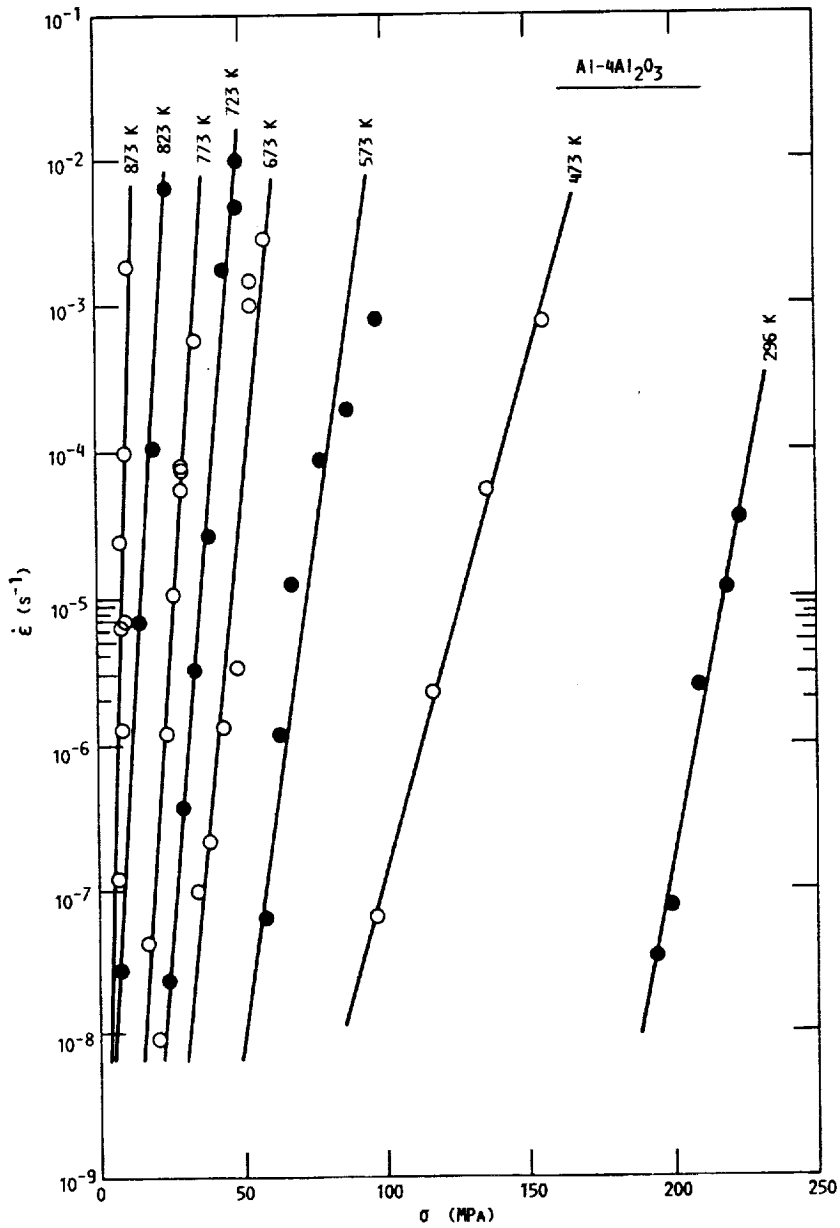

FIGURE 4. - SEMI-LOGARITHMIC PLOT OF THE STEADY-STATE CREEP RATE AGAINST THE APPLIED STRESS FOR Al-4 (wt %) Al_2O_3 SHOWING AN EXPONENTIAL STRESS DEPENDENCY FOR THIS MATERIAL (MILIČKA, ČADEK, RYŠ, 1970).

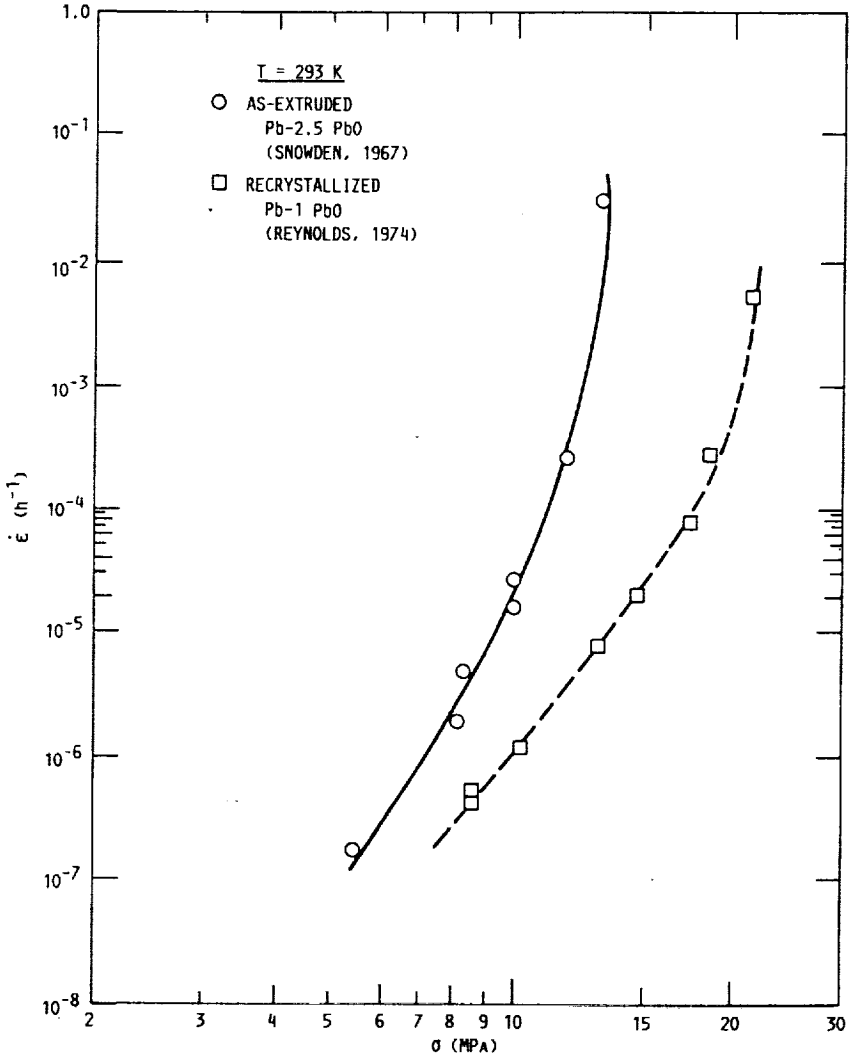

FIGURE 5. - VARIATION OF THE STEADY-STATE CREEP RATE WITH THE APPLIED STRESS FOR TWO DISPERSION-STRENGTHENED LEAD ALLOYS TESTED AT ABOUT 293 K. THE CREEP STRENGTH OF THE AS-EXTRUDED ALLOY CONTAINING 2.5 (WT %) PbO (SNOWDEN, 1967) IS LESS THAN THAT FOR THE RECRYSTALLIZED MATERIAL CONTAINING 1.0 (WT %) PbO (REYNOLDS, 1974).

Figure 5 demonstrates clearly that an increase in the volume fraction of the dispersoid may not always lead to an increase in the creep strength of the alloy. This situation would arise when the dominance of one mechanism is enhanced in preference to another, and this appears to be the case with the data shown in Fig. 5. Similarly, the presence of MgO dispersoids in an Al-3.9% Mg solid solution alloy effectively increases the role of one mechanism while suppressing class A behavior and results in a weaker material when $10^{-3} \lesssim \sigma/E \lesssim 3x10^{-3}$ (Fig. 6). The suppression of class A behavior has also been observed in an Al-5% Mg-0.25% Fe commercial alloy containing about 16 to 17 vol. % of $(FeMn)Al_6$ (Horita, 1983; and Horita and Langdon 1983). These observations are important in the development and application of dispersion-strengthened materials since they demonstrate the inherent dangers associated with particle weakening: The suppression of one creep mechanism can lead to the dominance of another, which could result in unforeseen deformation and failure of an engineering component.

3.3 The Temperature Dependence of The Creep Rate

The apparent activation energy for creep, Q_A, is given by

$$Q_A = -R[\partial \ln \dot{\varepsilon}/\partial(1/T)]_\sigma \tag{5}$$

In practice, Q_A is generally determined from plots of the temperature dependence of the creep rate at a constant value of stress or from temperature change experiments, where the creep rate is measured before and after small changes in temperature (typically, 5 % of the original temperature). The values of Q_A reported for a number of dispersion-strengthened materials are also tabulated in Table A.1. In some investigations, the reported value of Q_A was partially corrected for the temperature dependence of the elastic modulus in the manner proposed by Barrett, Ardell, and Sherby (1964), and this is indicated in the table. From Table A.1, it is clear that extremely large values of Q_A have been reported in several investigations, and these may exceed the activation energy for lattice self-diffusion in the matrix by a factor of up to 25 in some cases. In most instances, the corresponding magnitudes of the stress exponent are also high.

Figure 7 shows the distribution of the reported values of Q_A with T/T_m for a number of dispersion-strengthened materials. In general, three types of distribution functions are observed. First, Q_A does not depend significantly on stress and temperature when the materials are tested after relatively little or no prior mechanical processing followed by an annealing treatment. Typically, these materials contain equiaxed grains and a large interparticle spacing, and the values of Q_A and n are comparable to those for a pure metal. Second, high values of Q_A much greater than Q_l, but relatively independent of stress and temperature, are observed in alloys subjected to a complex thermomechanical processing history to produce recrystallized grains with very large grain aspect ratios. Third, the magnitude of

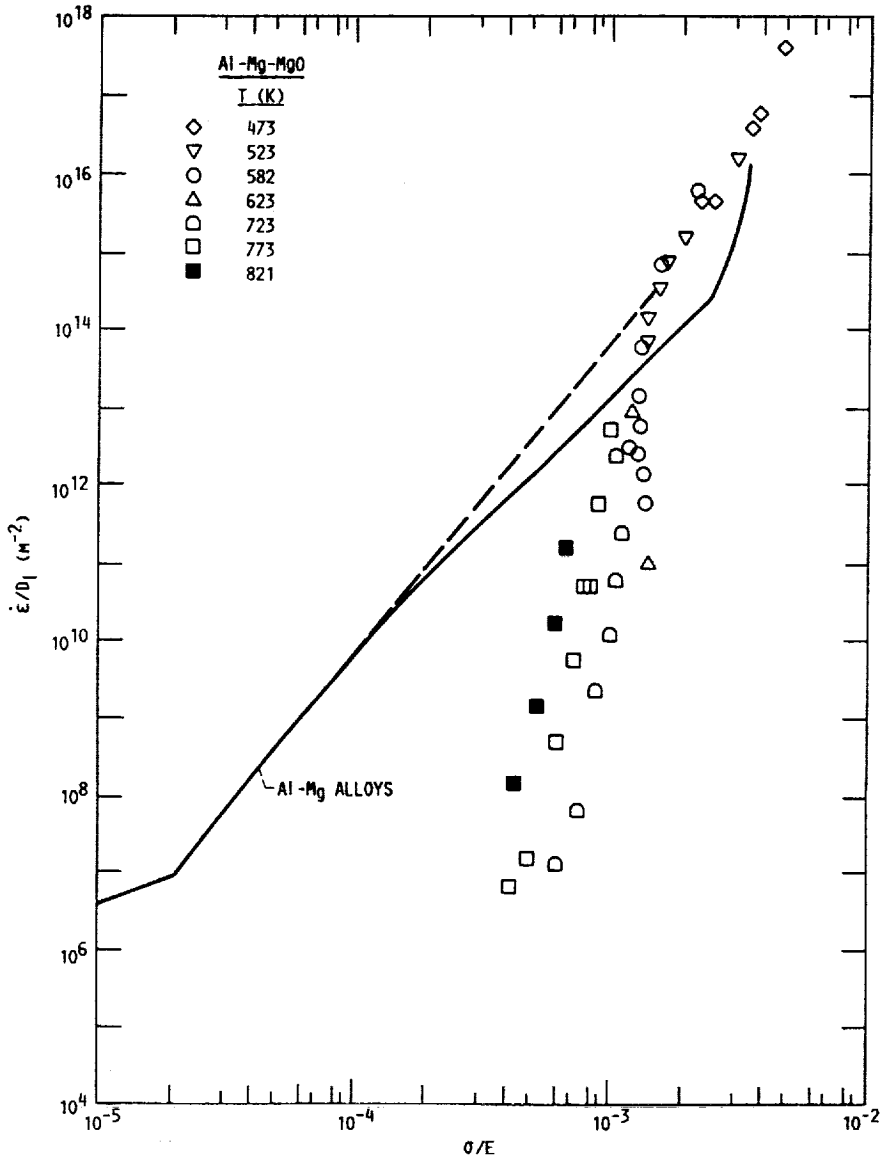

FIGURE 6. - EFFECT OF DISPERSION STRENGTHENING ON THE CREEP PROPERTIES OF Al-3.9 (wt %) Mg (OLIVER AND NIX, 1982). THE PRESENCE OF THE PARTICLES STRENGTHENS THE MATRIX ONLY WHEN $\sigma/E < 10^{3}$. ABOVE THIS VALUE, THE CREEP STRENGTH OF THE SOLID SOLUTION ALLOY CONTAINING DISPERSOIDS IS COMPARABLE OR LESS THAN THAT OF THE MATRIX MATERIAL. NOTE THAT THE VISCOUS GLIDE MECHANISM IS NOT OBSERVED IN THE ALLOY (REPRINTED WITH PERMISSION, PERGAMON JOURNALS LTD.).

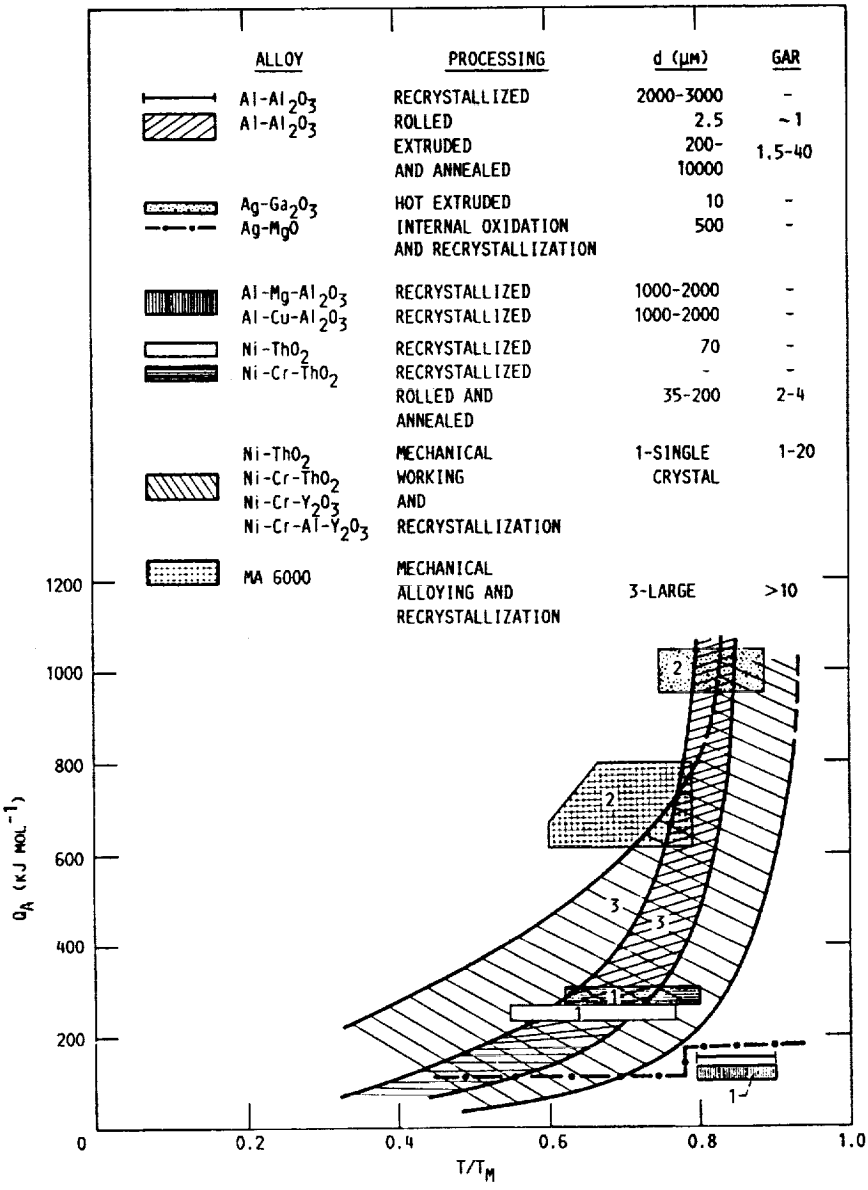

FIGURE 7. - TEMPERATURE DEPENDENCE OF THE APPARENT ACTIVATION ENERGY FOR CREEP OF SEVERAL DISPERSION-STRENGTHENED MATERIALS BASED ON THE VALUES OF Q_A TABULATED IN TABLE A1. IN REGION 1, $Q_A \approx Q_1$, WHILE $Q_A >> Q_1$ IN REGION 2. THE DATA CORRESPONDING TO REGION 3 IS STRONGLY DEPENDENT ON TEMPERATURE UNLIKE THOSE IN REGIONS 1 AND 2.

Q_A increases with temperature in some alloys,[4] which were tested in the mechanically-worked state (Milička, Čadek, and Ryš, 1970) or which possessed a large initial grain aspect ratio (Petrovic and Ebert, 1973). This observed temperature dependence of the activation energy could result from its dependence on the applied stress as shown in Fig. 8, where the true activation energy evaluated from the data reported by Milička, Čadek, and Ryš (1970) on Al-4% Al_2O_3 (Fig. 9), is plotted against the normalized applied stress. The values of the activation energies for lattice self-diffusion in Al and Al_2O_3 tabulated by Frost and Ashby (1982) are also shown in Fig. 8. As shown in Fig. 8, the magnitude of Q_c increases gradually with a decrease in σ/G till about 10^{-3}, below which the rate of change is much higher.

Lund and Nix (1975), and Malu and Tien (1975), attributed the high values of $Q_A >> Q_l$ to the importance of the temperature dependence of the elastic modulus which can be significant at high temperatures, especially if n is high. However, only a partial correction incorporating the modulus-compensated stress term in equation (1) was suggested, and the additional contribution because of the term, G/T, in the equation was ignored. For a power-law creep relation, such as equation (1), the true activation energy is given by Langdon and Mohamed (1977)

$$Q_c = Q_A + RT + (n - 1)(RT^2/G)(\partial G/\partial T)_P \qquad (6)$$

where $(\partial G/\partial T)_P$ is the rate of change in the shear modulus with temperature at a constant pressure, P. Alternatively, the true activation energy for creep may be obtained by plotting $\dot{\epsilon}T/G$ against $1/T$ semi-logarithmically for different values of the normalized stress (Fig. 9). Using equation (6), and the data for the shear modulus tabulated in Table A.2 in the Appendix, the values of Q_c were estimated for some of the materials listed in Table A.1. These are tabulated in Table A.3, along with the ratio, Q_c/Q_l, where the magnitudes of Q_l are given in Table A.2. Further details of the procedure followed in deriving Q_c are given in Appendix A.2. It is evident from Table A.3 that the magnitudes of the temperature-compensated activation energies are still much larger than Q_l in a number of instances. These results suggest that additional correction terms may have to be included in equation (6) in order to reduce Q_A to a value equal to about Q_l. This is discussed in Sec. 3.4.

Although the incorporation of other terms into equation (6) can lead to $Q_A \approx Q_l$ there is no *a priori* reason to assume that these corrections are necessarily valid, since the inclusion of such correction factors implicitly assumes that all deformation is restricted to the matrix. However, if the particles deform during creep, then these high values of activation energy may equal those associated with the creep of the dispersoids. If this be the case, it is then instructive to compare the experimental activation energies

[4]Relatively constant values of Q_A have been reported for some Ni-Cr-ThO_2, MA 754, and Ni-Cr-Al-Y_2O_3 alloys (Table A.1). However, for reasons of clarity, no attempt has been made to identify these results in Fig. 7.

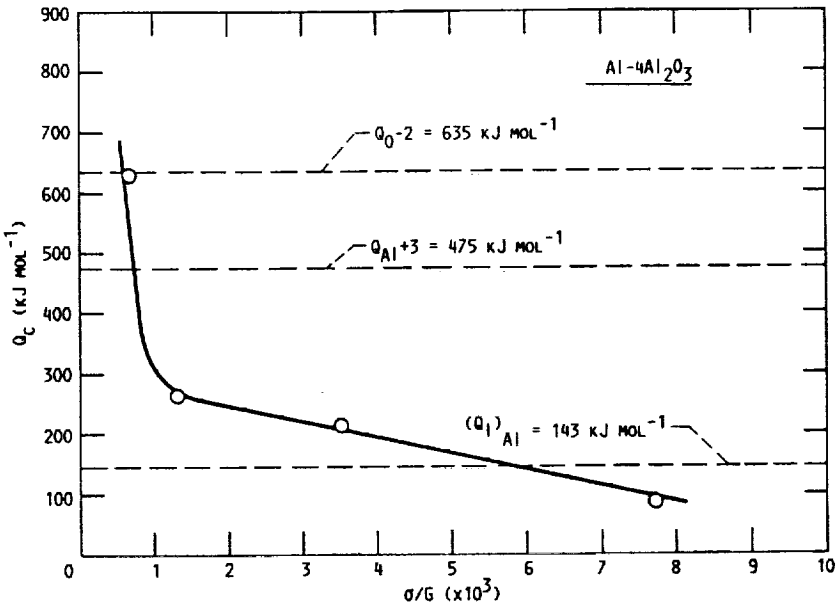

FIGURE 8. - VARIATION OF TRUE ACTIVATION ENERGY FOR CREEP WITH NORMALIZED STRESS FOR Al-4 (wt %) Al_2O_3 BASED ON THE DATA REPORTED BY MILIČKA, ČADEK, AND RYŠ, (1970). THE BROKEN LINES REPRESENT THE VALUES OF THE ACTIVATION ENERGIES FOR LATTICE SELF-DIFFUSION IN ALUMINUM (MOHAMED AND LANGDON, 1974b), AND INTRINSIC DIFFUSION OF ANIONS AND CATIONS IN Al_2O_3 (FROST AND ASHBY, 1982).

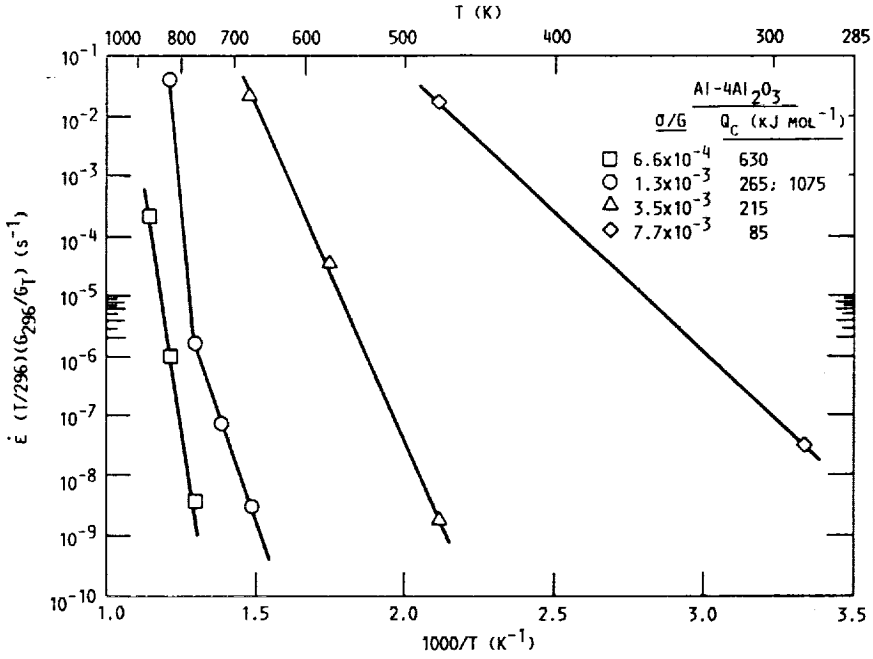

FIGURE 9. - TECHNIQUE FOR ESTIMATING THE TRUE ACTIVATION ENERGY FOR CREEP FOR Al-4 (wt %) Al_2O_3 (MILIČKA, ČADEK, RYŠ, 1970) FROM A PLOT OF THE TEMPERATURE-COMPENSATED CREEP RATE AGAINST THE INVERSE OF THE ABSOLUTE TEMPERATURE FOR DIFFERENT VALUES OF THE NORMALIZED STRESS.

with those for intrinsic diffusion of the slowest species in the dispersoids assuming that the deformation of the latter is controlled by a lattice diffusion mechanism such as high temperature climb or Nabarro-Herring creep. The latter possibility was considered by Oliver and Nix (1982) in their investigation on oxide dispersion-strengthened Al and Al-Mg alloys.

Table II compares the apparent activation energies for several ODS alloys for which $Q_A >> Q_l$ (Table A.1) with those for intrinsic lattice diffusion of the slowest diffusing species or for high temperature climb. The activation energies for intrinsic diffusion and creep are based on the tabulated data reported by Frost and Ashby (1982), and Gaboriaud (1981). It should be noted that the values of Q_c given in Table A.3 were obtained after correcting for the temperature dependence of the shear modulus of the *matrix*; thus it would be inappropriate to compare these with the activation energy data reported for the particle. Therefore, these values are not included in Table II. A more appropriate correction of the apparent activation energy would involve the temperature dependence of the shear modulus of the dispersoid, if the latter deforms by a nondiffusion creep mechanism with $n > 1$. However, the range of temperatures over which the data have been obtained constitutes only a small fraction of the absolute melting point of the dispersoids, and consequently this correction factor is expected to be small. Therefore, the data for the apparent activation energy included in Table II would be approximately equal to that corrected for the temperature dependence of the shear modulus of the particle.

As shown in Table II, the apparent activation energies compare reasonably well with those for cation and anion intrinsic diffusion in the dispersoid only in some cases. For example, the agreement is extremely good for the data reported by Oliver and Nix (1982) on ODS aluminum and Al-Mg but very poor for the more complex nickel-base materials. Therefore, the present evidence does not support the viewpoint that diffusional processes occurring within the particle contribute to the creep of most dispersion-strengthened materials. This does not however rule out the possibility that the dispersoid may deform by a nondiffusional mechanism, and this idea is examined in Sec. 4.2.

3.4 Phenomenological Equations for Creep

It was demonstrated in Secs. 3.2 and 3.3 that the stress exponents and activation energies for creep of several dispersion-strengthened materials tend to be much higher than those for the matrix material. One possible rationalization was considered in Sec. 3.3, where the activation energies were compared with those for intrinsic diffusion of the anion and cation in the dispersoids, and it was concluded that the available evidence does not support the hypothesis that the particle deforms by a diffusion-controlled process. In this section, a second and more commonly accepted viewpoint is discussed based on the existence of a threshold stress.

A common observation in many dispersion-strengthened materials is the large increase in the magnitude of the stress exponent at high temperatures and low stresses. This is shown in Fig. 10 for a Ni-20% Cr-2% ThO_2 alloy

TABLE II. - A COMPARISON OF THE APPARENT ACTIVATION ENERGIES, Q_A, FOR CREEP OF OXIDE DISPERSION-STRENGTHENED MATERIALS WITH THOSE FOR ANION, Q_{an}, AND CATION, Q_{cat}, DIFFUSION IN THE OXIDES

Matrix	Dispersoid[1]	Q_A, kJ mol^{-1}	Q_A/Q_{an}[2]	Q_A/Q_{cat}[3]	References
Al	Al_2O_3	540	0.9	1.1	Oliver and Nix (1982)
Al-Mg	MgO	500	1.1	-	Oliver and Nix (1982)
Ni	ThO_2	795	-	1.3	Wilcox and Clauer (1966)
Ni-Cr	ThO_2	390 990	- -	0.6 1.6	Lund and Mix (1976)
Ni-Cr	Y_2O_3	505 660	- -	1.3 1.7	Howson *et al.* (1980a)
Ni-Cr	Y_2O_3	351 400-670	- -	0.8 1.0-1.7	Stephens and Nix (1984, 1985)
Ni-Cr-Al	Y_2O_3	525-660 1530	- -	1.4-1.7 3.9	McAlarney *et al.* (1982)
MA 6000	Y_2O_3	670	-	1.7	Kim and Merrick (1979)
MA 6000	Y_2O_3	620	-	1.6	Howson *et al.* (1980b)
MA 6000	Y_2O_3	800	-	2.1	Wittenberger (1984)

[1]For MA 6000, the dispersoids probably consist of a mixture of yttrium and aluminum oxides (Singer and Artz, 1986).

[2]Q_{an} is the activation energy of the anion in the oxide. The values of Q_{an} were obtained from Frost and Ashby (1982), and are about 635 and 460 kJ mol^{-1} for Al_2O_3 and MgO, respectively.

[3]Q_{cat} is the activation energy for cation diffusion in the oxide. The values of Q_{cat} used were about 475 and 625 kJ mol^{-1} for Al_2O_3 and ThO_2, respectively (Frost and Ashby, 1982). A value of $Q_{cat} \approx 390$ kJ mol^{-1} was assumed for Y_2O_3 based on the creep data reported by Gaboriaud (1981).

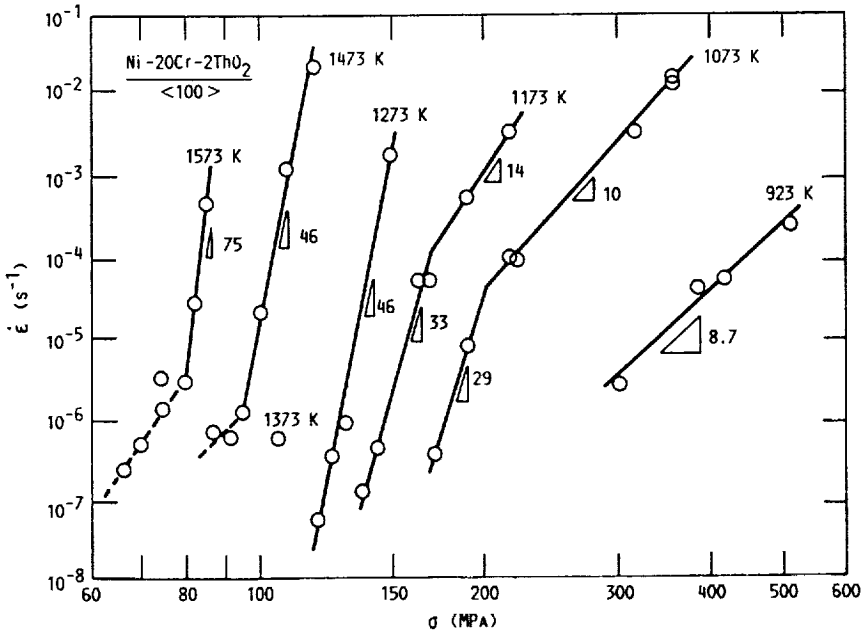

FIGURE 10. - MINIMUM CREEP RATE FOR Ni-20% Cr-2% ThO_2 SINGLE CRYSTALS AS A FUNCTION OF CREEP STRESS AT VARIOUS TEMPERATURES (LUND AND NIX, 1976). (REPRINTED WITH PERMISSION, PERGAMON JOURNALS LTD.).

(TD-Nichrome) based on the data reported by Lund and Nix (1976). In this case, the stress exponent increased from $n = 8.7$ at 923 K to $n = 75$ at 1573 K. However, if these are replotted as $\dot{\varepsilon}/D_1$ against σ/G using the data tabulated in Table A.2, then it is seen that the normalized creep rate decreases sharply with a small decrease in the normalized stress (Fig. 11). Two points may be noted about Fig. 11. First, at low temperatures and high stresses $\dot{\varepsilon}/D_1$ varies relatively gradually with σ/G. Second, there is almost a vertical drop in the $\dot{\varepsilon}/D_1 - \sigma/G$ plot at high temperatures and low stresses which suggests the existence of a critical stress below which the creep rate is expected to be zero if there is no change in the deformation mechanism. However, if the rate-controlling process changes, then $\dot{\varepsilon}/D_1$ can decrease more gradually at lower values of σ/G after the sharp drop in the $\dot{\varepsilon}/D_1 - \sigma/G$ plot. Similar observations relating to these two modes of behavior in the $\dot{\varepsilon}/D_1 - \sigma/G$ plot have been reported for dispersion-strengthened aluminum (Fig. 3) and Al-Mg (Fig. 6) alloys (Oliver and Nix, 1982). These results suggest the occurrence of two deformation regions which act sequentially with each other.

The observation of an apparent threshold behavior during creep of dispersion-strengthened alloys has led to the suggestion that it is the effective stress, $(\sigma - \sigma_{th})$, and not the applied stress, that is the important variable in the creep rate equation. Therefore, the power-law creep equation may be represented by

$$\dot{\varepsilon} = A_4(D_0Gb/kT)[(\sigma - \sigma_{th})/G]^{n_1}\exp(-Q_{c1}/RT) \tag{7}$$

where D_0 is a frequency factor, Q_{c1} is the activation energy for creep in the modified equation, and n_1 and A_4 are constants. Alternatively, the exponential relation may be modified to include the threshold stress as

$$\dot{\varepsilon} = A_5(\sigma - \sigma_{th})^2\exp[B'(\sigma - \sigma_{th})/G]\exp(-Q_{c2}/RT) \tag{8}$$

where Q_{c2} is the activation energy for creep, and A_5 and B' are constants. The stress exponent of two incorporated in the pre-exponential term is assumed to result from the dependence of the dislocation density on the effective stress. Both equations (7) and (8) predict that $\dot{\varepsilon} = 0$ when $\sigma = \sigma_{th}$.

Equations (7) and (8) are an attractive, although empirical, representation of the creep rate equation for a dispersion-strengthened material since they provide a rationale for the high values of the stress exponent and the activation energies reported in the literature (table A.1). This arises as a result of the relationship that exists between the measured stress exponent given by equation (1) and that predicted by equation (7) (Purushotham and Tien, 1978):

$$n = n_1\left[\left\{1 - \left(\partial\sigma_{th}/\partial\sigma\right)_T\right\}\Big/\left\{1 - \sigma_{th}/\sigma\right\}\right] \tag{9}$$

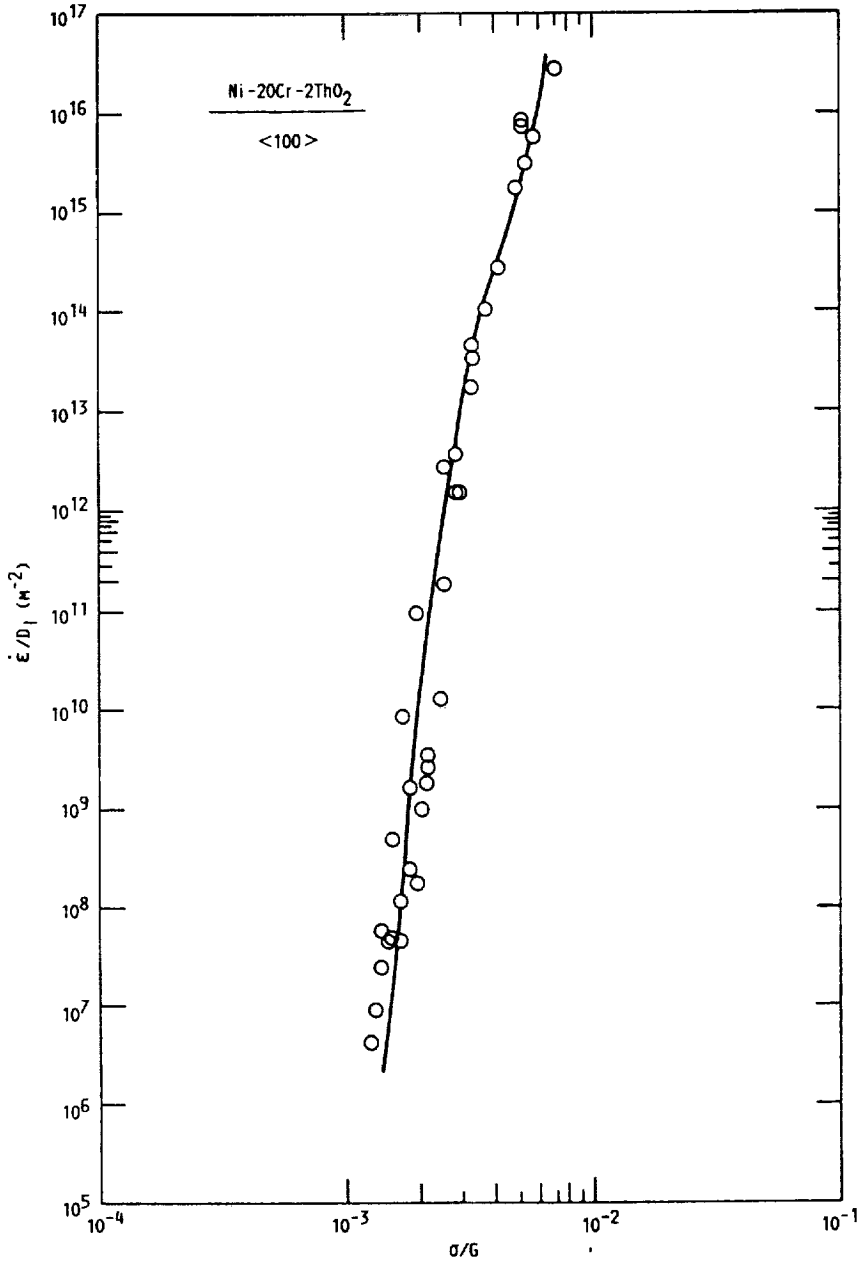

FIGURE 11. - VARIATION OF $\dot{\epsilon}/D_l$ WITH σ/G FOR Ni-20% Cr-2% ThO_2 SINGLE CRYSTALS BASED ON THE DATA SHOWN IN FIG. 10. AN APPARENT THRESHOLD STRESS BEHAVIOR IS OBSERVED AT THE LOWER VALUES OF σ/G.

Similarly, a pseudo stress exponent can be calculated from the exponential stress relation given by equation (8) as

$$n = (\partial \ln \dot{\varepsilon}/\partial \ln \sigma)_T = \left[2 + B'(\sigma - \sigma_{th})\right]\left[\left\{1 - (\partial \sigma_{th}/\partial \sigma)_T\right\} \Big/ \left\{1 - \sigma_{th}/\sigma\right\}\right] \tag{10}$$

Equations (9) and (10) predict high values of n when σ approaches σ_{th}. Purushotham and Tien (1978) suggested that the exact magnitude of n would be determined by the stress dependence of σ_{th}. Therefore, when σ_{th} is independent of the applied stress, and $\sigma >> \sigma_{th}$, equations (9) and (10) lead to $n \approx n_1$ and $n \approx [2 + B'(\sigma - \sigma_{th})]$, respectively. Although similar results are obtained when σ_{th} is assumed to be linearly dependent on the applied stress, this assumption is inconsistent with the definition of the threshold stress which requires that the latter be stress independent.

The activation energy for creep can be expressed in terms of the threshold stress utilizing either equations (7) or (8). Thus, equation (7) leads to

$$Q_{c1} = Q_A + RT + (n_1 - 1)(RT^2/G)(\partial G/\partial T)_P + [n_1 RT^2/(\sigma - \sigma_{th})](\partial \sigma_{th}/\partial T)_P \tag{11}$$

and equation (8) gives

$$Q_{c2} = Q_A - (RT^2/A_5)(\partial A_5/\partial T) + (RT^2/G)(\partial G/\partial T)_P[2 + B'/G]$$

$$+ RT^2(\partial \sigma_{th}/\partial T)_P[2/(\sigma - \sigma_{th}) + B'/G] \tag{12}$$

Equation (11) reduces to equation (6) when $(\partial \sigma_{th}/\partial T)_P = 0$ and $n = n_1$. The quantity $(\partial \sigma_{th}/\partial T)_P$ is negative (Artz, 1992), so that the effect of the fourth term in equation (11) or (12) leads to a significant decrease in the magnitude of the apparent activation energy as σ approaches σ_{th}. This correction is in addition to that incorporated in the third term in these equations.

Although the incorporation of the threshold stress in the creep rate equation provides an attractive rationale for the observed values of the stress exponent and the activation energy for creep, Gibeling and Nix (1980) have cautioned against an indiscriminate use of the effective stress approach since there is a danger of overlooking a genuine deformation mechanism. For example, the threshold stress approach is not always consistent as is evident through a comparison of Figs. 11 and 12, where the experimental creep rates shown in Fig. 10 for TD-nichrome (Lund and Nix, 1976) have been normalized by two different procedures. In Fig. 11 the creep rates have been normalized by the diffusion coefficient for lattice diffusion and an apparent threshold stress behavior is observed. However, if the creep rates are normalized in accordance with equation (1) as shown in Fig. 12, there is a gradual deviation in the data from the apparent threshold effect observed in Fig. 11 at low stresses and high temperatures owing to the additional influence of (T/G).

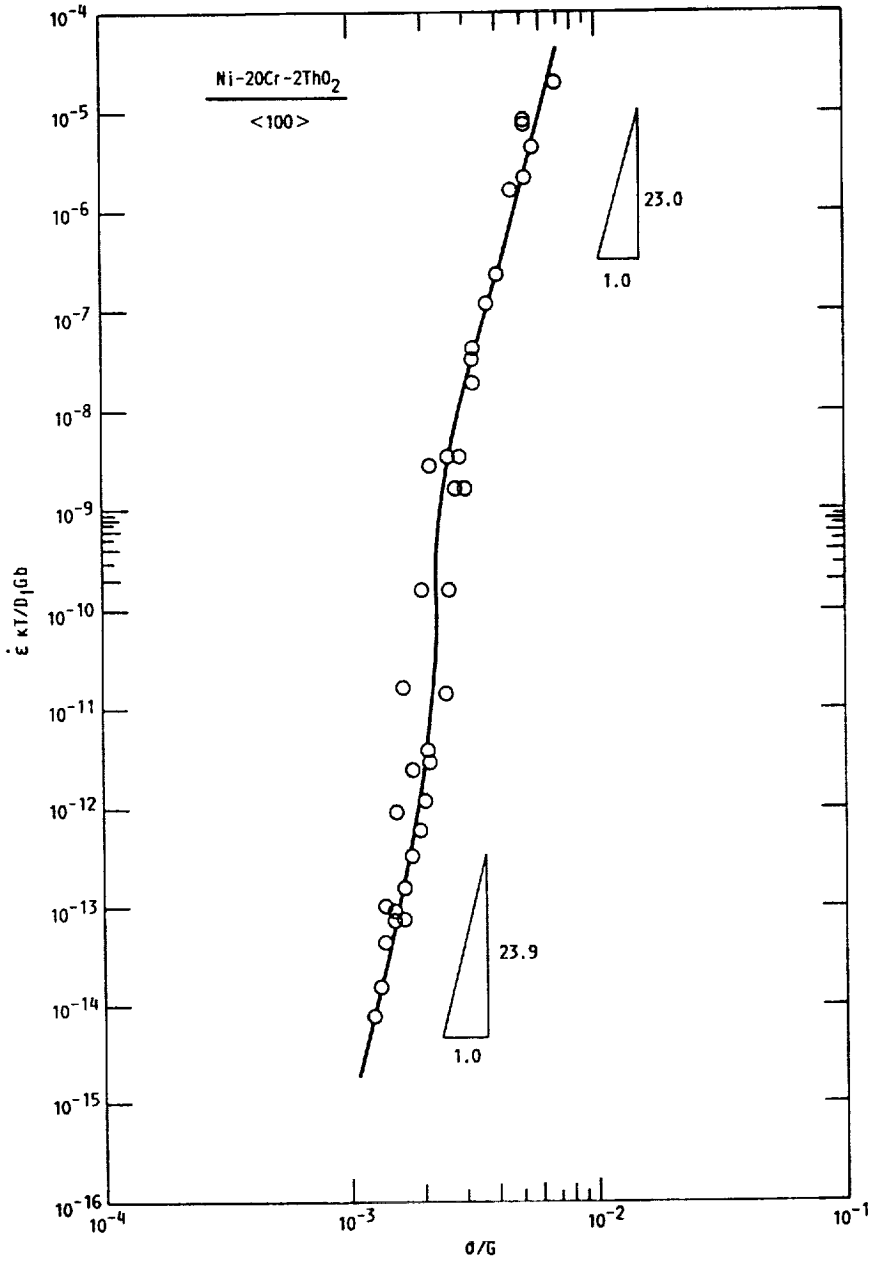

FIGURE 12. - PLOT OF $\dot{\varepsilon}kT/D_1Gb$ AGAINST σ/G FOR THE DATA SHOWN IN FIG. 10. A DEVIATION FROM THE THRESHOLD STRESS BEHAVIOR SHOWN IN FIG. 11 IS OBSERVED BELOW $\sigma/G \approx 2\times10^{-3}$ OWING TO THE ADDITIONAL INFLUENCE OF T/G IN THE NORMALIZING PARAMETER FOR THE CREEP RATE.

This deviation is consistent with a value of $n < 75$ observed at 1573 K when $\sigma < 80$ MPa (Fig. 10). These results cannot be easily rationalized using the threshold stress approach since the latter should lead to $\dot{\varepsilon} = 0$ when $\sigma = \sigma_{th}$ independent of the manner in which the data were normalized.

Three additional difficulties exist with the incorporation of a threshold stress in the creep rate equation. First, there is no unique or universally accepted technique for determining the magnitude of the threshold stress, and the value of σ_{th} is dependent on the method employed. Second, back stresses due to solid solution alloying, precipitates, and forest dislocations can complicate the measured value of σ_{th}, and it is not always possible in practice to correct for these effects. Third, a physical interpretation of the origin of these threshold stresses and the microstructural parameters which influence their magnitude is still poorly understood.

Despite these difficulties, the potential importance of the σ_{th} concept lies in the fact that the high values of n and Q_c can be easily rationalized. Therefore, a considerable amount of effort has been expended in evolving techniques for measuring the magnitude of the threshold stress and in understanding the nature of the deformation mechanisms responsible for this type of creep behavior. Some of these techniques used in the, estimation of σ_{th} are discussed in the next section while the possible origins of threshold stress behavior are reviewed separately by Artz (1992).

3.5 Techniques For Determining The Threshold Stress

Although several procedures have been developed for measuring σ_{th}, none of these are entirely satisfactory or universally accepted. Wilshire and co-workers (Davies *et al.*, 1973; Williams and Wilshire, 1973; Threadgill and Wilshire, 1974; Parker and Wilshire, 1975; Nelmes and Wilshire, 1976; Parker and Wilshire, 1978; Burt *et al.*, 1979; and Evans and Harrison, 1979), suggested that equation (7) with $n_1 = 4$ is valid for pure metals, solid solutions, precipitate-hardened alloys, and dispersion-strengthened materials and that σ_{th} could be evaluated from stress reduction experiments. Typically, these experiments are performed by decreasing the stress by small amounts in a creep experiment and noting the length of the "incubation" period of zero creep rate following the stress reduction before measurable creep occurs. The threshold stress is then estimated from plots of cumulative incubation times against the cumulative stress decrease. However, this technique is controversial since the existence of an incubation period is in doubt (Blum, Hausselt, and König, 1976; and Gibeling and Nix, 1977) so that this, procedure is not widely accepted. In addition, Lin and Sherby (1981) have pointed out that σ_{th} as determined by this technique is empirical and cannot be correlated independently with microstructural parameters, such as the interparticle spacing.

An alternative procedure for evaluating the threshold stress was suggested by Lin and Sherby (1981) based on the assumption that the subgrain microstructure can be considered to be constant during creep of a dispersion-

strengthened material. This condition would be fulfilled when the interparticle spacing is equal to or less than the equivalent subgrain size predicted by equation (3). Therefore, equation (3) may be modified to include the threshold stress

$$\dot{\varepsilon} = A_6(d_s/b)^3(DGb/kT)\left\{(\sigma - \sigma_{th})/G\right\}^8 \tag{13}$$

The magnitude of d_s is determined by the initial subgrain size or the interparticle spacing when the latter is smaller than the equivalent subgrain size. This condition is expected to be satisfied at relatively low stresses and equation (13) predicts a constant stress exponent of eight. However, if the stress is sufficiently high so that the equivalent subgrain size is smaller than the interparticle spacing, the stress dependence of the subgrain size becomes important, and equation (13) predicts a stress exponent of five, if $d_s \propto (\sigma - \sigma_{th})^{-1}$.

The threshold stress can be estimated from a graphical analysis of equation (13) by extrapolating a linear plot of $[\dot{\varepsilon}kTb^2/(d_s)^3DG]^{1/8}$ against σ/G to zero. In this case, the magnitude of d_s is obtained from experimental measurements of the initial subgrain size or the interparticle spacing.

The Lin-Sherby technique is attractive in that it permits the determination of σ_{th} based on an estimate of a single microstructural parameter. However, its applicability is dependent on the validity of equation (13), and a uniform distribution of dispersoids which is seldom observed in practice. In addition, an examination of Table A.1 shows that subgrains are not always observed in dispersion-strengthened materials even when $n \approx 4$ and the interparticle spacing is large (Reynolds, Lenel, and Ansell, 1971). The Lin and Sherby hypothesis (1981) is also not supported by the observations of Durber and Davies (1974) on several Ni-ThO_2 alloys. A value of $n = 3.5$ was obtained in this investigation although the interparticle spacing was smaller than the subgrain size of about 20 μm estimated from equation (3).

A more direct technique for determining the threshold stress utilizes the power-law creep relationship such as that given by equation (7). In this case, σ_{th} can be determined by extrapolating a linear plot of $(\dot{\varepsilon}kT/DGb)^{1/n_1}$ against (σ/G) to a zero value of the normalized creep rate. However, this method requires some knowledge of the value of n_1 which is often assumed to equal that for the matrix (Artz, 1992). This assumption is valid only when the deformation of the matrix remains unchanged in the presence of the dispersoids which may not necessarily be valid. In addition, the choice of n_1 is somewhat arbitrary since the stress exponent of the matrix material can vary with stress and temperature. However, a major advantage of this technique is its relative simplicity.

For the specific case when σ_{th} is equal to the Orowan stress, the threshold stress can be identified with the magnitude of the yield stress obtained at room temperature if this corresponds to the a thermal region of the yield stress-temperature plot. Alternatively, the threshold stress can be estimated theoretically if the particle size and spacing are known. Another technique for estimating the threshold stress is based on the "additive rule" proposed by Lund and Nix (1976), and later modified by Pharr and Nix (1976). This procedure assumes that the high temperature strength of the alloy at a constant value of $\dot{\epsilon}/D$ can be represented by

$$(\sigma/G)_{alloy} = (\sigma/G)_{matrix} + (\sigma_{th}/G) \qquad (14)$$

where $(\sigma/G)_{alloy}$ is the measured normalized strength of the dispersion-strengthened alloy and $(\sigma/G)_{matrix}$ is the normalized strength of the matrix. Therefore, σ_{th} may be estimated from equation (14) if the magnitudes of $(\sigma/G)_{alloy}$ and $(\sigma/G)_{matrix}$ are known. Lin and Sherby (1981) have raised two objections to this concept. First, equation (14) assumes that the matrix and the dispersion-strengthened material exhibit similar creep behavior. This may not always be valid since the matrix material exhibits primary creep (e.g., nichrome) whereas the dispersion-strengthened alloy may show very little strain hardening (e.g., TD-nichrome) in some cases. Second, σ_{th} cannot be correlated easily with the microstructural parameters.

To summarize, there is as yet no satisfactory technique for measuring the threshold stress, although the extrapolation method utilizing equation (7) appears to be the simplest and the most general procedure available at present despite the inherent subjectiveness involved in the choice of the stress exponent.

3.6 Characteristics of the Threshold Stress

The creep of dispersion-strengthened alloys is strongly influenced by the initial microstructure. The addition of dispersoids to a metallic matrix generally tends to reduce the creep rate although other effects, such as the suppression of the dominant creep mechanism in the pure metal or solid solution alloy and the relative enhancement of another process, can lead to dispersion weakening of the material (Figs. 5 and 6). Although it would be useful to correlate this decrease in the creep rate directly with the microstructural parameters, such as the interparticle spacing, such relationships are difficult to make in practice since other variables, such as the particle size, can also vary. Therefore, there are very few investigations where such correlations have been attempted. Durber and Davies (1974) observed that the creep rate decreased with an increase in the volume fraction of ThO_2 in recrystallized Ni-ThO_2 alloys. No significant variation was observed in the particle size, so that the decrease in the creep rate can be correlated directly with the interparticle spacing as shown in Fig. 13, where it is evident that even small additions of ThO_2 ($\approx$ 0.01 vol %) to nickel reduce the creep rate significantly.

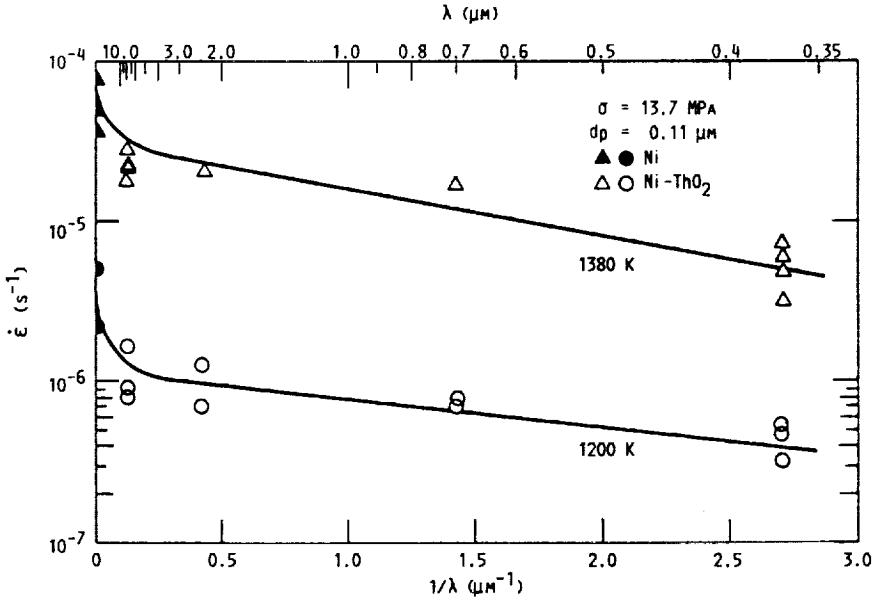

FIGURE 13. - EFFECT OF INTER-PARTICLE SPACING ON THE STEADY-STATE CREEP RATE FOR Ni-ThO_2. THE DATA ARE BASED ON THE INVESTIGATION OF DURBER AND DAVIES (1974).

However, from engineering considerations, it is the threshold behavior exhibited by some dispersion-strengthened alloys that is of primary interest. It was mentioned earlier that the addition of dispersoids to a metallic matrix does not necessarily result in threshold stress behavior, and alloys with similar compositions may exhibit differences in creep behavior (Table A.1). Therefore, for dispersion-strengthened alloys to be useful in engineering applications, it is important to understand the characteristics of threshold stresses.

At low temperatures, the magnitude of the threshold stress compares reasonably well with the calculated value of the Orowan stress, σ_{OR}. However, at high temperatures, the magnitude of the threshold stress is often found to be less than the experimental and the estimated values of the Orowan stress (Shewfelt and Brown, 1974; Pharr and Nix, 1976; Hausselt and Nix, 1977(a) and (b); Petkovic-Luton, Srolovitz, and Luton, 1983; and Clauer and Hansen, 1984). An example of this behavior is shown in Fig. 14 for a number of Cu-SiO_2 alloys (Shewfelt and Brown, 1974), where the ratio of the shear modulus-corrected values of the yield stress, σ_T, to the Orowan stress decreases with temperature above about 300 °C. At 1050 °C, the temperature-compensated yield stress, which is about 0.6 σ_{OR}, is only weakly dependent on the volume fraction and size of the particles. Similarly, the estimated values of σ_{th} have been found to be about half the Orowan stress for many other materials (Artz and Ashby, 1982; and Artz, 1992). Shewfelt and Brown (1974) also concluded that the threshold stress was not strongly influenced by the type or shape of the dispersoids used in copper-based alloys. Although this conclusion was based on a comparison of their data with those obtained on Cu-Al_2O_3 and Cu-BeO (Humphreys, Hirsch, and Gould, 1970), it is noted that this rationale may be erroneous owing to the large scatter in the data.

The simple interrelation that exists between the threshold and the Orowan stress (Artz, 1992) suggests that they are affected in a similar manner by the same microstructural parameters. Most calculations for the Orowan stress suggest that:

$$\sigma_{OR} = C(Gb/\lambda)\ln(d_p/b) \qquad (15)$$

where C is a geometrical constant. Alternatively, λ may be replaced by $\lambda_m = (\lambda - d_p)$ as suggested by Lund and Nix (1976). In the present paper, C was estimated to be about 0.5 using the equation given by Artz (1992).

Equation (15) predicts that σ_{OR} and σ_{th} are inversely related to the interparticle spacing, and this is shown in Fig. 15 for a number of materials tested in the power-law and diffusion creep regimes (Sautter and Chen, 1968; Burton, 1971; Moon, 1972; Pugh, 1973; Blickensderfer, 1974; Shewfelt and Brown, 1974; Lund and Nix, 1976;[5] Hausselt and Nix, 1977; Sinha and Blachere,

[5]The threshold stress estimated from the data of Lund and Nix (1976) may not be valid in view of the results shown in Fig. 12. However, this data point is shown in figure 15 for the sake of completeness.

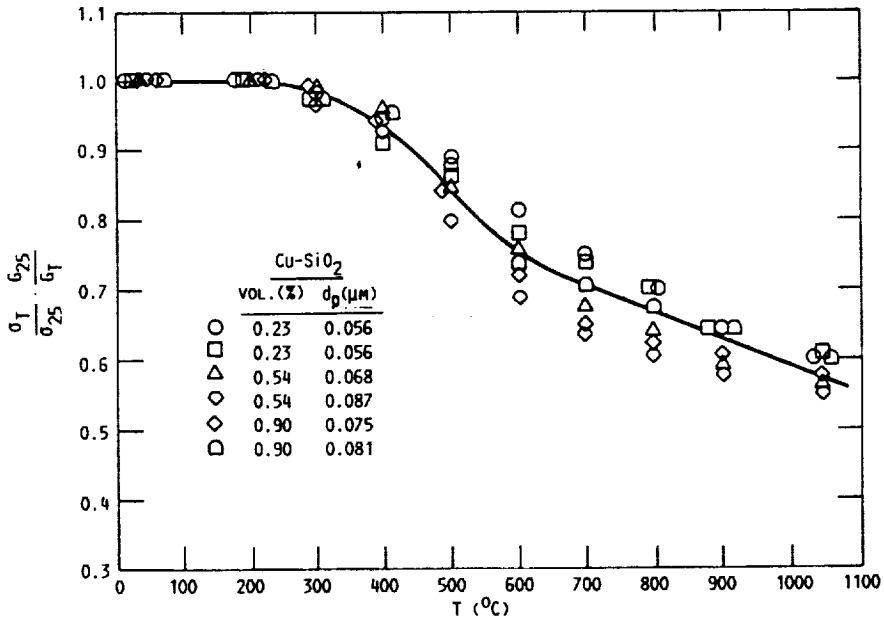

FIGURE 14. - THE RATIO OF THE MODULUS-CORRECTED YIELD STRESS, σ_T/G_T, FOR Cu-SiO_2 ALLOYS DETERMINED BETWEEN 20 AND 1050 °C TO THAT OBTAINED AT 25 °C AS A FUNCTION OF TEMPERATURE (SHEWFELT AND BROWN, 1974).

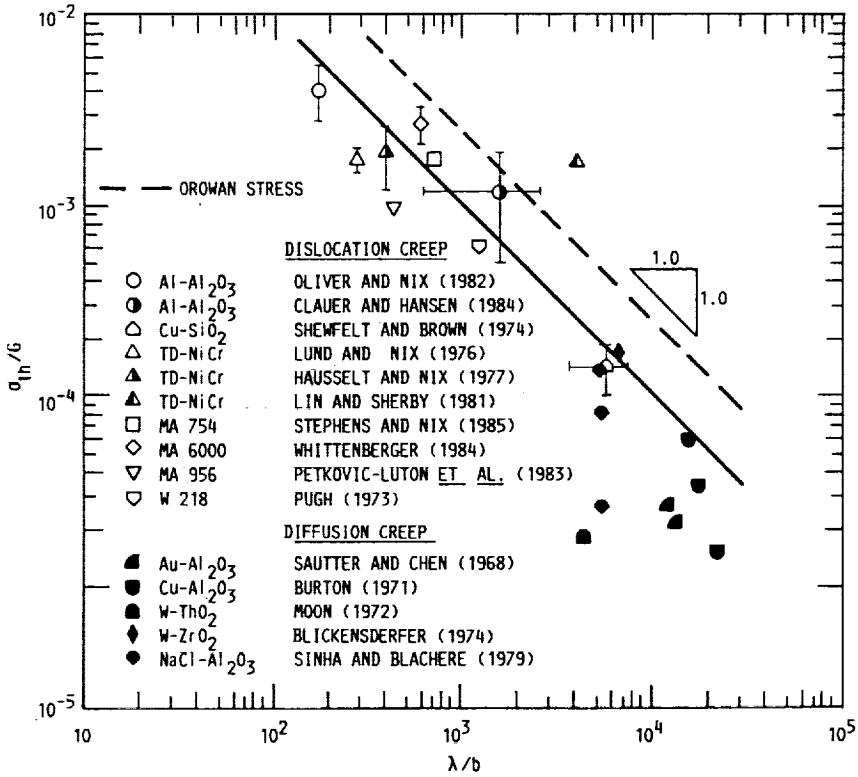

FIGURE 15. - VARIATION OF THE NORMALIZED EXPERIMENTAL THRESHOLD STRESS WITH THE NORMALIZED INTER-PARTICLE SPACING FOR SEVERAL DISPERSION-STRENGTHENED ALLOYS TESTED IN THE POWER-LAW AND DIFFUSION CREEP REGIMES. THE VALUES OF σ_{th} HAVE BEEN REPORTED ELSEWHERE (ARTZ AND ASHBY, 1982; ARTZ, 1991). THE BROKEN LINE REPRESENTS THE PREDICTED VALUE OF THE OROWAN STRESS GIVEN BY EQUATION (15) FOR dp/b = 100. THE INTER-PARTICLE SPACING REPORTED BY LIN AND SHERBY (1981) IS FOR COARSE PARTICLES.

1979; Lin and Sherby, 1981;[6] Oliver and Nix, 1982; Petkovic-Luton, Srolovitz,and Luton, 1983; Clauer and Hansen, 1984; Whittenberger, 1984; and Stephens and Nix, 1985). The threshold stress data for most of the materials tested in the power-law creep region are those tabulated by Artz (1992). However, the data on Cu-SiO_2 and the 218 tungsten alloy are based on the investigations of Artz and Ashby (1982), and Pugh (1973), respectively. The threshold stresses corresponding to the diffusion creep regime were obtained from the original references and these are included only for the sake of comparison. Alternatively, the normalized threshold stress can be plotted against the normalized effective interparticle spacing, $(\lambda - d_p)/b$ as shown in Fig. 16.

Assuming $d_p/b \approx 100$, the Orowan stress was calculated from equation (15), and the predicted values are compared with the threshold stress data in Fig. 15. Some general conclusions can be made based on Figs. 15 and 16. First, these plots demonstrate that σ_{th}/G is inversely dependent on the interparticle or the effective interparticle spacing; thus the form of equation (15) is satisfied. Second, the estimated values of the Orowan stress are nearly equal to or higher than the experimental values of the threshold stress for most of the materials. However, it should be noted that the calculated values of σ_{OR} are sensitive to the choice of the constant, C, in equation (15). Third, the normalized values of diffusion creep threshold stress generally tend to be much smaller than those for dislocation creep, and they are essentially independent of the interparticle spacing.

Figure 17 shows the variation of $(\sigma_{th}/G)(\lambda/b)$ with (d_p/b) plotted semi-logarithmically in accordance with equation (15). The slope of the linear regression line shown in the figure is about 1.0.[7] In comparison to the effect of the interparticle spacing, Fig. 17 suggests that the threshold stress is only weakly dependent on the particle size. There is very little direct experimental evidence on the effect of particle size on the creep rate and on the magnitude of the threshold stress. However, the observations of NcNelley, Edwards, and Sherby (1977) on dispersion-strengthened zinc containing a high volume fraction of Al_2O_3 dispersoids suggests that the threshold stress decreases with an increase in the particle size. This is shown in Fig. 18 where the data have been replotted by Blum and Reppich (1985). It is seen that the threshold stress decreases as the particle size increases in the Zn-30% Al_2O_3 alloys. These results appear to contradict the predictions of recent theoretical models on the origin of the creep threshold stress, which suggest that the threshold stress is not influenced by the size of the dispersoids (Artz and Schröder, 1986; and Artz and Wilkinson, 1986). One possible explanation of these observations is to attribute them to a

[6]The interparticle spacing reported by Lin and Sherby (1981) corresponds to coarse particle only. This may account for the relatively large deviation of this datum point from the mean line shown in Fig. 15.

[7]The data of Lin and Sherby (1981) were not considered in the regression analysis for reasons stated earlier.

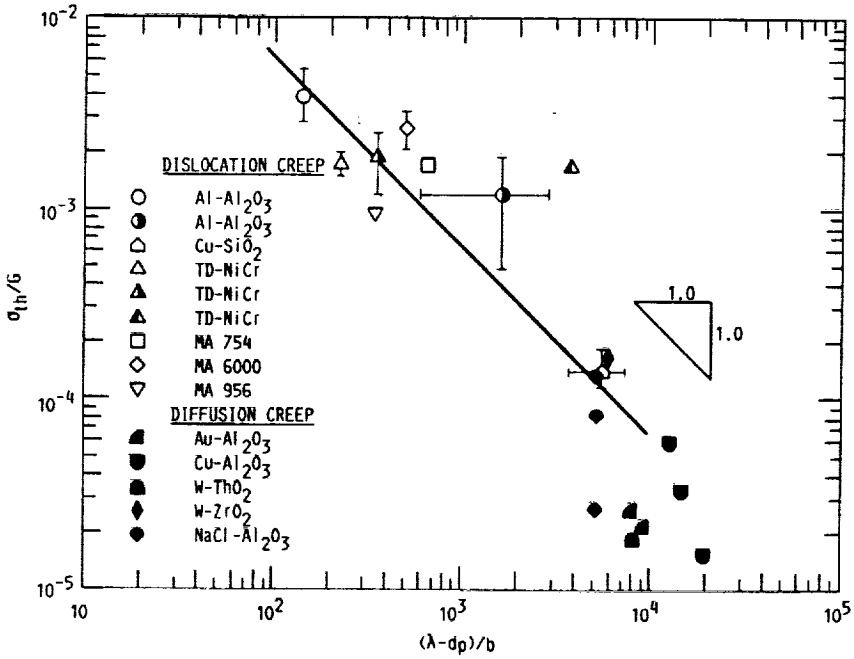

FIGURE 16. - VARIATION OF THE NORMALIZED EXPERIMENTAL THRESHOLD STRESS WITH THE NORMALIZED EFFECTIVE INTER-PARTICLE SPACING FOR THE DATA SHOWN IN FIG. 15.

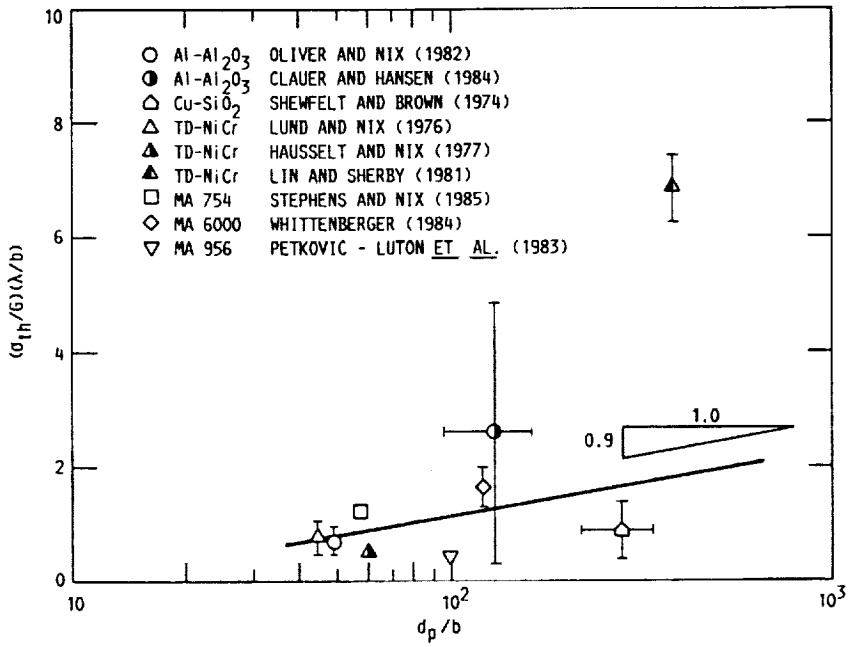

FIGURE 17. - PLOT OF (σλ/Gb) AGAINST dp/b IN THE DISLOCATION CREEP REGION.

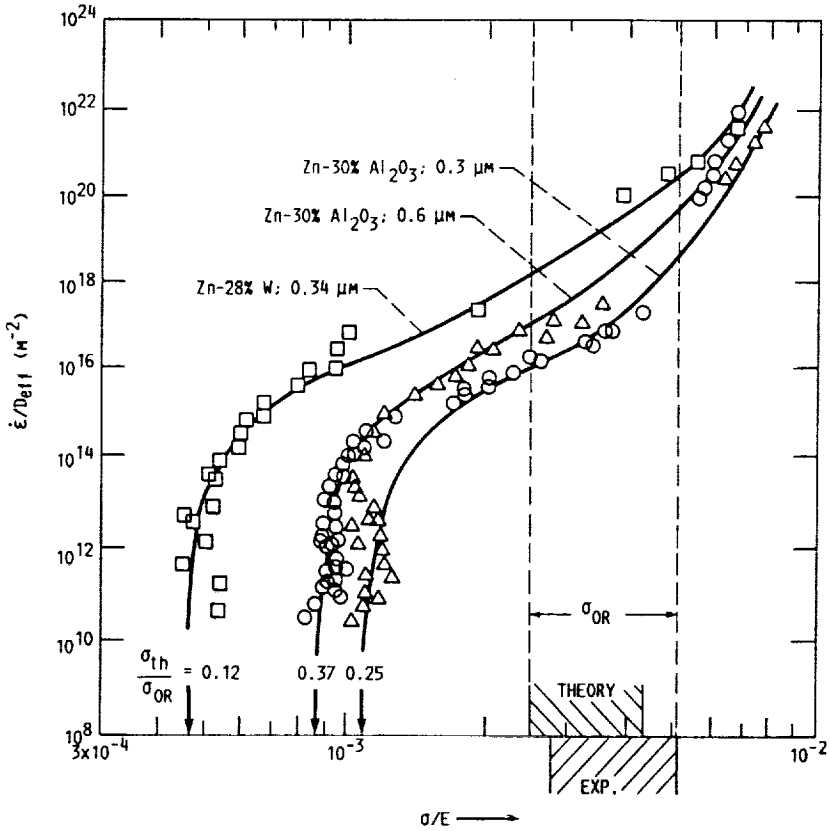

FIGURE 18. - PLOT OF THE CREEP RATE, NORMALIZED BY THE EFFECTIVE DIFFUSION COEFFICIENT, D_{eff}, AGAINST THE NORMALIZED STRESS FOR ZINC CONTAINING LARGE VOLUME FRACTIONS OF ALUMINA AND TUNGSTEN DISPERSOIDS (McNELLEY, EDWARDS, AND SHERBY, 1977). σ_{OR} DENOTES THE OROWAN STRESS IN THE FIGURE AND THE ARROWS INDICATE THE EXTRAPOLATED VALUES OF THE THRESHOLD STRESS GIVEN IN UNITS OF THE OROWAN STRESS. THE RANGE OF MEASURED AND PREDICTED VALUES OF σ_{OR} IS ALSO SHOWN (BLUM AND REPPICH, 1985) (COURTESY PINERIDGE PRESS).

variation in the interparticle spacing. This is an area where more research is required to establish the exact nature of this dependence on particle size.

Interestingly, Fig. 18 also shows that the Zn-W alloys are considerably weaker and exhibit a lower threshold stress than Zn-Al_2O_3 containing about the same size and volume fraction of dispersoids. These observations do not agree with the observations of Shewfelt and Brown (1974) on dispersion-strengthened copper alloys that the type of dispersoids do not influence creep behavior. Blum and Reppich (1985) attributed the observed differences in the creep behavior of the dispersion-strengthened Zn alloys to the possible effect of interfacial characteristics but there is insufficient evidence to verify this suggestion. However, it is also possible that these observations can be rationalized on the basis that the tungsten particles deform to a larger extent than the relatively stronger Al_2O_3 disperoids during creep, thereby resulting in a lower value of the threshold stress. The effect of particle deformation on the threshold stress is discussed in Sec. 4.2.

3.7 Microstructural Observations

The type of microstructures reported in the literature are also noted in Table A.1. In general, the nature and morphology of the substructure in Al-Al_2O_3, Ni-ThO_2, and NiCr-ThO_2 after creep remains unchanged from the initial microstructure, and large areas with little or no dislocations are often seen (Wilcox and Clauer, 1966(a) and (b), Miliča, Čadek, and Ryš, 1970; and Reynolds, Lenel, and Ansell, 1971). This is true even in those cases where class M behavior was observed (Reynolds, Lenel, and Ansell, 1971). These observations indicate that dislocation creep probably occurs rather heterogeneously in dispersion-strengthened materials.

Only limited observations of subgrains have been reported in dispersion-strengthened alloys deformed at elevated temperatures. This may be due to the fact that the total strain in the secondary creep region is usually less than 3%. However, subgrains have been observed in specimens deformed to strains greater than 10%. For example, in an investigation on a Ni-20% Cr-2% ThO_2 alloy, Hausselt and Nix (1977a) observed that the subgrain size decreased with an increase in stress in accordance with equation (3) with a stress exponent of about 1.0. Even in this instance, subgrains were found to be distributed inhomogeneously. The subgrain size also decreased with increasing strain and correlated extremely well with the dislocation density. These investigators concluded that the subgrain size was determined only by the applied stress and not by the interparticle spacing.

In those areas of the specimens where dislocations are observed, it is often observed that they are pinned down by the particles. An example of this is shown in Fig. 19 for a Ni-1 vol % ThO_2 alloy creep tested at 1073 K (Wilcox and Clauer, 1968). Two points may be noted. First, there is no evidence of dislocation loops around the particles as would be expected from the Orowan mechanism. Second, the dislocations appear to be joined to the particle-matrix interfaces (Fig. 19(a)) or to directly emanate from them (Fig. 19(b)). Similar microstructural observations have also been reported more recently on MA 754 (Nardone and Tien, 1983; Cooper, Nardone, and Tien, 1984), MA 956

ORIGINAL PAGE
BLACK AND WHITE PHOTOGRAPH

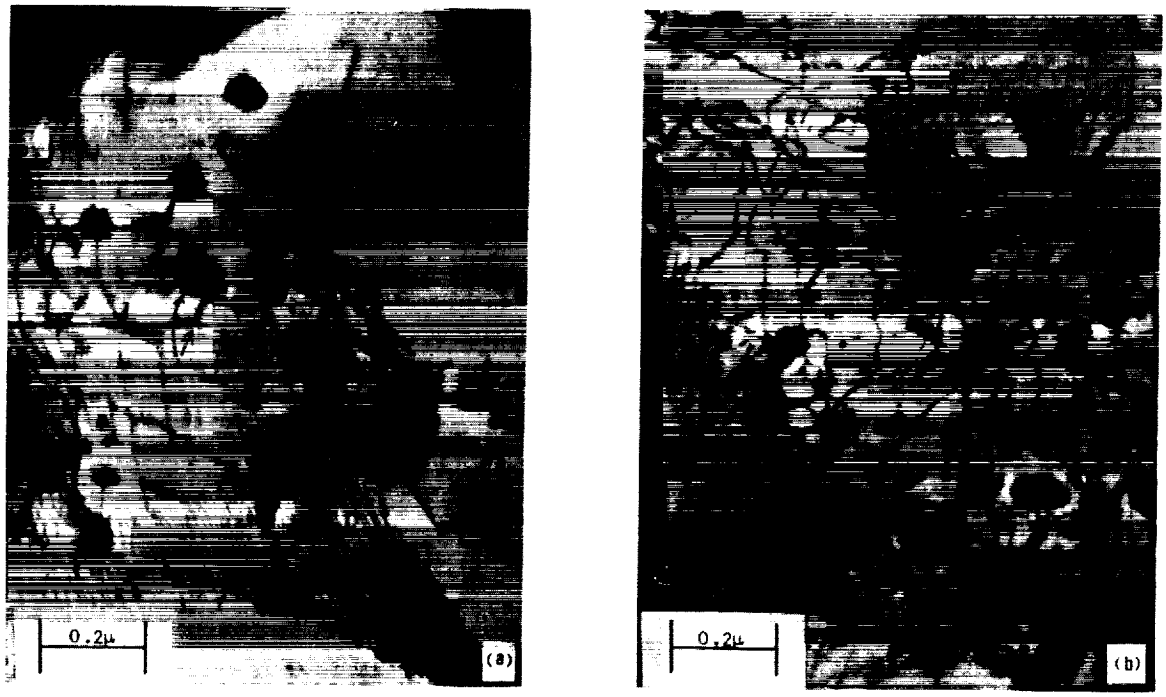

FIGURE 19. - MICROSTRUCTURE OF A Ni-1 vol % ThO_2 ALLOY TESTED AT 1073 K UNDER A STRESS OF 27.6 MPa TO A STRAIN OF ABOUT 1%. THE DISLOCATIONS ARE EITHER (a) ATTACHED TO THE DISPERSOIDS OR (b) APPEAR TO EMANATE FROM THEM (WILCOX AND CLAUER, 1968) (COURTESY GORDON AND BREACH, SCIENCE PUBLISHERS).

(Petkovic-Luton and Luton, 1985), and MA 6000 (Schröder and Artz, 1985). Examples of these are shown in Figs. 20 and 21 for MA 754 (Nardone, Matejczyk, and Tien, 1984) and MA 6000 (Schröder and Artz, 1985), respectively. These figures suggest that the dislocation-particle interaction is attractive in nature despite the fact that these dispersoids are harder than the matrix. It was concluded from observations of bowed dislocation segments between particles that the attractive interaction existed on the "departure," side of the dispersoid (Nardone and Tien, 1983; and Cooper, Nardone, and Tien, 1984). These observations are discussed by Artz (1992) as to their influence on the threshold stress behavior below the Orowan stress, and form the basis of recent models for dislocation creep in dispersion-strengthened materials (Srolovitz, Petkovic-Luton, and Luton, 1982; Srolovits, Petkovic-Luton, and Luton, 1983; Srolovitz *et al.*, 1984; Nardone, Matejcsyk, and Tien, 1984; and Artz and Wilkinson, 1986).

Srolovitz *et al.* (1982, 1983, 1984) suggested that the occurrence of slip and diffusion at the particle-matrix interface at elevated temperatures results in an attractive dispersoid-dislocation interaction, which permits the dislocation core to delocalize completely and relax into the interface. Under these conditions, the threshold stress is determined by the magnitude of this attractive interaction, and dislocation detachment from the dispersoid becomes the strength-determining factor. However, microstructural observations by Nardone, Matejczyk, and Tien (1984), and Schröder and Artz (1985, 1986), indicate that the dislocation does not lose its identity completely in the vicinity of the dispersoid (Fig. 21(b)). As a result, Nardone, Matejczyk, and Tien (1984), and Artz and Wilkinson (1986), proposed alternative derivations of the threshold stress based on the assumption that the dislocation core undergoes only a partial relaxation in the vicinity of a particle. The dislocation detachment theories are attractive from the point of view of the initial microstructures which often show dislocations attached to dispersoids in the as-received material (Fig. 22).

To summarize, the microstructure after creep is generally similar to that observed in undeformed samples where very few dislocations are normally seen. However, in those instances where dislocations have been observed, particle pinning of the dislocations are commonly observed. Even in these cases, the dislocation density is usually low (Schröder and Artz, 1985) often resulting in a single dislocation lying between two or more particles (Figs. 20 and 21) thereby suggesting the possibility of a localized interaction between the dislocation and the individual particles, especially at stresses close to the threshold stress.

4.0 THEORETICAL CONSIDERATIONS IN THE CREEP OF SINGLE CRYSTALLINE AND COARSE-GRAINED DISPERSION-STRENGTHENED MATERIALS

4.1 Discrepancies Between Theory and Experimental Observations

Current theories relating to the creep of dispersion-strengthened materials have been reviewed by Bilde-Sorensen (1983), and Blum and Reppich (1985), and no detailed discussion of these will be presented here. In

ORIGINAL PAGE
BLACK AND WHITE PHOTOGRAPH

FIGURE 20. - MICROSTRUCTURES OBSERVED IN A MA 754 ALLOY CREPT TO A STRAIN OF 2% AT 1033 K AND 221 MPa SHOWING EVIDENCE OF AN ATTRACTIVE DISLOCATION-PARTICLE INTERACTION AT THE POINTS INDICATED BY THE ARROWS (NARDONE, MATEJCZYK, AND TIEN, 1984) (REPRINTED WITH PERMISSION, PERGAMON JOURNALS LTD.).

ORIGINAL PAGE
BLACK AND WHITE PHOTOGRAPH

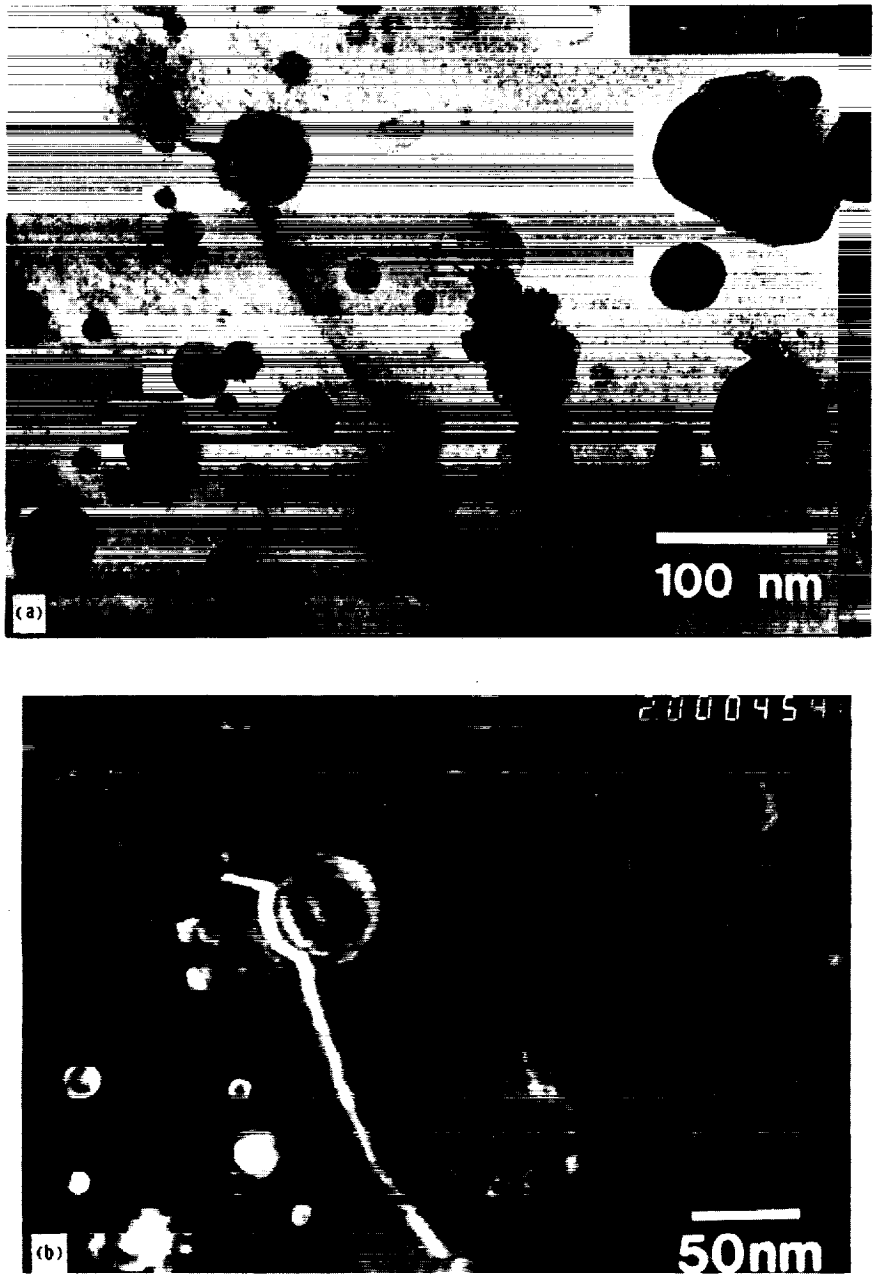

FIGURE 21. - (a) BRIGHT-FIELD AND (b) WEAK-BEAM IMAGES SHOWING DISLOCATION PARTICLE INTERACTION IN CREPT MA 6000 (SCHRODER AND ARTZ, 1985) (REPRINTED WITH PERMISSION, PERGAMON JOURNALS LTD.).

ORIGINAL PAGE
BLACK AND WHITE PHOTOGRAPH

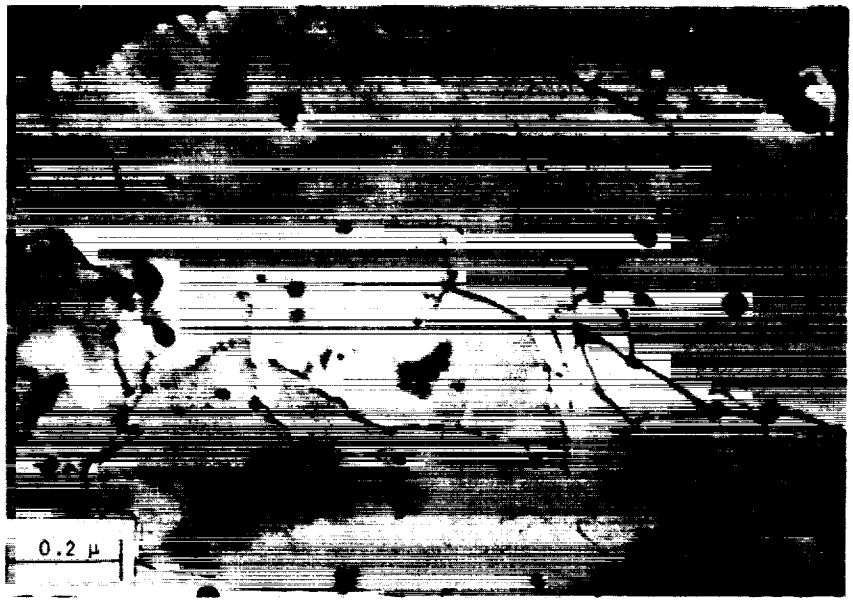

FIGURE 22. - MICROSTRUCTURE OF AN AS-RECEIVED Ni-1 vol % ThO_2 ALLOY SHOWING DISLOCATION PINNING BY THE DISPERSOIDS (WILCOX AND CLAUER, 1966b).

general, these models predict that the threshold stress is less than or equal to the Orowan stress with σ_{th} inversely proportional to λ or $(\lambda - d_p)$. In particular, the particle-dislocation interaction models proposed by Srolovitz *et al.*, (1982, 1983, 1984), Nardone, Matejczyk, and Tien (1984), and Artz and Wilkinson (1986), predict that the threshold stress is independent of the size and shape of the particle. In addition, the partial dislocation core relaxation models proposed by Nardone, Matejczyk, and Tien (1984), and Artz and Wilkinson (1986), suggest that σ_{th} can depend on the nature of the dispersoid matrix interface through the core relaxation parameter, k_r.

Despite the fact that the interparticle spacing is expected to influence the creep of dispersion-strengthened materials through its effect on the threshold stress, an examination of Table A.1 shows that this is not always the case even when the interparticle spacing is about the same for two materials. For example, it is seen that dispersion-strengthened silver alloys containing MgO dispersoids did not show a threshold stress behavior (Leverant, Lenel, and Ansell, 1966; and Nieh and Nix, 1979) despite the fact that the interparticle spacings in these materials were comparable or smaller than those reported in investigations where a threshold stress behavior was observed (Oliver and Nix, 1982; Lund and Nix, 1976; and Hausselt and Nix, 1977a). The reason for these variations is not understood at present, but could arise from a number of factors: processing techniques which result in differences in the uniformity of particle distribution and the degree of elongated grain morphology, differences in the dislocation-particle interaction brought about by the presence of different dispersoids or differences in the yield strength of the dispersoids. Nevertheless, these results appear to indicate that the threshold stress behavior is not solely dependent on the interparticle spacing.

Even in those instances where similar processing techniques have been employed and the interparticle spacing is more or less the same, differences in creep behavior have been observed. For example, considering the data on the 218 potassium-doped tungsten alloy strengthened by the presence of bubbles, two types of creep behavior have been reported (Table A.1). Pugh (1973) observed a threshold stress of about 69.0 MPa in a wire-drawn 218 alloy with an interparticle spacing of about 0.3 μm[8] and tested at 3000 K. Similar observations have been reported by Wright (1978), who suggested that the interaction between the dislocations and the bubbles is significant only when the grain aspect ratio is high (typically, GAR > 11) owing to the relative unimportance of grain boundary sliding in these microstructures. In comparison, Gaal, Harmat, and Füle (1983) did not observe any threshold stress behavior in this alloy under similar testing conditions despite a grain aspect ratio of about 15, and a similar interparticle spacing. Clearly, these observations cannot be rationalized entirely on the basis of an attractive interaction between the voids and dislocations in this material or due to differences in the amount of grain boundary sliding.

Finally, as shown in Fig. 18, the magnitude of the threshold stress for Zn-W alloy is less than that for the $ZnAl_2O_3$ material although the volume

[8]Estimated from the published micrograph.

fraction and the size of the dispersoids were quite similar for both alloys. As mentioned in Sec. 3.6, this observation may be attributed to differences in the deformation behavior of the dispersoids during creep. The possibility that dispersoids may deform by a nondiffusional mechanism during creep is examined in the next section.

4.2 Deformation of the Dispersoids During Creep

Modern theories of creep of dispersion-strengthened materials can be classified into (a) those involving local climb of portions of dislocation segments in close proximity to the particle-matrix interface (Brown and Ham, 1971; and Shewfelt and Brown, 1977); (b) those involving general climb of additional segments of the dislocation out of the glide plane (Lagneborg, 1973; and Hausselt and Nix, 1977 (b); and (c) those involving dislocation core relaxation at the dispersoid-matrix interface (Srolovitz *et al.*, 1982, 1983, 1984; Nardone, Matejczyk, and Tien, 1984; and Artz and Wilkinson, 1986). The climb models assume that the particle exerts a repulsive force on the dislocation so that the latter can only overcome the barrier by climbing over it. Typically, these models attribute the origin of the threshold stress to an increase in the dislocation line energy. On the other hand, the models involving dislocation core relaxation attribute the origin of the threshold stress to the attractive nature of the dislocation-particle interaction on the "departure" side of the dispersoid. Artz and Wilkinson (1986) examined the case when the dislocation core undergoes only partial relaxation at the interface, and showed that only a modest relaxation of about 6 percent is sufficient to ensure that dislocation detachment from the interface is more important than processes involving local climb.

A major assumption incorporated in these models is that the dispersoid does not deform during creep. Instead, the dislocation is assumed to be stationary or move slowly in the immediate vicinity of the particle, so that diffusional mechanisms become significant enough to permit dislocation climb over these obstacles with partial or total relaxation of the dislocation core at the dispersoid-matrix interface. Srolovitz *et al.* (1984) showed that the typical relaxation times, τ_r associated with interfacial and volume diffusion are extremely small in comparison to the usual duration of a creep experiment, so that the stress concentration at the particle-matrix interface can relax by a diffusion-controlled process. This results in an attractive interaction between the particle and the dislocation if the glide plane intersects the dispersoid thereby resulting in a complete delocalization of the dislocation core.

Although the diffusional relaxation times are shorter than the total duration of a creep experiment, this comparison may not be valid since it is the time required for the dislocation to traverse from particle, A, to another, B, that is important (Fig. 23). In many instances the dislocation velocity can be quite high and limited only by phonon damping in the matrix. These situations arise when a dislocation escapes from a solute atmosphere, a pinning particle, dislocation tangles or has been newly created (Srolovitz *et al.*, 1984). For the specific case of a dislocation escaping from a pinning

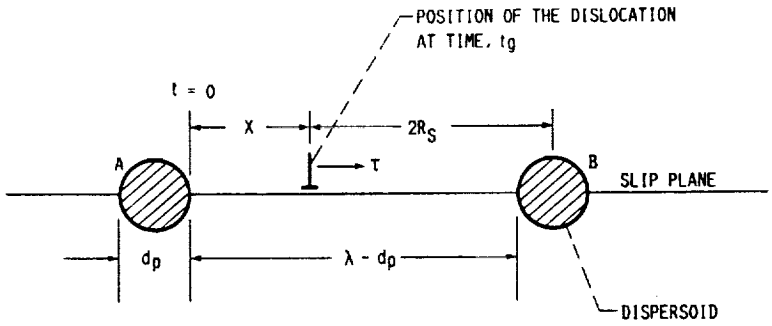

FIGURE 23. - POSITION OF A DISLOCATION AT TIME, t_g, AFTER IT HAS ESCAPED FROM A PARTICLE, A, AS IT TRAVELS AT A VERY HIGH VELOCITY TOWARDS THE DISPERSOID, B, UNDER THE ACTION OF A SHEAR STRESS, τ.

dispersoid, A, under the action of a shear stress, τ ($\approx \sigma/2$), the glide time, t_g, for the dislocation to traverse a certain distance, X, where $0 \leq X \leq (\lambda - d_p)$ (Fig. 23), would be insufficient to allow diffusional relaxation to occur. This is demonstrated in Fig. 24 for the specific geometrical configuration shown in Fig. 23, where the relaxation times for interfacial and volume diffusion in TD-Nichrome at 1200 K are compared with the times required for phonon drag-limited dislocation glide through two distances, and at two different stresses. The relaxation times associated with the reduction of the stress concentration at the particle-matrix interface by volume and interfacial diffusion were estimated for spherical particles from the equations given in the paper by Srolovitz *et al.*, (1984), and these estimates are based on the data tabulated by Frost and Ashby (1982).[9] The time for dislocation glide was estimated from

$$t_g = (X/v_g) \tag{16}$$

where the glide velocity, v_g, is by (Frost and Ashby, 1982)[10]

$$v_g = (\sigma b/2B_g(T)) \tag{17}$$

The drag coefficient, $B_g(T)$, was estimated to be about 4×10^{-4} Nt s m^2 at 1200 K. Typically, $\lambda \approx 10\ d_p$ for nickel base alloys, so that a value of $X = 5\ d_p$ is equal to about half the effective spacing between the particles. As shown in Fig. 24, the relaxation times for volume and interfacial diffusion are much larger than t_g when $d_p > 0.02\ \mu$m. The relaxation time for interfacial diffusion is comparable to t_g only for dispersoids smaller than 0.02 μm when $\sigma = 10$ MPa.

The above discussion assumes that the dislocation is not slowed down by interaction with other dislocations as it traverses from one particle to the next. This appears to be a reasonable assumption for dispersion-strengthened materials since the initial and the final microstructures generally contain little or no dislocations (Sec. 3.7). For example, Figs. 20 and 21 show that there is generally one dislocation visible between two adjacent dispersoids while in most other instances the interparticle spacing appears to be free of dislocations. The observations of Schröder and Artz (1985) also confirm this viewpoint. In this investigation, it was found that the dislocation density was sufficiently low to permit the interaction of single dislocations with the incoherent dispersoids in a MA 6000 alloy. However, the presence of immobile dislocations between adjacent particles can interact with a fast moving dislocation and slow it down sufficiently to permit processes, such as

---

[9]The interfacial diffusion coefficient was assumed to be equal to that for grain boundary diffusion.

[10]The back stress on the dislocation due to the particle has been ignored but this is expected to be significant only when the dislocation is at a distance of about d_p from the dispersoid.

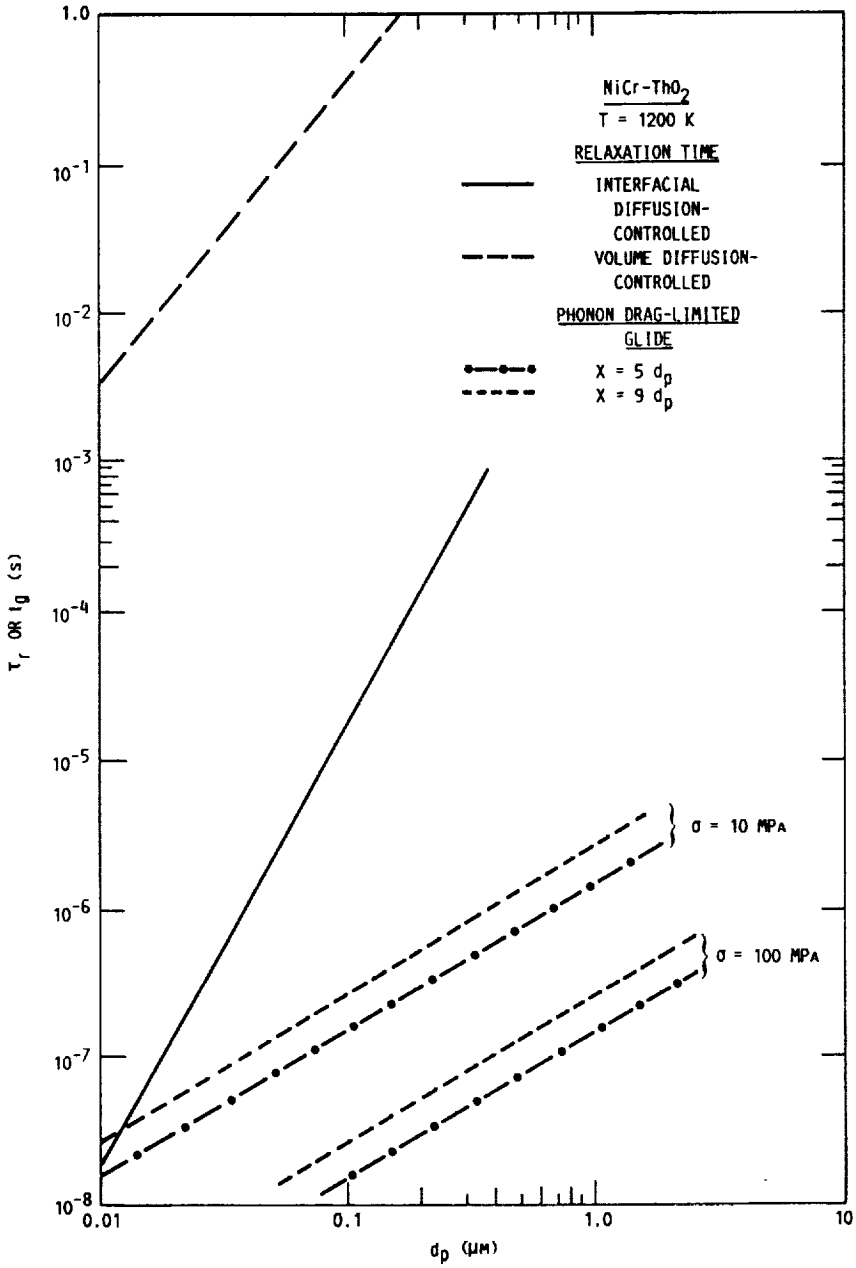

FIGURE 24. - VARIATION OF τ_r AND t_g WITH d_p FOR TWO VALUES OF X AND σ.

dislocation climb and dislocation core relaxation mechanisms to become important. In the following, the discussion is limited to the case where the fast moving dislocation is not slowed down.

In most investigations on NiCr-ThO_2 alloys, the experimental values of the average particle size and the applied stress were usually greater than 0.015 μm and 10.0 MPa, respectively, (Table A.1), so that Fig. 24 suggests that there is insufficient time to allow any diffusional relaxation of the stresses at the particle-matrix interface. In the absence of diffusional relaxation, interfacial slip would be insignificant, and the stress concentration on the dispersoid owing to the combined effects of the applied stress and the dislocation would increase as the latter approaches the particle. Under these conditions, the stresses at the particle-matrix interface could be sufficiently high to deform the particle. This would occur when the stress acting on the dispersoid exceeds its microscopic yield stress, σ_Y, which would be determined by the defect concentration in the particle and at its surface in the interface.

It is expected that the dislocation structure inside extremely small dispersoids would anneal out so that the yield strength of such particles should approach the theoretical limit. This would be the case when the particle surface at its interface with the matrix is defect free so that the stress required to deform the dispersoid would be about $G_p/30$, where G_p is the shear modulus of the dispersoid. However, it is more likely that the complex techniques used in processing these alloys introduce defects at the particle surface so that the stress required to deform it would be less than $G_p/30$. In addition, larger particles could also contain defects in the interior which would also reduce their microscopic yield strength below the theoretical value. Therefore, in any attempt to establish whether the particles deform during creep of dispersion-strengthened materials, it is necessary to estimate the magnitude of σ_Y and to characterize the microstructure of the dispersoids after deformation. One approach is to assume that σ_Y equals about $0.5\ G_p b(\rho_s)^{1/2}$, where ρ_s is the average density of dislocation sources in a dispersoid, but since measurements of ρ_s in particles with a diameter of about 0.02 μm are difficult to make in practice, there is a large uncertainty with this method. A second approach is to simply assume that $\sigma_Y \approx G_p/1000$ (Ansell, 1968) although there is no certainty that this assumption is valid in practice as it requires that the yield strength of the dispersoid be equal to its bulk properties. However, in the absence of a more reliable method of assessing the magnitude of the microscopic yield strength of the particle, the following discussion is based on the assumption that $\sigma_Y = G_p/1000$.

The maximum normal stress, σ_p, acting on the particle due to a dislocation is given by Oliver and Nix (1982)[11]

$$\sigma_p = (2G_{Mb}/\pi)[1 + (G_p - G_M)/(G_M + G_p)][1/(2R_s - d_p)] \quad (18)$$

where G_M is the shear modulus of the matrix, and $2R_s$ is the distance of interaction between the center of the dispersoid, B, and the approaching dislocation (Fig. 23). The variation of σ_p, normalized by $[(2G_Mb/\pi d_p)\{1 + (G_p - G_M)/(G_p + G_M)\}]$, is plotted against $2R_s/d_p$ in Fig. 25. The particle yield stresses were assumed to be about $G_p/1000$, and these are indicated by the horizontal broken line in the figure. The normalized values of σ_y shown in Fig. 25 were calculated for d_p = 0.015, 0.02, and 0.02 μm for Al-Al_2O_3, Ni-ThO_2, and Ni-Y_2O_3, respectively, and using G_{Al} = 1.6×10^4 MPa, $G_{Al_2O_3}$ = 1.5×10^5 MPa, G_{Ni} = 5.5×10^4 MPa, G_{ThO_2} = 9.2×10^4 MPa, and $G_{Y_2O_3}$ = 5.8×10^4 MPa. Figure 25 indicates that the Al_2O_3 particles in aluminum can deform only when $2R_s/d_p \lesssim 3$. Similarly, particle deformation in Ni-ThO_2 and Ni-Y_2O_3 alloys can occur when $2R_s/d_p$ is less than about 7 and 9, respectively. It is appropriate at this stage to pose two questions: Are these values of $2R_s/d_p$ achieved in practice which would indicate that particle deformation is a genuine possibility? Does the threshold stress associated with a dispersion-strengthened alloy represent the average microscopic yield strength of the particles?

Two factors suggest that these questions may be important in understanding the creep behavior of dispersion-strengthened materials. First, noting that the maximum value of $2R_s$ represents the interparticle spacing, an examination of the experimental data on aluminum and nickel-base alloys, which exhibited a threshold stress, suggests that the magnitudes of λ/d_p are generally comparable with the critical values of $2R_s/d_p$ required for particle deformation. For example, Oliver and Nix (1982) observed a threshold stress behavior in an Al-Al_2O_3 alloy with a $(2R_s)_{max}/d_p \approx \lambda/d_p \approx 4$. Similarly, threshold stresses are generally observed in nickel-based alloys with $\lambda/d_p \approx 10$. It is noted that these values of λ/d_p are greater than the critical values of $2R_s/d_p$ discussed above so that it can be concluded that the dispersoid, B, in Fig. 23 begins to deform when the dislocation is more than half the interparticle spacing from it. Second, the magnitudes of σ_p and σ_{th} are comparable for aluminum and nickel base dispersion-strengthened alloys. This is shown in Figs. 26 and 27, where the magnitudes of σ_p/G_M calculated from equation (18) are shown as a function of $(2R_s - d_p)$, while the experimental values of σ_{th}/G_M are plotted against $(\lambda - d_p)$. As shown in Figs. 26 and 27, σ_p/G_M and σ_{th}/G_M are in agreement with each other to within a factor of three. Therefore, it is concluded that particle deformation remains a genuine possibility in these alloys. It is now instructive to examine the case when

[11]Equation (18) represents a modified form of the original expression given by Oliver and Nix (1982). The elastic modulii terms have been interchanged to reflect the fact that $G_p > G_M$ for a hard particle. It is also assumed that $\sigma_p = 2\tau_p$, and it is noted that G_M is used instead of G in the normalization of the experimental data.

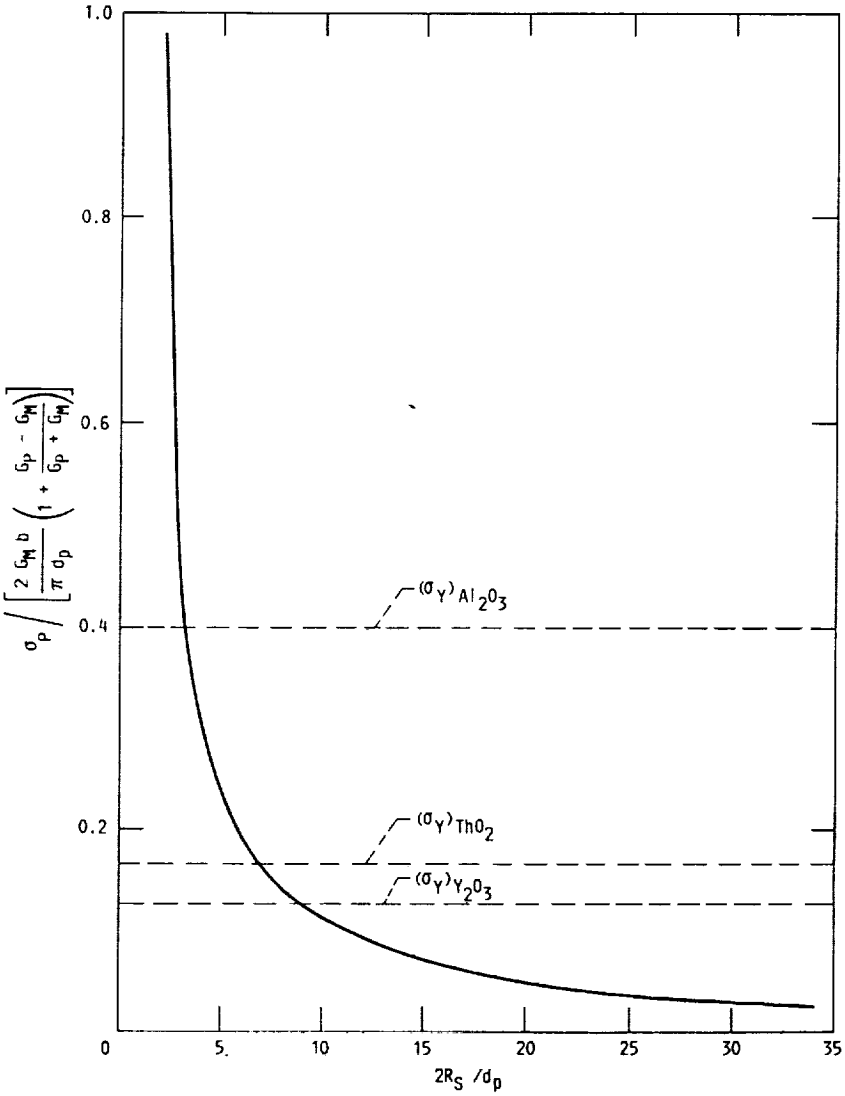

FIGURE 25. - VARIATION OF THE STRESS ON A PARTICLE, NORMALIZED ACCORDING TO EQUATION (18), WITH $2R_S/d_p$. THE HORIZONTAL BROKEN LINES INDICATE THE NORMALIZED VALUES OF $\sigma_Y \approx G_p/1000$ FOR Al_2O_3, ThO_2 AND Y_2O_3.

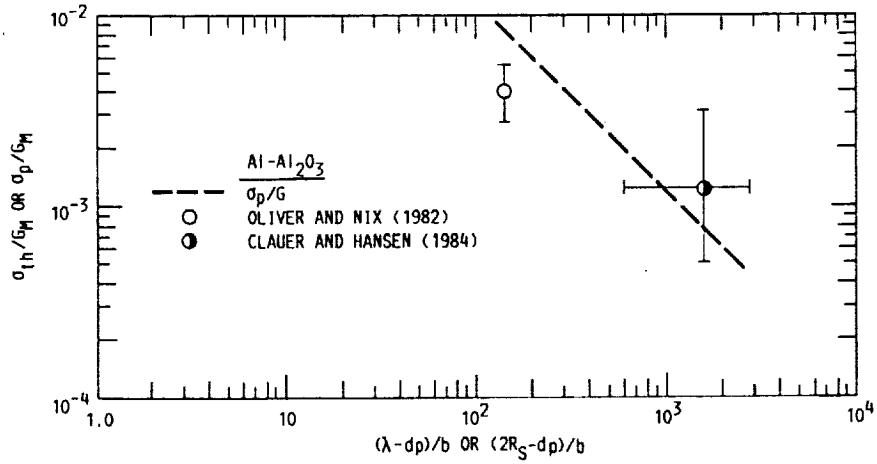

FIGURE 26. - VARIATION OF σ_p/G_M AGAINST $(2R_S-d_p)/b$ AND σ_{th}/G AGAINST $(\lambda-d_p)/b$ FOR Al-Al_2O_3 ALLOYS (OLIVER AND NIX, 1982; CLAUER AND HANSEN, 1984).

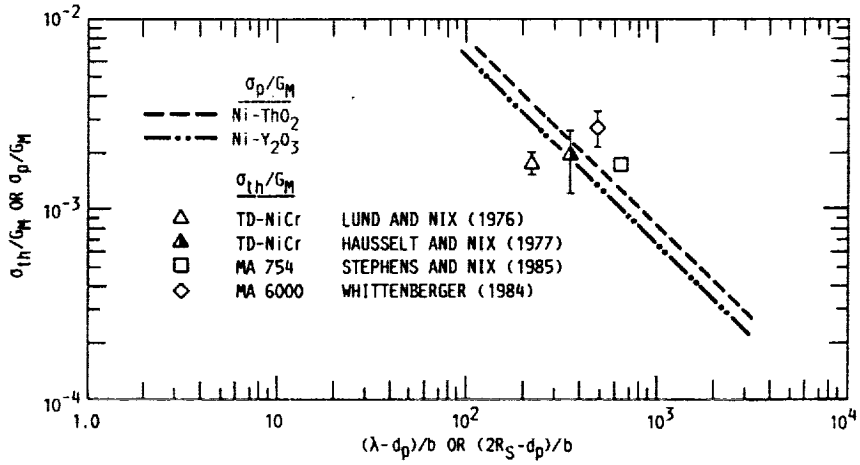

FIGURE 27. - VARIATION OF σ_p/G_M AGAINST $(2R_S-d_p)/b$ AND σ_{th}/G AGAINST $(\lambda-d_p)/b$ FOR DISPERSION-STRENGTHENED NICKEL ALLOYS (LUND AND NIX, 1976; HAUSSELT AND NIX, 1977; WHITTENBERGER, 1984; STEPHENS AND NIX, 1985).

particle deformation governs the creep behavior of these materials and its contribution to the creep threshold stress.

Oliver and Nix (1982) assumed that the oxide particle deforms by Nabarro-Herring creep owing to a low oxygen partial pressure at the dispersoid-matrix interface and a correspondingly high defect concentration in the oxide. This rationalization appears to be improbable owing to the higher stresses acting on the dispersoids. This viewpoint is supported by the lack of complete agreement between the apparent activation energies for creep of the dispersion-strengthened alloys and those for intrinsic diffusion of the slowest moving species in the dispersoids (Table II).

The above comparison between the activation energies for creep and diffusion also suggests that the deformation of the dispersoids is not controlled by dislocation climb. In the absence of these diffusion-controlled mechanisms, it follows that the deformation of the particles must involve some other dislocation mechanism such as dislocation generation from sources surfaces of the dispersoids. The threshold stress can then be identified with σ_Y so that the additive rule given by equation (14) can be expressed as

$$\left[(\sigma/G)_{alloy}\right] \dot{\varepsilon}_{/D} = \left[(\sigma/G_M)_{Matrix}\right] \dot{\varepsilon}_{/D} + \left[(\sigma_Y/G_P)_{Particle}\right] \dot{\varepsilon}_{/D} \qquad (19)$$

Equation (19) represents a "composite" approach in describing the creep behavior of dispersion-strengthened alloys. The physical significance of equation (19) lies in the fact that the deformation of the matrix and the dispersoids are coupled, so that as the dislocation approaches the dispersoid, B, in Fig. 23, the load is increasingly taken up by the particle. Assuming that the stress due to the dislocation is taken up entirely by the matrix when $\sigma > \sigma_{OR}$ and by the particles when $\sigma < \sigma_{OR}$, equation (19) can be represented schematically as shown in Fig. 28.[12] The deformation of the particle and the matrix occurs sequentially, and exponential creep is expected to be dominant when $\sigma > \sigma_{PLB}$. Below the Orowan stress, the deformation of the dispersion-strengthened material will be determined by the creep of the dispersoid, while above the Orowan stress, the deformation of the matrix would determine the creep behavior of the alloy. In the absence of other creep mechanisms (e.g., grain boundary sliding and diffusion creep), Fig. 28 suggests that the threshold stress would lie between σ_{PLB} and σ_{OR}, so that these define the limits of σ_{th} for dislocation creep. The average value of σ_{PLB}/G for pure f.c.c. metals is about 5×10^{-4} (Fig. 1) (Raj, 1986), and the experimental magnitudes of σ_{th}/G exceed this value for most dispersion-strengthened materials (Fig. 15). Thus, the maximum allowable interparticle spacing for observing threshold stress behavior can be estimated from

$$\lambda = \alpha b (G/\sigma)_{PLB} \qquad (20)$$

where α is a constant varying between 0.5 and 1.0. Therefore, the critical interparticle spacing would vary between about 0.3 and 0.5 μm corresponding to

[12]The values of the normalized creep rates given in the figure have no special significance.

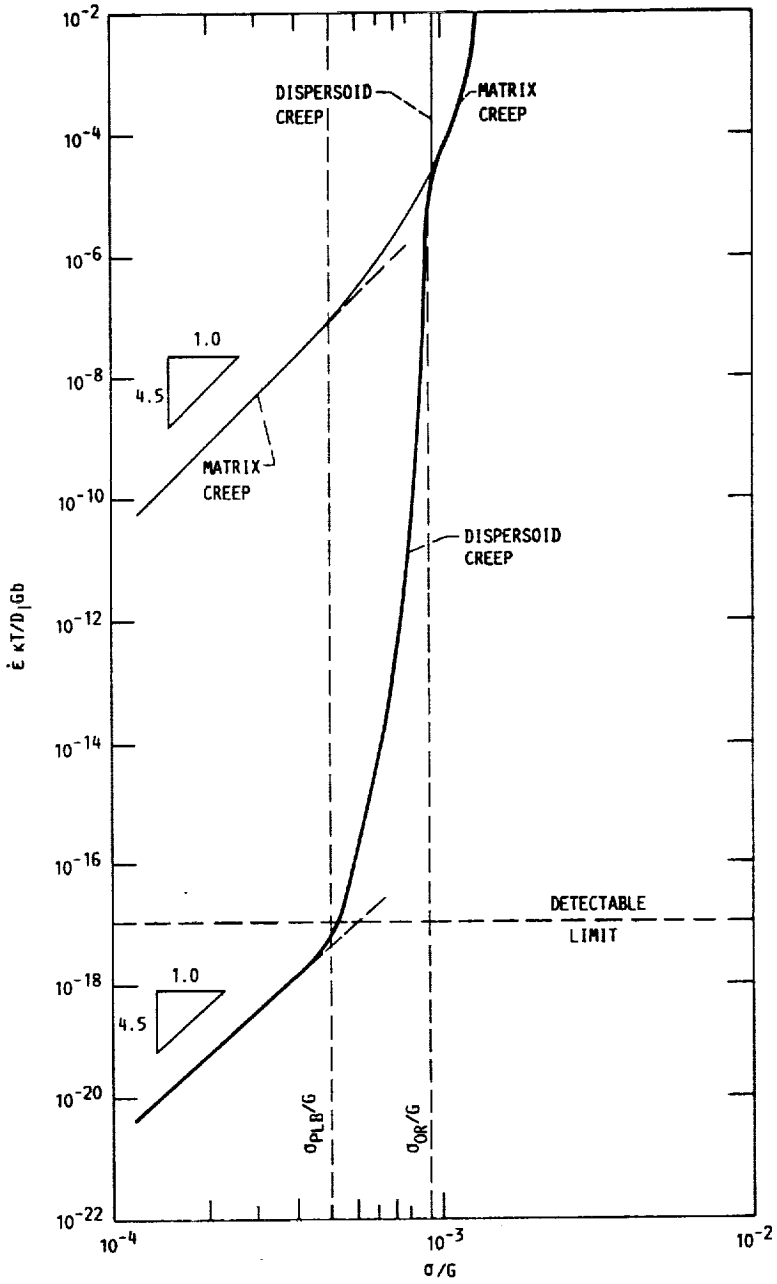

FIGURE 28. - SCHEMATIC PLOT OF $\dot{\varepsilon}kT/D_1Gb$ VERSUS σ/G SHOWING THE CONTRIBUTION OF MATRIX AND PARTICLE DEFORMATION TO THE TOTAL CREEP STRENGTH. THE DEFORMATION OF THE MATRIX AND THE PARTICLE ARE ASSUMED TO BE COUPLED, AND EXPONENTIAL CREEP OCCURS ABOVE σ_{PLB}/G. THE CREEP OF THE DISPERSOID IS IMPORTANT IN THE REGION $\sigma_{PLB}/G < \sigma/G < \sigma_{OR}/G$, WHILE MATRIX DEFORMATION DOMINATES WHEN $\sigma/G > \sigma_{OR}/G$. THE BOLD LINE REPRESENTS THE OBSERVED VARIATION OF THE NORMALIZED CREEP RATE WITH NORMALIZED STRESS FOR THE DISPERSION-STRENGTHENED ALLOY.

$\lambda/b \approx 1000$ and 2000, respectively. If the particle spacing exceeds these values, the threshold stress behavior due to particle deformation would not be observed, and the coupling of the matrix and particle deformation processes would not be applicable. As shown in Fig. 15, λ/b is less than 2000 for most engineering alloys which exhibit dislocation threshold stress behavior.

4.3 Contribution to the Threshold Stress from Different Mechanisms

At a distance of about d_p from the particle-matrix interface when the back stress due to the dispersoid is significant, the dislocation can slow down considerably to allow climb and detachment-controlled mechanisms to become important. Two types of detachment-controlled mechanisms have been proposed. Srolovitz *et al.* (1982, 1983, and 1984) considered the case where the dislocation core relaxes completely into the interface as a result of interfacial slip so that a particle essentially behaves as a void. On the other hand, Nardone, Matejczyk and Tien (1984), and Artz and Wilkinson (1986), suggested the possibility of a partial relaxation of the dislocation core at the interface as local segments climb around the dispersoid. The stress required to detach the dislocation from the interface at the "departure" side of the dispersoid can be calculated for the latter conditions based on the assumption that the dislocation line energy decreases by a factor of k_r at the particle-matrix interface over that in the matrix. In comparison, the classical local climb-controlled mechanisms do not account for the reduction in the line energy.

It is now instructive to examine the extent to which local climb, detachment-controlled, and the particle deformation mechanisms contribute to the threshold stress. In the absence of particle deformation, Artz and Wilkinson (1986), and Artz (1991), showed that the dislocation core need only relax by about 6 percent for the detachment-controlled process to become important. However, when particle deformation occurs, the difference in the shear moduli of the dispersoid and the matrix must also be considered.

This is shown in Fig. 29, where σ_p, estimated from equation (18) for $2R_s >> d_p$ and normalized by $(G_M b/2R_s)$, is plotted against the relaxation parameter, k_r, employed in the Artz-Wilkinson model (Artz and Wilkinson, 1986; and Artz, 1991). These normalized values of σ_p, which were calculated for three matrix-dispersoid combinations, reflect the fact that differences in the shear moduli between the particle and the matrix would play an important role in determining the creep behavior of these alloys. A value of $k_r = 1$ signifies complete repulsion, while $k_r = 0$ indicates complete attraction between the particle and the dislocation. The predicted values of the threshold stresses, normalized by $(G_M b/\lambda)$, for detachment- and local climb-controlled mechanisms are also plotted against k_r in Fig. 29 using the relations used by Artz and Wilkinson (1986). The conditions for which one of these mechanisms would be important can be identified through a comparison of the predicted threshold strengths assuming that $\sigma_p = \sigma_Y$ with the threshold stress for the dominant mechanism being the largest.

Figure 29 shows that local climb of dislocation segments does not contribute significantly to the threshold stress in comparison to the particle

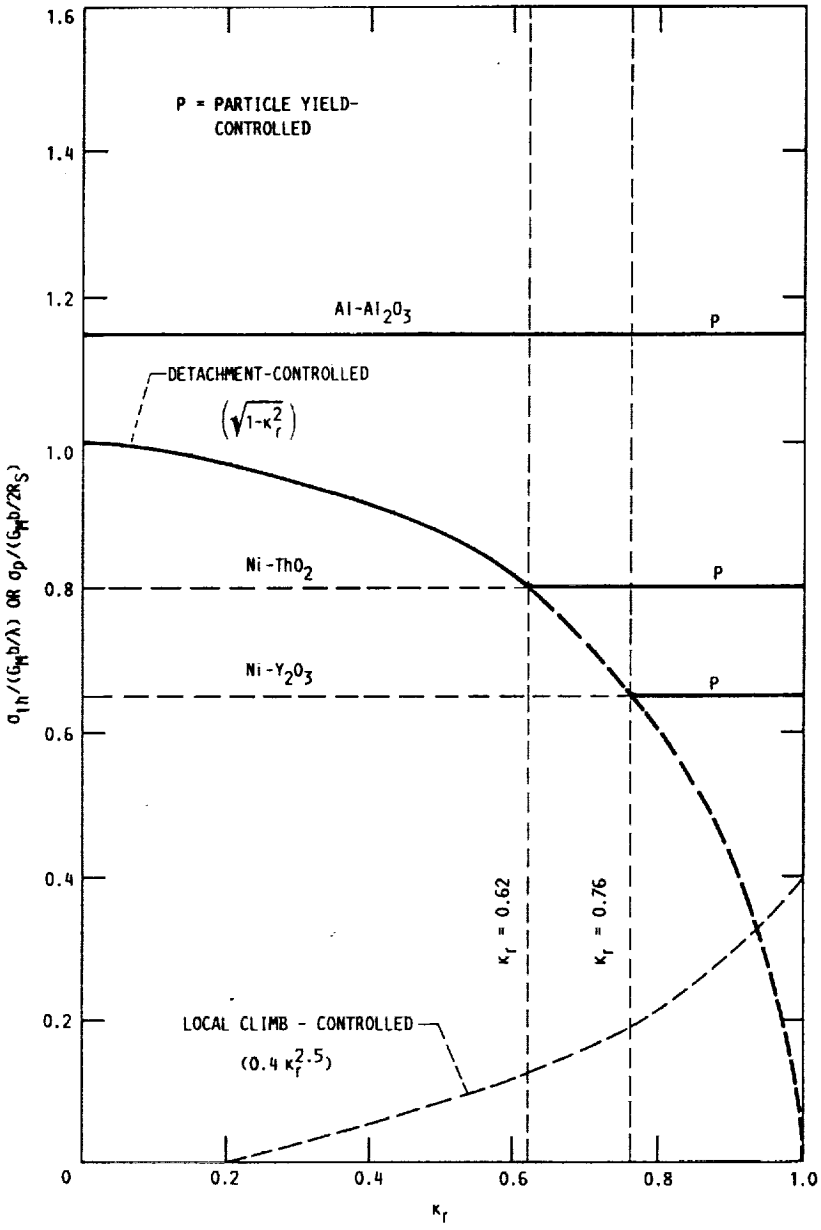

FIGURE 29. - PLOT OF $[\sigma_p/(G_M b/2R_S)]$ AND $[\sigma_{th}/(G_M b/\lambda)]$ AGAINST k_r. THE HORIZONTAL LINES INDICATE THE NORMALIZED VALUES OF σ_p FOR THREE MATRIX-DISPERSOID COMBINATIONS. THE EQUATIONS USED FOR ESTIMATING THE MAGNITUDES OF σ_{th} FOR THE DETACHMENT-CONTROLLED AND THE LOCAL CLIMB PROCESSES ARE THOSE USED BY ARTZ AND WILKINSON (1986).

yield- and the detachment-controlled mechanisms. The threshold stress behavior of the Al-Al_2O_3 alloys is expected to be determined entirely by the yield properties of alumina. On the other hand, the threshold properties of nickel-based alloys containing ThO_2 or Y_2O_3 is determined by the particle yield strength only if the dislocation core relaxation at the interface is less than about 40 and 25 percent, respectively. The extent of dislocation core relaxation must exceed these values for the detachment mechanism to control the threshold stress. This requirement is larger than that suggested by Artz and Wilkinson (1986) but it is still smaller than that predicted by the model proposed by Srolovitz *et al.* (1982, 1983, 1984). Figure 29 predicts that the critical value of the relaxation parameter governing the transition from the particle yield-controlled to the detachment-dominated mechanism is dependent on the relative magnitudes of G_M and G_p. The importance of the particle yield mechanism increases with G_p/G_M, and this can have important implications in the design of new dispersion-strengthened alloys. For example, the threshold stress is expected to be determined mainly by the detachment-controlled mechanism in bubble-strengthened materials since $G_p = 0$ and $\sigma_p = 0$ in equation (18).

Therefore, based on the discussion in this section, three parameters are identified which are expected to determine the strength of dispersion-strengthened alloys. First, materials containing dispersoids with $G_p >> G_M$ are expected to have a high threshold stress determined by the yield strength of the dispersoid, e.g., Al-Al_2O_3 alloys. Therefore, the strength of the dispersion-strengthened material would depend on the relative strengths of the matrix and the dispersoid. Second, the threshold stress appears to be governed by the particle yield strength in alloys with $\lambda/d_p \lesssim 10$ in the absence of considerable dislocation core relaxation. Third, the deformation processes occurring in the matrix and the particle can be coupled only when $\lambda/b \lesssim 2000$.

5.0 THE EFFECT OF GRAIN BOUNDARIES ON THE CREEP AND FRACTURE OF DISPERSION-STRENGTHENED MATERIALS

In the previous sections, the role of grain boundaries on the creep behavior of dispersion-strengthened materials was ignored. However, it is now fairly well-established that the grain size and the grain aspect ratio can have a considerable influence on the threshold stress and the fracture behavior of these materials. This is demonstrated in Fig. 30 for TD-Nichrome (Lin and Sherby, 1981), where the creep rate for the coarse-grained alloy decreases more sharply than for the fine-grained material when $\sigma/E < 10^{-3}$. This indicates that single crystals and coarse-grained materials are stronger than those with a smaller grain size, and this conclusion is confirmed by the observations of Kane and Ebert (1976) shown in Fig. 31. This decrease in creep strength with decreasing grain size can be attributed to the increasing importance of grain boundary sliding.

Wilcox and Clauer (1966a) first suggested that grain boundary sliding contributes significantly to the deformation of TD-Nickel. In a later investigation, they (Wilcox and Clauer, 1972) demonstrated that the yield, creep, and rupture strengths of several dispersion-strengthened alloys increased with

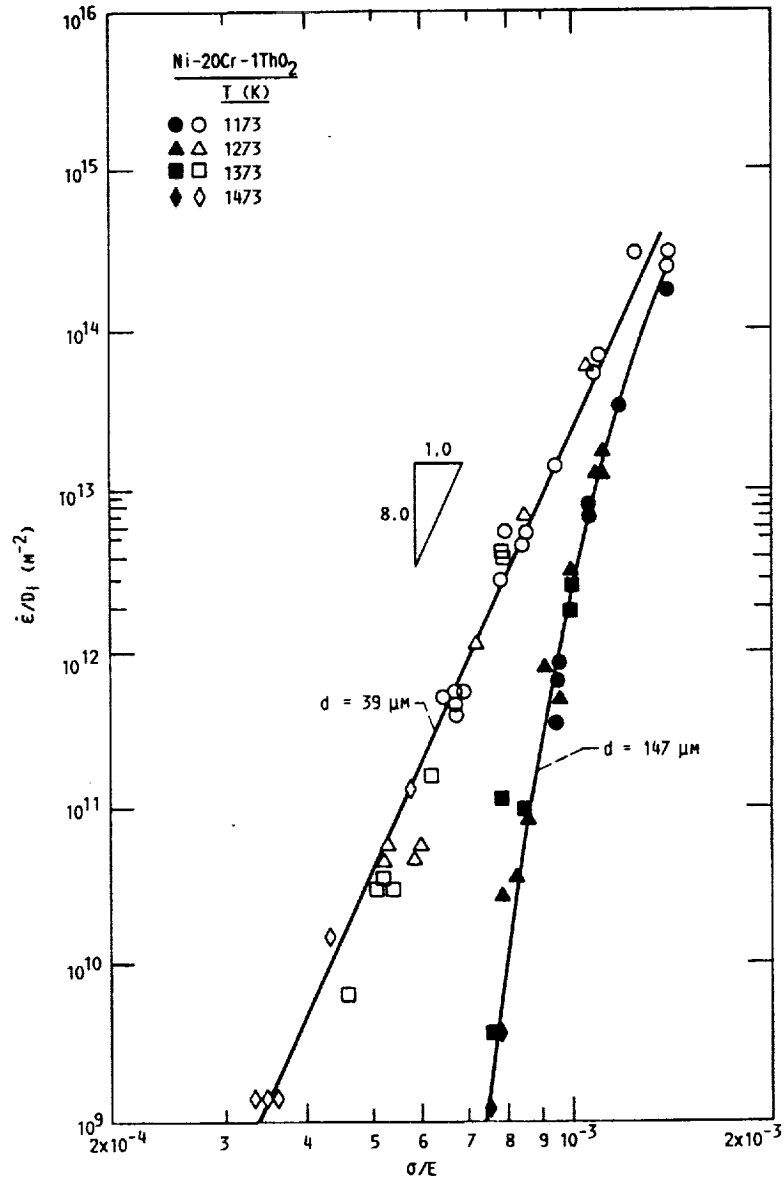

FIGURE 30. - VARIATION OF $\dot{\varepsilon}/D_\ell$ WITH σ/E FOR COARSE (d = 147 μm) AND FINE-GRAINED (d = 39 μm) TD-NICHROME (LIN AND SHERBY, 1981) (COURTESY ELSEVIER APPLIED SCIENCE PUBLISHERS).

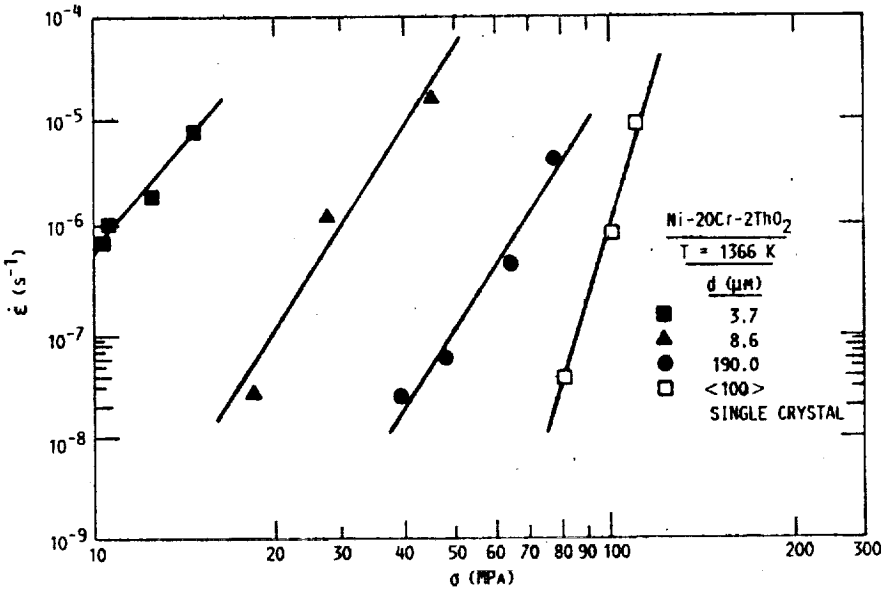

FIGURE 31. - EFFECT OF GRAIN SIZE ON THE CREEP BEHAVIOR OF TD-NICHROME (KANE AND EBERT, 1976).

an increase in the grain aspect ratio (Fig. 32). These results were attributed to a lower tendency for sliding in microstructures containing elongated grains than in those where the grains were relatively equiaxed.

In an important observation, Whittenberger (1977) reported that the experimental threshold stresses correlated extremely well with the grain aspect ratio[13] for several dispersion-strengthened nickel base alloys (Fig. 33). The increase in σ_{th} with the grain aspect ratio (Fig. 33) can be also attributed to a decrease in the amount of grain boundary sliding. Similar observations were also reported by Lin and Sherby (1981). This observed variation of σ_{th} with the grain aspect ratio is relevant in the thermomechanical processing of complex alloys, such as MA 754 and MA 6000, which result in the development of long, elongated, and recrystallized grains several millimeters in length. Interestingly, recrystallization does not always lead to the observation of a threshold stress behavior, especially in the simpler alloy systems (Table A.1). This may be due to the presence of an equiaxed recrystallized microstructure which does not slow down the rate of grain boundary sliding in these materials. Additionally, as discussed in Sec. 4.1, discrepancies also exist in the observations of Pugh (1973), and Gaal, Harmat, and Füle (1983), on potassium-doped, void-strengthened 218 tungsten alloy. The grain aspect ratios in these two investigations were 10 and 15, respectively, and the observed differences in the creep behavior of this alloy cannot be rationalized on the basis of the decreasing importance of grain boundary sliding with an increase in the grain aspect ratio as suggested by Wright (1978).

The decrease in the rate of grain boundary sliding with an increase in the grain aspect ratio, and the corresponding increase in the magnitude of the threshold stress, results in an improvement in the rupture life owing to a change in the fracture path from intergranular to transgranular fracture (Fig. 34). Similar observations have been also reported by Artz and Singer (1984) on a MA 6000 alloy, and they rationalized their observations on the basis of a grain boundary sliding-controlled cavitation model.

The Artz-Singer model (Artz and Singer, 1984) assumes that cavity growth on grain boundaries transverse to the stress axis leads to grain separation along the longitudinal direction and develops local incompatibilities between neighboring grains (Fig. 35). These incompatibilities are assumed to be accommodated by grain boundary sliding along the longitudinal grain boundaries. Thus, the predicted strain rate associated with cavity growth coupled with grain boundary sliding is given by

$$\dot{\varepsilon} = \left(\beta\delta D_{gb}\Omega/kTh^2L_1\right)\left[(\sigma - \sigma_c - \sigma_{gb}GAR) \Big/ \left(\left\{1_c/h\right\}^2 + 2\ GAR\right)\right] \qquad (21)$$

where β is a constant equal to about 10, δ is the grain boundary width, D_{gb} is the grain boundary diffusion coefficient, Ω is the atomic volume, h is the average height of grain boundary steps or serrations, L_1 is the grain

[13]The grain aspect ratio was defined with respect to the testing direction in this investigation.

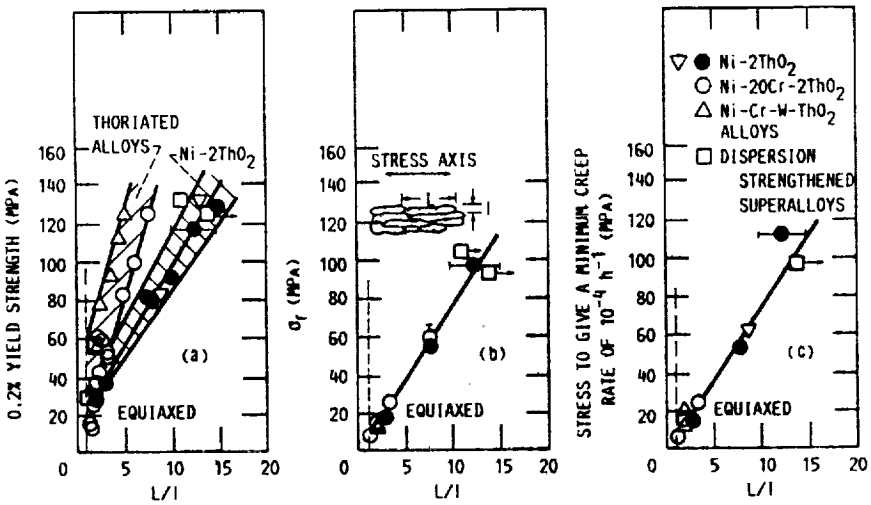

FIGURE 32. - EFFECT OF GRAIN ASPECT RATIO ON THE (a) 0.2% YIELD STRENGTH, (b) 100 h RUPTURE STRENGTH, AND (c) STRESS TO GIVE A MINIMUM CREEP RATE OF 2.8×10^{-4} h^{-1} IN DISPERSION-STRENGTHENED NICKEL ALLOYS TESTED AT 1366 K. THE OPEN AND CLOSED POINTS REPRESENT ALLOYS WITH RECRYSTALLIZED AND NONRECRYSTALLIZED MICROSTRUCTURES, RESPECTIVELY (WILCOX AND CLAUER, 1972) (REPRINTED WITH PERMISSION, PERGAMON JOURNALS LTD.).

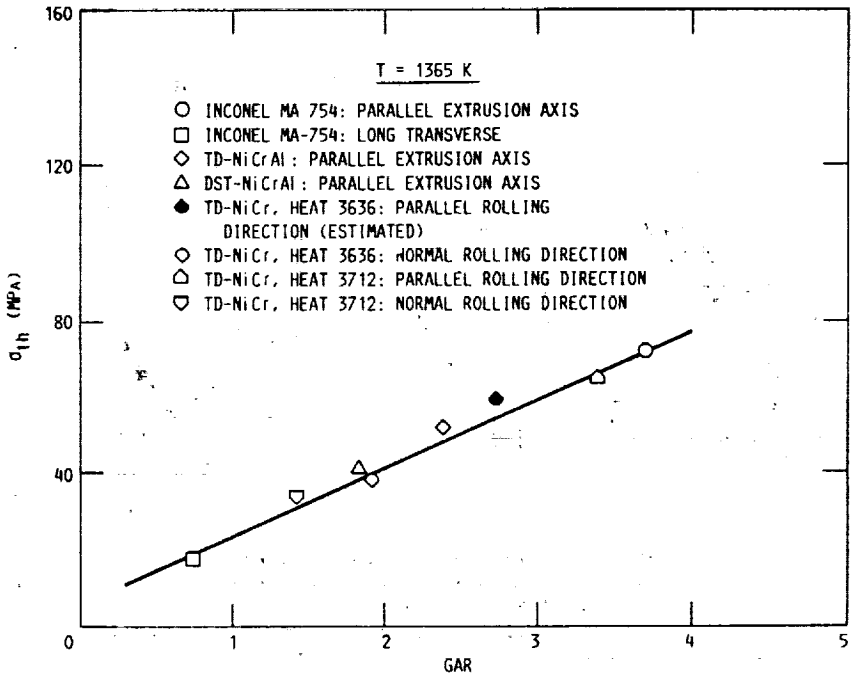

FIGURE 33. - VARIATION OF THE EXPERIMENTAL THRESHOLD STRESS OBTAINED AT 1365 K WITH THE GRAIN ASPECT RATIO FOR SEVERAL COARSE-GRAINED DISPERSION-STRENGTHENED NICKEL ALLOYS (WHITTENBERGER, 1977) (COURTESY AMERICAN SOCIETY FOR METALS).

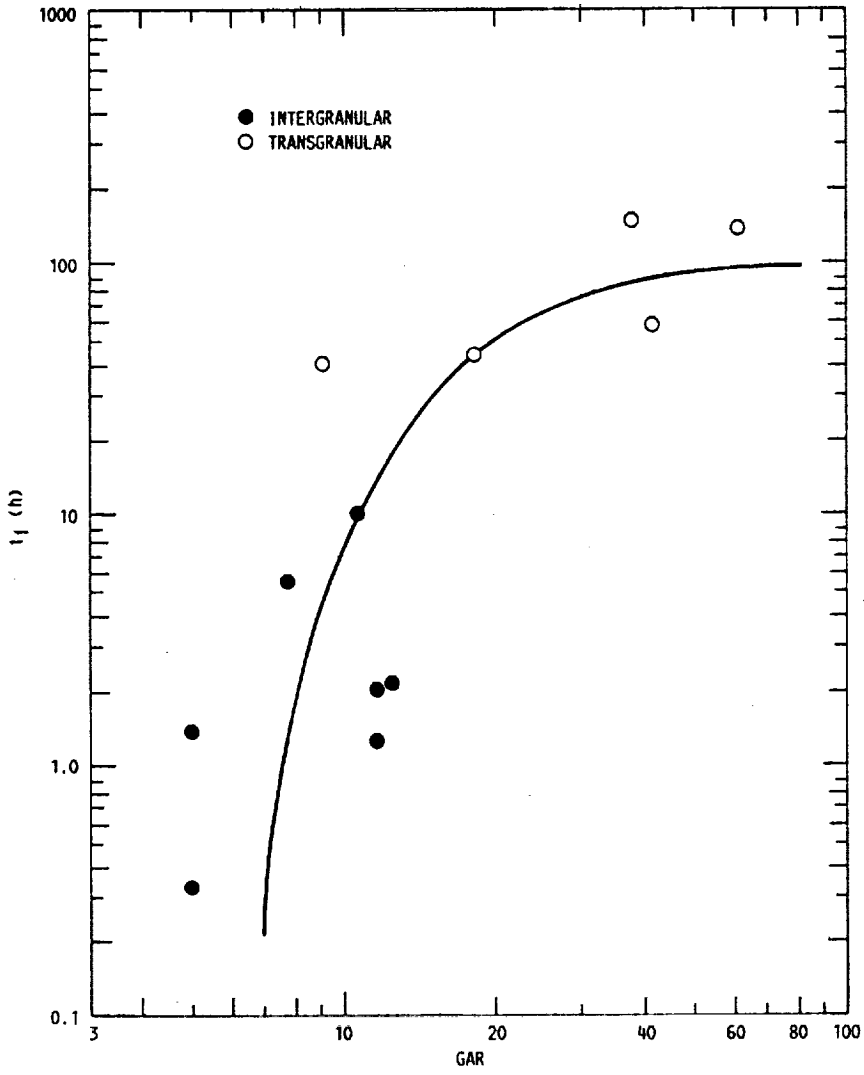

FIGURE 34. - EFFECT OF GRAIN ASPECT RATIO ON RUPTURE LIFE AND FRACTURE MODE IN A MA 6000 ALLOY (SINGER, BENN, AND KANG, 1983) (COURTESY INCO ALLOYS INTERNATIONAL).

ARTZ - SINGER MODEL

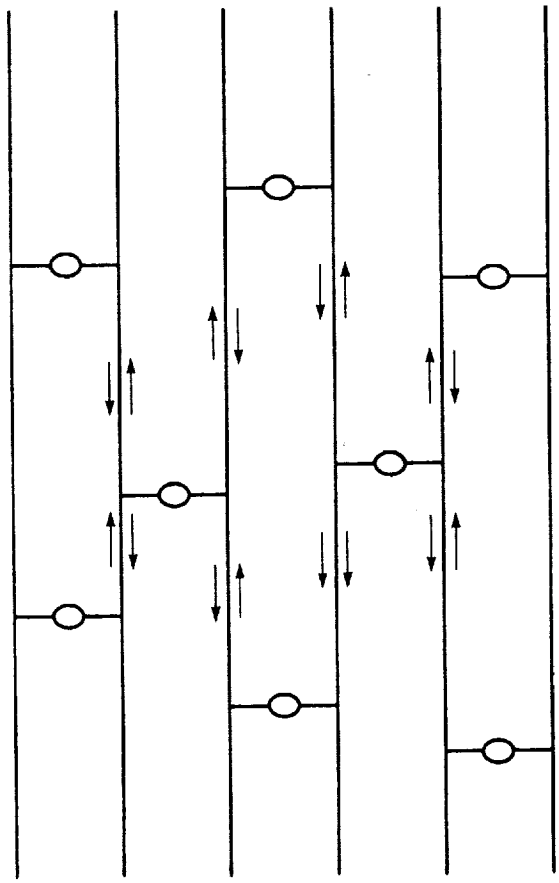

FIGURE 35. - SCHEMATIC REPRESENTATION OF THE ARTZ-SINGER MODEL. CAVITY GROWTH ON THE TRANSVERSE GRAIN BOUNDARIES LEADS TO INCOMPATIBILITY BETWEEN NEIGHBORING GRAINS, AND THESE ARE ELIMINATED BY GRAIN BOUNDARY SLIDING ALONG THE LONGITUDINAL GRAIN BOUNDARIES (ARTZ AND SINGER, 1984) (REPRINTED WITH PERMISSION FROM THE METALLURGICAL SOCIETY, AIME).

diameter in the longitudinal direction, σ_c and σ_{gb} are the threshold stresses for cavity growth and grain boundary sliding, respectively, and l_c is the planar spacing of the cavities in the transverse grain boundaries. The grain aspect ratio used in equation (21) is similar to the definition given in appendix A.1.0. Artz and Singer (1984) suggested that the condition $(l_c/h)^2 >> 2$ GAR corresponds to an equiaxed grain morphology, few cavity nuclei, and smooth grain boundaries, and cavity growth would not be affected by grain boundary sliding. However, when $(l_c/h)^2 << 2$ GAR, corresponding to elongated grains, many cavities, and serrated grain boundaries, the cavity growth would be controlled by accommodated grain boundary sliding. This condition predicts a fracture life, t_f, given by equation (22)

$$t_f = [kTh^2 l_c GAR/\delta D_{gb}\Omega(\sigma - \sigma_c - \sigma_{gb}GAR)] \tag{22}$$

The Artz-Singer model (Artz and Singer, 1984) specifically assumed that the applied stress is distributed between that required for continued cavity growth and that causing grain boundary sliding. Two alternative models proposed by Stephens and Nix (1986) consider the cases when cavity growth can be accommodated by power-law creep of the adjoining grains or by grain boundary sliding owing to the presence of fine grains interspersed along the longitudinal boundaries of coarser, elongated grains. This approach is more realistic than the simpler model proposed by Artz and Singer (1984) partly because it considers a duplex microstructure, and partly because it recognizes the difficulties associated with sliding along the grain boundaries of elongated grains. In this case, the Stephens-Nix model (Stephens and Nix, 1986) requires that the applied stress be distributed equally between the grain interior and the transverse grain boundaries.

For the case when the dispersion-strengthened alloy has a duplex microstructure of fine, equiaxed grains, which permit grain boundary sliding to occur easily, and coarse, elongated grains which do not slide past each other, the predicted creep rate is

$$\dot{\varepsilon}_{coupled} = [80\, D_l w_f \Omega/kT(d_f)^2 L_l] \times [\sigma - (1 - f_c)\sigma_o/\{10\pi h_c w_f k_f/(d_f)\}^2 + GAR] \tag{23}$$

where w_f is the width of the equiaxed fine grain pockets comprised of grains of size, d_c, f_c the a real fraction of the grain boundaries that are cavitated, σ_o' is the cavity sintering stress, h_c is the volumetric aspect ratio of the cavity, and

$$k_f = [\ln(1/f_c) - 0.5(3 - f_c)(1 - f_c)] \tag{25}$$

Equation (23) must be considered as an upper bound since the model assumes that all longitudinal grain boundaries contain pockets of fine grains.

An examination of equations (21) and (23) shows that mechanisms involving the accommodation of cavity growth by grain boundary sliding result in a stress exponent of unity, although the predicted values of the activation energy for creep depends on the nature of the assumptions used in developing

the models. Additionally, equation (21) predicts a much stronger dependence of the creep rate on the grain aspect ratio than equation (23).

In the second model proposed by Stephens and Nix (1986), it was assumed that the microstructure consisted uniformly of coarse and highly elongated grains which cannot slide along the longitudinal boundaries. The basic premise of this model is that a cavitating grain boundary transverse to the applied stress sheds load to the adjacent grains. Using an iterative technique, Stephens and Nix (1986) showed that the creep rate and rupture strength were influenced significantly by the grain aspect ratio (Fig. 36). The results of this investigation suggest that a microstructure consisting solely of coarse, fibrous grains was more desirable when long term creep properties are important in comparison to a duplex microstructure consisting of fine equiaxed and coarse elongated grains. Stephens and Nix (1986) pointed out that although an increase in the volume fraction of particles could improve the short term creep properties, it is more likely to result in the formation of the duplex microstructure which would lead to poor long term creep properties.

6.0 PRESENT OUTLOOK AND FUTURE RESEARCH

Perhaps, the single most important mechanical property of a dispersion-strengthened alloy for commercial applications is the occurrence of a threshold stress behavior. In principle, the material should never fracture by creep when the design stress is less than the threshold limit. This appears to be the case for MA 6000 which exhibits an almost stress independent rupture life when the stress corresponds to values in Region II in Fig. 37 (Benn and Kang, 1984). However, as discussed earlier, the nature of the threshold stress is complex, and it can arise as a result of particle-dislocation interactions within the grain interior or owing to difficulties in grain boundary sliding and cavitation due to a high grain aspect ratio. Additionally, the presence of particles at the grain boundaries can also decrease the efficiency of vacancy sources and sinks at these sites, which would result in the occurrence of a threshold stress behavior in the diffusion creep region (Burton, 1971; and Whittenberger, 1991). Figure 38 illustrates how each of these processes can influence the creep behavior of dispersion-strengthened alloys. It should be noted that the relative portions of each of these mechanisms can be greatly influenced by the microstructure. For example, significant diffusion creep nor grain boundary sliding cannot occur in materials with an elongated and coarse-grained microstructure.

In commercial applications where the structural components are required to have an almost infinite lifetime, the design stress should be less than the threshold stress for diffusion creep. In principle, it is possible to suppress diffusion creep and grain boundary sliding by increasing the grain size and the grain aspect ratio, respectively. This philosophy has led to the development of complex thermomechanical procedures for processing alloys which result in coarse and highly elongated grains. However, as pointed out by Stephens and Nix (1986) this microstructure is favored with only smaller volume fractions of the dispersoids, which result in the improvement of long term creep properties at the expense of short term creep characteristics. The

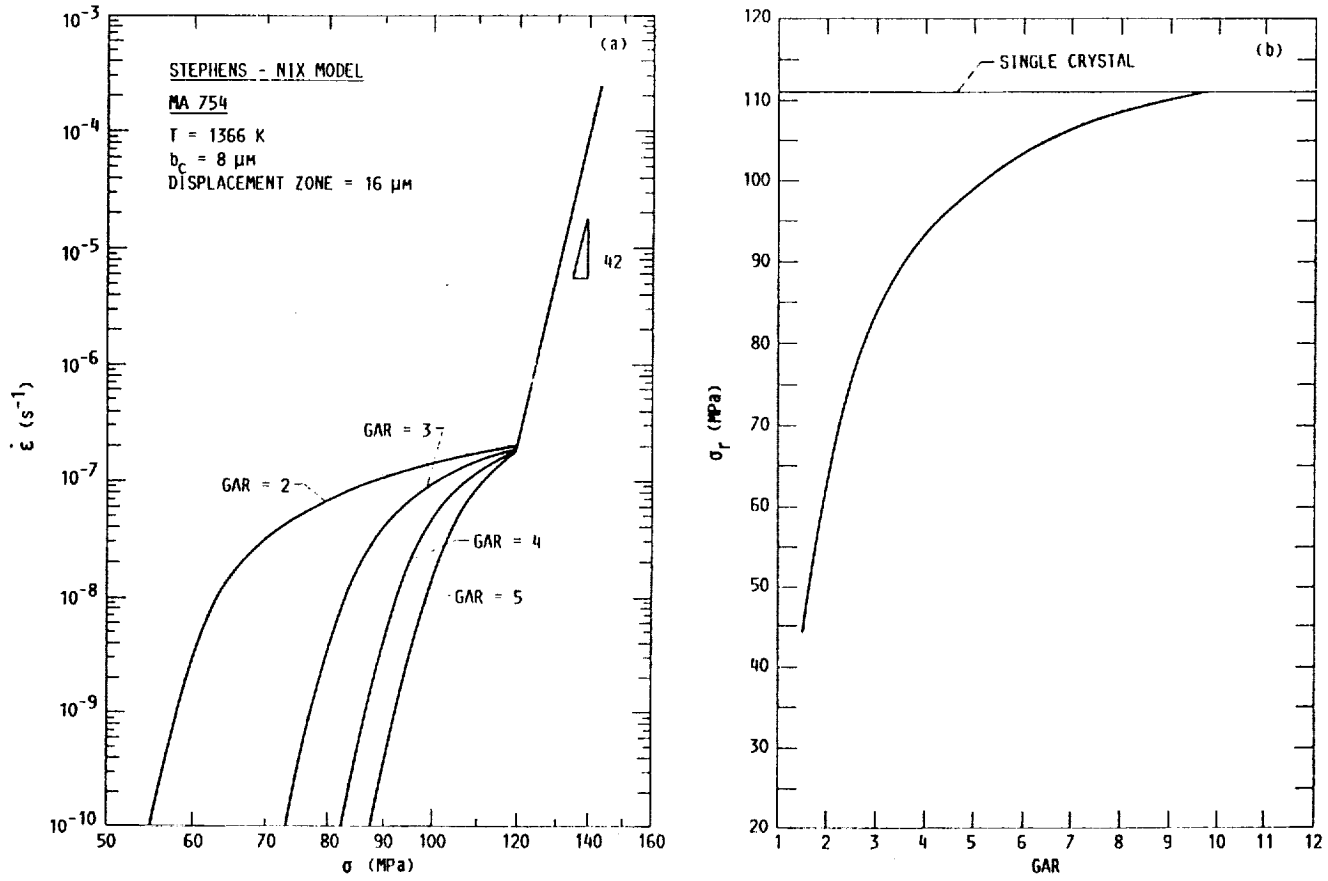

FIGURE 36. - EFFECT OF GRAIN ASPECT RATIO ON (a) THE MINIMUM CREEP RATE, AND (b) THE 100 h RUPTURE STRENGTH, σ_r, OF MA 754 PREDICTED BY THE STEPHENS - NIX MODEL FOR CAVITY GROWTH IN TRANSVERSE GRAIN BOUNDARIES. THE MICROSTRUCTURE WAS ASSUMED TO CONSIST OF AN UNIFORM DISTRIBUTION OF COARSE ELONGATED GRAINS, WHICH COULD NOT SLIDE ALONG THE LONGITUDINAL GRAIN BOUNDARIES. THE SPACING BETWEEN THE CAVITIES AT THE GRAIN BOUNDARIES IS GIVEN BY $2b_c$ (STEPHENS AND NIX, 1986) (COURTESY AMERICAN SOCIETY FOR METALS).

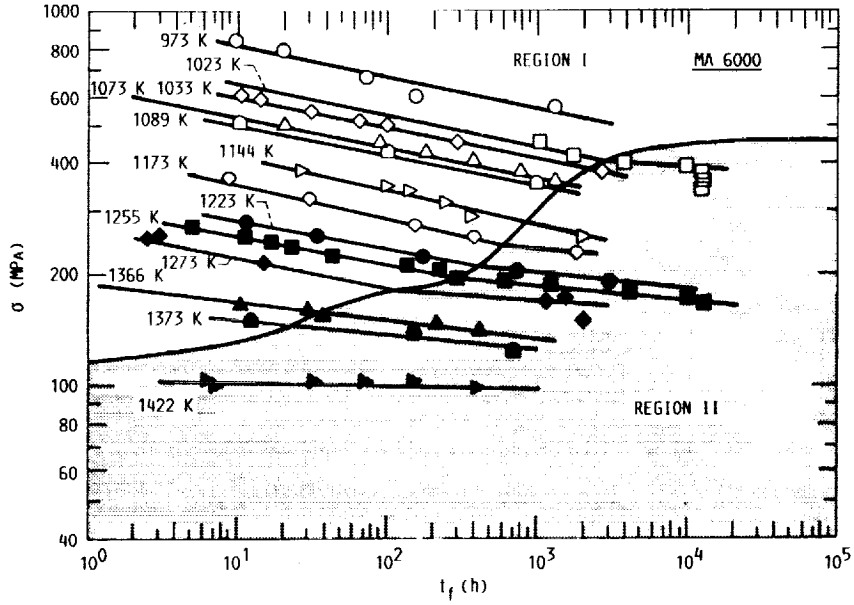

FIGURE 37. - STRESS RUPTURE DATA FOR MA 6000 SHOWING AN APPROXIMATELY INFINITE LIFETIME IN REGION II (BENN AND KANG, 1984) (REPRINTED WITH PERMISSION FROM THE METALLURGICAL SOCIETY, AIME).

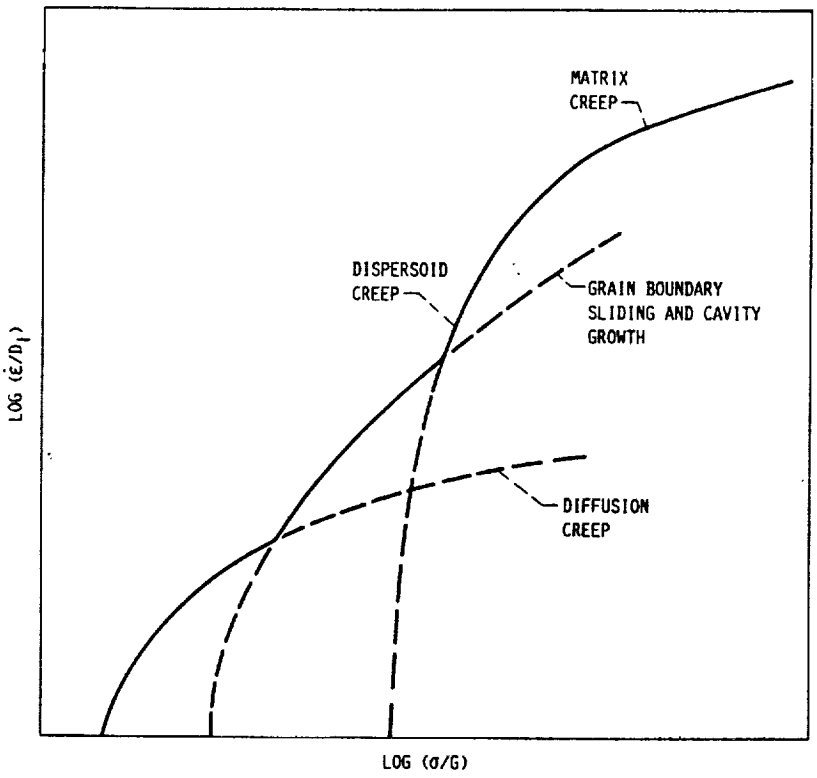

FIGURE 38. - SCHEMATIC PLOT OF THE CONTRIBUTION OF DISLOCATION CREEP, GRAIN BOUNDARY SLIDING AND CAVITY FORMATION, AND DIFFUSION CREEP TO DEFORMATION BEHAVIOR OF POLYCRYSTALLINE DISPERSION-STRENGTHENED MATERIALS (SELLARS AND PETKOVIC-LUTON, 1980).

short term, low temperature creep properties can be improved by precipitate-hardening, and this philosophy of dual particle strengthening because of the presence of precipitates and dispersoids has been employed quite effectively in the development of dispersion-strengthened superalloys, such as MA 6000 (Singer and Artz, 1986).

However, several problems still remain which restrict the use of dispersion-strengthened alloys in commercial applications. Whittenberger (1973) observed dispersoid-free zones at the grain boundaries in a TD-NiCr alloy because of conventional diffusion creep and suggested that these regions led to a degradation in the mechanical properties owing to their decreased resistance to grain boundary cavitation. An alternative explanation has been advanced by Stephens and Nix (1984, 1985), who suggest that the dispersoid-free zones associated with cavities lying on transverse grain boundaries result from localized diffusion involving atom plating in the adjacent regions. Nevertheless, a change in the initial microstructure during creep, either by the formation of cavity containing dispersoid-free zones at the grain boundaries or by the coarsening of the large particles (Singer and Artz, 1986), can lead to a degradation of the long-term creep properties of the alloy.

In comparison to some pure metals, many commercial ODS alloys possess poor creep rupture ductility generally less than 3 percent. In the particular case of an early heat of the b.c.c. iron-based MA 956 ODS alloy, the tensile fracture strain was less than 1 percent at strain rates less than 10^{-4} s^{-1} (Whittenberger, 1979), although the ultimate tensile strength was not strongly dependent on the initial strain rate. In this case, the specimens tested at low strain rates failed without warning. This behavior could be potentially hazardous in an engineering application and there is considerable scope for improving the ductility of these alloys.

On a more fundamental level, the mechanism responsible for the observed threshold stress behavior in the dislocation creep region is still poorly understood. Current theoretical models suggest that voids and hard particles can attract dislocations, so that the nature of the dispersoids do not appear to be important in determining the creep strength of a dispersion-strengthened alloy for similar values of k_r. These theories implicitly assume that particle deformation is unimportant during creep and no attempt has been made to verify this assumption. However, as shown in Sec. 4.2, this assumption may not be entirely justified and the stress acting on the particle can be sufficiently high to exceed its yield strength. These results are however limited by the definition of the particle yield stress and further research is required to establish a better criteria for estimating the magnitude of σ_y. The choice of the dispersoid-matrix combination would influence the magnitude of the threshold stress when significant deformation of the particles occurs (Fig. 29) and this could be important in the design of new dispersion-strengthened alloys. As mentioned earlier, there are significant differences in the creep behavior of some dispersion-strengthened materials which cannot be attributed to variations in the interparticle spacing or processing variables. The solution of these problems would require a universal theoretical approach applicable to all dispersion-strengthened alloys. Finally, the

question remains: How genuine is the concept of a threshold stress and would creep occur below the experimental values of σ_{th}?

7.0 SUMMARY AND CONCLUSIONS

1. A compilation of the high temperature creep and constant strain rate data is presented for several dispersion-strengthened alloys.

2. The reported values of the creep stress exponents vary between 3.5 (Durber and Davies, 1974) and 100 (Whittenberger, 1977), and the dispersion-strengthened alloys fall into three categories depending on their stress dependencies. The first group consists of alloys which exhibit class M behavior with values of $n \approx 4.5$ and $Q_c \approx Q_l$. The second category includes materials with values of n varying between 6.5 and 8.0, and $Q_c \geq Q_l$. The last class of alloys show extremely high values of n and Q_c at low stresses and high temperatures, and a tendency towards a threshold stress behavior. In this case, the magnitude of Q_c is usually greater than Q_l.

3. The high values of the true activation energy for creep cannot be rationalized on the basis of anion or cation diffusion in the dispersoid.

4. It is demonstrated that the local stress acting on the particle due to a fast-moving dislocation can be very high since there is insufficient time to relax it by diffusional mechanisms. If the particle yield strength is about $G_p/1000$, then this stress can exceed the yield strength of the dispersoid when the dislocation is within a distance of 5 d_p from the particle. The case when the deformation of the dispersoid is important is examined and it is suggested that σ_{th} in the additive rule proposed by Nix and coworkers (Lund and Nix, 1976; and Pharr and Nix, 1976) represents the yield strength of the particle. The present results suggest that three parameters are important in determining the nature of the dislocation threshold stress in dispersion-strengthened alloys. First, materials containing dispersoids with $G_p >> G_M$ are expected to have a high threshold stress determined by the yield strength of the particle, e.g., Al-Al_2O_3. Second, the threshold stress appears to be governed by the particle yield strength in alloys with $\lambda/d_p \leq 10$. Third, the deformation processes occurring in the matrix and the particle can be coupled only when $\lambda/b \leq 2000$.

5. The effect of grain size and grain shape on the creep and fracture behavior of dispersion-strengthened alloys is discussed. The creep rate increases with a decrease in the grain size or in the grain aspect ratio owing to the relative increase in the amount of grain boundary sliding. The magnitude of the threshold stress is similarly affected. The current models proposed to account for these effects are examined.

ACKNOWLEDGMENTS

The author thanks Dr. J. Daniel Whittenberger of the Lewis Research Center for suggesting the topic of this review, and for his interest, encour-

agement and support during the period of this investigation. He also gratefully acknowledges his discussions with Professor W.D. Nix of Stanford University on certain aspects of this investigation. Thanks are also due to Mr. Joe Stephens and Dr. Mike Nathal of the Lewis Research Center for reading the manuscript, and to Professor J.K. Tien of Columbia University and Professor E. Artz of the Max Planck Institute, Stuttgart, F.R.G., for providing copies of the original micrographs reproduced in Figs. 20 and 21, respectively.

References

Ansell, G.S.; and Weertman, J.: Creep of a Dispersion-Hardened Aluminum Alloy. Trans. AIME, vol. 215, no. 5, Oct. 1959, pp. 838-843.

Ansell, G.S.: The Mechanism of Dispersion-Strengthening: A Review. Oxide Dispersion Strengthening, G.E. Ansell, T.D. Cooper, and F.V. Lenel, eds., Gordon and Breach, New York, 1968, pp. 61-141.

Artz, E.; and Ashby, M.F.: Threshold Stresses in Materials Containing Dispersed Particles. Scr. Metall., vol. 16, no. 11, Nov. 1982, pp. 1285-1290.

Artz, E.; and Singer, R.F.: The Effect of Grain Shape on Stress Rupture of the Oxide Dispersion Strengthened Superalloy Inconel MA 6000. Superalloys 1984, M. Gell, et al., eds., TMS-AIME, Warrendale, PA., 1984, pp. 367-376.

Artz, E.; and Schröder, J.H.: High Temperature Strength of ODS Superalloys Due to Dispersoid-Dislocation Interaction. High Temperature Alloys for Gas Turbines and Other Applications, W. Betz, et al., eds., Reidel Publishing Company, Dordrecht, Netherlands, 1986, pp. 1037-1048.

Artz, E.; and Wilkinson, D.S.: Threshold Stresses for Dislocation Climb Over Hard Particles: The Effect of an Attractive Interaction. Acta Metall., vol. 34, no. 10, Oct. 1986, pp. 1893-1898.

Artz, E.: Threshold Stress for Creep of Dispersion Strengthened Materials. Handbook of Metallic Composites, S. Ochiai, ed., Marcel Dekker, New York, 1992, to be published.

Ault, G.M.; and Burte, H.M.: Technical Applications for Oxide Dispersion-Strengthened Materials. Oxide Dispersion Strengthening, G.E. Ansell, T.D. Copper, and F.V. Lenel, eds., Gordon and Breach, Science Publishers, New York, 1968, pp. 3-57.

Barrett, C.R.; Ardell, A.J.; and Sherby, O.D.: Influence of Modulus on the Temperature Dependence of the Activation Energy for Creep at High Temperatures. Trans. AIME, vol. 230, no. 1, Feb. 1964, pp. 200-204.

Barrett. C.R.; and Sherby, O.D.: Influence of Stacking-Fault Energy on High-Temperature Creep of Pure Metals. Trans. AIME, vol. 233, no. 6, June 1965, pp. 1116-1119.

Bendersky, L.; Rosen, A.; and Mukherjee, A.K.: Creep and Dislocation Substructure. Int. Met. Rev., vol. 30, no. 1, 1985, pp. 1-15.

Benn, R.C.; and Kang, S.K.: Long-Term Mechanical Behavior of Some ODS Alloys. Superalloys 1984, M. Gell, et al., eds., TMS-AIME, Warrendale, PA, 1984, pp. 319-326.

Bilde-Sørensen, J.B.: Creep in Particle-Containing Materials. Deformation of Multi-Phase and Particle Containing Materials, J.B. Bilde-Sørensen, et al., eds., Risø National Laboratory, Roskilde, Denmark, 1983, pp. 1-14.

Bird, J.E.; Mukherjee, A.K.; and Dorn, J.E.: Correlations Between High-Temperature Creep Behavior and Structure. Quantitative Relation Between Properties and Microstructure, R.G. Brandon and A. Rosen, eds., Israel Universities Press, Jerusalem, Israel, 1969, pp. 255-341.

Blickensderfer, R.: Creep Behavior of a Tungsten Alloy Dispersion Strengthened by ZrO_2. Met. Trans., vol. 5, no. 11, Nov. 1974, pp. 2347-2350.

Blum, W.; and Reppich, B.: On the Stress Dependence of the Stationary Deformation Rate. Acta Metall., vol. 17, no. 8, Aug. 1969, pp. 959-966.

Blum, W.; Hausselt, J.; and König, G.: Transient Creep and Recovery After Stress Reduction During Steady State Creep of AlZn. Acta Metall., vol. 24, no. 4, Apr. 1976, pp. 293-297.

Blum, W.: Dislocation Models of Plastic Deformation of Metals at Elevated Temperatures. Z. Metallk., vol. 68, July 1977, pp. 484-492.

Blum, W.; and Reppich, B.: Creep of Particle-Strengthened Alloys. Creep Behavior of Crystalline Solids, B. Wilshire and R.W. Evans, eds., Pineridge Press, Swansea, U.K., 1985, pp. 83-136.

Brown, L.M.; and Ham, R.K.: Dislocation-Particle Interactions. Strengthening Methods in Crystals, A. Kelly and R.B. Nicholson, eds., Elsevier, Amsterdam, 1971, pp. 9-135.

Burt, H.; Dennison, J.P.; and Wilshire, B.: Friction Stress Measurements During Creep of Nimonic 105. Met. Sci., vol. 13, no. 5, May 1979, pp. 295-300.

Burton, B.: The Influence of Alumina Dispersions on the Diffusion-Creep Behavior of Polycrystalline Copper. Met. Sci. J., vol. 5, no. 1, Jan. 1971, pp. 11-15.

Čadek, J.: Creep in Particle Strengthened Metals. Czech. J. Phys., vol. 31B, no. 2, 1981, pp. 177-186.

Clauer, A.H.; and Wilcox, B.A.: Steady-State Creep of Dispersion-Strengthened Nickel. Met. Sci. J., vol. 1, May 1967, pp. 86-90.

Clauer, A.H.; and Hansen, N.: High Temperature Strength of Oxide Dispersion-Strengthened Aluminum. Acta Metall., vol. 32, no. 2, Feb. 1984, pp. 269-278.

Cooper, A.H.; Nardone, V.C.; and Tien, J.K.: Attractive Dislocation and Particle Interactions in ODS Superalloys and Implications. Superalloys 1984, M. Gell, et al., eds., TMS-AIME, Warrendale, PA, 1984, pp. 357-366.

Davies, P.W., et al.: Stress-Change Experiments During High-Temperature Creep of Copper, Iron, and Zinc. Met. Sci. J., vol. 7, May 1973, pp. 87-92.

Durber, G.L.R.; and Davies, T.J.: Observations on the Stress-Dependence of Steady-State Creep of a Dispersion-Strengthened Alloy. Met. Sci., vol. 8, no. 7, July 1974, pp. 225-227.

Evans, W.J.; and Harrison, G.F.: Validity of Friction Stress σ_o Measurements for High-Temperature Creep. Met. Sci., vol. 13, no. 6, June 1979, pp. 346-350.

Frost, H.J.; and Ashby, M.F.: Deformation-Mechanism Maps: The Plasticity and Creep of Metals and Ceramics. Pergamon, Oxford, 1982.

Fuentes-Samaniego, R.; and Nix, W.D.: Appropriate Diffusion Coefficients for Describing Creep Processes in Solid Solution - Alloys. Scr. Metall., vol. 15, no. 1, Jan. 1981, pp. 15-20.

Gaal, I.; Harmat, P.; and Füle, G.: Creep at Low Stresses in Bubble Strengthened Tungsten. Deformation of Multi-Phase and Particle Containing Materials, J.B. Bilde-Sørensen, et al., eds., Risø National Laboratory, Roskilde, Denmark, 1983, pp. 257-262.

Gaboriaud, R.J.: Fluage Haute Temperature du Sequioxyde d' Yttrium: Y_2O_3. Philos. Mag., vol. 44A, no. 3, 1981, pp. 561-587.

Gibeling, J.C.; and Nix, W.D.: The Existence of a Friction Stress for High-Temperature Creep. Met. Sci., vol. 11, no. 10, Oct. 1977, pp. 453-457.

Gibeling, J.C.; and Nix, W.D.: The Description of Elevated Temperature Deformation in Terms of Threshold Stresses and Back Stresses: A Review. Mater. Sci. Eng., vol. 45, Sept. 1980, pp. 123-135.

Gilman, P.S.: The Development of Aluminum-Aluminum Oxide Alloys by Mechanical Alloying. Ph.D. Thesis, Standford University, 1979.

Grant, N.J.: Dispersion Strengthening. Strengthening Mechanisms: Metals and Ceramics, J.J. Burke, N.L. Reed, and V. Weiss, eds., Syracuse University Press, Syracuse, New York, 1966, pp. 63-82.

Guard, R.W.: Mechanisms of Fine-Particle Stengthening. Strengthening Mechanisms in Solids, American Society for Metals, Metals Park, OH, 1962, pp. 253-278.

Hancock, J.; Dillamore, I.L.; and Smallman, R.E.: The Creep of Dispersion-Strengthened Ni-Co Alloys. Met. Sci. J., vol. 6, Sept. 1972, pp. 152-156.

Hansen, N.: Dispersion-Strengthened Aluminum Powder Products for Nuclear Application. Powder Metall., vol. 10, no. 20, 1967, pp. 94-115.

Hansen, N.: Dispersion-Strengthened Aluminum Products Manufactured by Powder Blending. Powder Metall., vol. 12, no. 23, 1969, pp. 23-44.

Hausselt, J.H.; and Nix, W.D.: Dislocation Structure of Ni-20Cr-2ThO_2 After High Temperature Deformation. Acta. Metall., vol. 25, no. 6, June 1977, pp. 595-607.

Hausselt, J.H.; and Nix, W.D.: A Model for High Temperature Deformation of Dispersion Strengthened Metals Based on Substructural Observations in Ni-20Cr-2ThO_2. Acta Metall., vol. 25, no. 12, Dec. 1977, pp. 1491-1502.

Hoffman, R.E.; Pikus, F.W.; and Ward, R.A.: Self-Diffusion in Solid Nickel. Trans. AIME, vol. 206, no. 5, May 1956, pp. 483-486.

Horita, Z.: Creep and Grain Boundary Sliding in the Presence of Precipitate Particles. Ph.D. Thesis, University of Southern California, Los Angeles.

Horita, Z.; and Langdon, T.G.: The Creep Behavior of a Commerical Al-5% Mg-0.25% Fe (5083) Alloy. Deformation of Multi-Phase and Particle Containing Materials, J.B. Bilde-Sørensen, et al., eds., Risø National Laboratory, Roskilde, Denmark, 1983, pp. 307-312.

Howson, T.E.; Stulga, J.E.; and Tien, J.K.: Creep and Stress Rupture of Oxide Dispersion Strengthened Mechanically Alloyed Inconel Alloy MA 754. Metall. Trans. A, vol. 11, no. 9, Sept. 1980, pp. 1599-1607.

Howson, T.E.; Mervyn, D.A.; and Tein, J.K.: Creep and Stress Rupture of a Mechancially Alloyed Oxide Dispersion and Precipitation Strengthened Nickel-Base Superalloy. Metall. Trans. A, vol. 11, no. 9, Sept. 1980, pp. 1609-1616.

Humphreys, F.J.; Hirsch, P.B.; and Gould, D.: The Effect of Temperature on the Mechanical Properties and Microstructure of Single Crystals of Copper Containing Dispersed Oxide particles. Second Conference on the Strength of Metals and Alloys, vol. 2, American Society for Metals, 1970, pp. 550-554.

High Temperature High Strength Nickel Base Alloys, third ed., International Nickel Company, Inc., New York, 1977, p. 21.

Kane, R.D.; and Ebert, L.J.: Creep Deforamtion of TD-Nickel Chromium. Metall. Trans. A., vol. 7, no. 1, Jan. 1976, pp. 133-137.

Kim, Y.G.; and Merrick, H.F.: Characterization of an Oxide Dispersion Strengthened Superalloy, MA-6000E, for Turbine Blade Applications. NASA CR-159493, 1979.

Lagneborg, R.: Bypassing of Dislocations Past Particles by a Climb Mechanism. Scr. Metall., vol. 7, no. 6, June 1973, pp. 605-614.

Langdon, T.G.; and Mohamed, F.A.: The Characteristics of Independent and Sequential Creep Processes. J. Austral. Inst. Metl., vol. 22, no. 3-4, Sept.-Dec. 1977, pp. 189-199.

Langdon, T.G.: Deformation of Polycrystalline Materials at High Temperatures. Deformation of Polycrystals: Mechanisms and Microstructures, N. Hansen, et al., eds., Risø National Laboratory, Roskilde, Denmark, pp. 45-54.

Langdon, T.G.: Deformation at High Temperatures. Strength of Metals and Alloys (ICSMA 6), R.C. Gifkins, ed., Pergamon, Oxford, 1983, pp. 1105-1120.

Lenel, F.V.; Ansell, G.S.; and Nazmy, M.Y.: The Creep Properties of Dispersion-Strengthened Silver-Gallium Oxide Alloys. High Temperatures-High Pressures, vol. 3, no. 4, 1971, pp. 439-444.

Leverant, G.R; Lenel, R.V.; and Ansell, G.S.: The High-Temperature Steady-State Creep of Pure Silver and Internally Oxidized Silver-Magnesium Alloys. Trans. ASM, vol. 59, 1966, pp. 890-898.

Lin, J.; and Sherby, O.D.: Creep of Oxide Dispersion Strengthened Materials (with special reference to TD nichrome). Res. Mech., vol. 2, June 1981, pp. 251-293.

Lund, R.W.; and Nix, W.D.: On High Creep Activation Energies for Dispersion Strengthened Metals. Metall. Trans. A, vol. 6, no. 7, July 1975, pp. 1329-1333.

Lund, R.W.; and Nix, W.D.: High Temperature Creep of Ni-20Cr-2ThO_2 Single Crystals. Acta Metall., vol. 24, no. 5, May 1976, pp. 469-481.

Malu, M.; and Tien, J.K.: The Elastic Modulus Correction Term in Creep Activation Energies: Application to Oxide Dispersion Strengthened Super-alloys. Scr. Metall., vol. 9, no. 10, Oct. 1975, pp. 1117-1120.

McAlarney, M.E., et al.: Creep and Rupture of an ODS Alloys with High Stress Rupture Ductility. Metall. Trans. A, vol. 13, no. 8, Aug. 1982, pp. 1453-1462.

McLean, D.: The Physics of High Temperature Creep in Metals. Reports Prog. Phys., vol. 29.

McNelley, T.R.; Edwards, G.R.; and Sherby, O.D.: A Microstructureal Correlation Between the Mechanical Behavior of Large Volume Fraction Particulate Composites at Low and High Temperatures. Act. Metall., vol. 25, no. 2, Feb. 1977, pp. 117-124.

Meyers, C.L.; and Sherby, O.D.: Creep of Sintered Aluminum Powder Above and Below the Melting Point of Aluminum. J. Inst. Metals, vol. 90, pt. 10, June 1962, pp. 380-382.

Milička, K.; Čadek, J.; and Ryš, P.: Creep of Aluminum Strengthened by Alumina Particles. Acta Metall., vol. 18, no. 7, July 1970, pp. 733-746.

Millan, P.P.; and Mays, J.C.: Oxide-Dispersion-Strengthened Turbine Blades, Vol. 1, NASA CR-179537-VOL-1, 1986, pp. 97-98.

Mohamed, F.A.; and Langdon, T.G.: The Transition from Dislocation Climb to Viscous Glide in Creep of Solid Solution Alloys. Acta Metall., vol. 22, no. 6, June 1974, pp. 779-788.

Mohamed, F.A.; and Langdon, T.G.: Deformation Mechanism Maps Based on Grain Size. Metall. Trans., vol. 5, no. 11, Nov. 1974, pp. 2339-2345.

Moon, D.M.; and Stickler, R.: Creep Behavior of Fine Wires of Powder-Metallurgical Pure, Doped, and Thoriated Tungsten. High Temp.-High Press., vol. 3, no. 5, 1971, pp. 503-516.

Moon, D.M.: Creep of Fine Wires of W-ThO_2 Alloys. Metall. Trans., vol. 3, Dec. 1972, pp. 3097-3102.

Morral, F.R.: Dispersion Strengthening of Metals. MCIC Report No. 77-30, Metals and Ceramics Information Center, Battelle Columbus Laboratories, Columbus, OH, 1977.

Mukherjee, A.K.; Bird, J.E.; and Dorn, J.E.: Experimental Correlations for High-Temperature Creep. Trans. ASM, vol. 62, no. 1, Mar. 1969, pp. 155-179.

Nardone, V.C.; and Tien, J.K.: Pinning of Dislocations on the Departure Side of the Strengthening Dispersoids. Scr. Metall., vol. 17, no. 4, Apr. 1983, pp. 467-470.

Nardone, V.C.; Matejczyk, D.E.; and Tien, J.K.: The Threshold Stress and Departure Side Pinning of Dislocations by Dispersoids. Acta Metall., vol. 32, no. 9, Sept. 1984, pp. 1509-1517.

Nelmes, G.; and Wilshire, B.: Some Factors Affecting the Creep Resistance of Single-Phase Copper Alloys. Scr. Metall., vol. 10, no. 8, Aug. 1976, pp. 697-700.

Nieh, T.G.; and Nix, W.D.: A Study of Intergranular Cavity Growth in Ag + 0.1% MgO at Elevated Temperatures. Acta Metall., vol. 27, no. 6, June 1979, pp. 1097-1106.

Nix, W.D.; and Ilschner, B.: Mechanisms Controlling Creep of Single Phase Metals and Alloys. Strength of Metals and Alloys (ICSMA 5), P. Haasen, V. Gerold, and G. Kostorz, eds., Pergamon, Oxford, Oxford, 1980, pp. 1503-1530.

Oliver, W.; and Nix, W.D.: High Temperature Deformation of Oxide Dispersion Strengthened Al and Al-Mg Solid Solutions. Acta Metall., vol. 30, no. 7, July 1982, pp. 1335-1347.

Parker, J.D.; and Wilshire, B.: The Effect of a Dispersion of Cobalt Particles on High-Temperature Creep of Copper. Met. Sci., vol. 9, 1975, pp. 248-252.

Parker, J.D.; and Wilshire, B.: Friction-Stress Measurements During High-Temperature Creep of Polycrystalline Copper. Met. Sci. J., vol. 12, Oct. 1978, pp. 453-458.

Petkovic-Luton, R.; Srolovitz, D.J.; and Luton, M.J.: Microstructural Aspects of Creep in Oxide Dispersion Strengthened Alloys. Frontiers of High Temperature Materials II, INCOMAP, J.S. Benjamin and R.C. Benn, eds., Inco Alloys International, New York, pp. 73-99.

Petkovic-Luton, R.; and Luton, M.J.: Mechanisms of Creep of Oxide Dispersion Strengthened Alloys. Strength of Metals and Alloys (ICSMA 7), vol. 1, H.J. McQueen, et al., eds., Pergamon, Oxford, pp. 743-748.

Petrovic, J.J.; and Ebert, K.J.: Elevated Temperature Deformation of TD-Nickel. Met. Trans., vol. 4, no. 5, May 1973, pp. 1301-1308.

Pharr, G.M.; and Nix, W.D.: A Comparison of the Orowan Stress with the Threshold Stress for Creep for Ni-20Cr-2ThO_2 Single Crystals. Scr. Metall., vol. 10, no. 11, Nov. 1976, pp. 1007-1010.

Pugh, J.W.: On the Short Time Creep Rupture Properties of Lamp Wire. Met. Trans., vol. 4, no. 2, Feb. 1973, pp. 533-538.

Purushothaman, S.; and Tien, J.K.: Role of Back Stress in the Creep Behavior of Particle Strengthened Alloys. Acta Metall., vol. 26, no. 4, Apr. 1978, pp. 519-528.

Raj, S.V.: The Effect of Stacking Fault Energy on the Creep Power-Law Breakdown Criterion in FCC Metals. Scr. Metall., vol. 20, no. 10, Oct. 1986, pp. 1333-1338.

Raj, S.V.; and Pharr, G.M.: A Compilation and Analysis of Data for the Stress Dependence of the Subgrain Size. Mater. Sci. Eng., vol. 81, 1986, pp. 217-237.

Raj, S.V.; and Langdon, T.G.: Creep Behavior of Copper at Intermediate Temperatures-I. Mechanical Characteristics. Acta Metall., vol. 37, no. 3, Mar. 1989, pp. 843-852.

Raj, S.V.; and Pharr, G.M.: Creep Substructure Formation in Sodium Chloride Single Crystals in the Power Law and Exponential Creep Regimes. Mater. Sci. Eng. A, vol. 122, 1989, pp. 233-242.

Raj, S.V.; and Langdon, T.G.: Creep Behavior of Copper at Intermediate Temperatures-II. Surface Microstructural Observations. Acta Metall., vol. 39, 1991, to be published.

Raj, S.V.; and Langdon, T.G.: Creep Behavior of Copper at Intermediate Temperatures-III. A Comparison With Theory. Acta Metall., vol. 39, 1991, to be published.

Reynolds, G.H.; Lenel, F.V.; and Ansell, G.S.: The Effect of Solute Additions on the Steady-State Creep Behavior of Dispersion-Strengthened Aluminum. Metall. Trans., vol. 2, Nov. 1971, pp. 3027-3034.

Reynolds, G.H.: Room Temperature Creep of Recrystallized Dispersion-Strengthened Lead. Scr. Metall., vol. 8, no. 7, July 1974, pp. 781-784.

Robinson, S.L.; and Sherby, O.D.; Mechanical Behavior of Polycrystalline Tungsten at Elevated Temperature. Acta Metall., vol. 17, no. 2, Feb. 1969, pp. 109-125.

Sands, R.L.; Phelps, L.A.; and Morgan, W.R.: Dispersion-Strengthened Stainless Steel. Powder Metall., no. 10, 1962, pp. 158-170.

Sautter, F.K.; and Chen, E.S.: Surface and Interfacial Energy of Gold and Gold-Al_2O_3 Alloys. Oxide Dispersion Strengthening, G.S. Ansell, T.D. Cooper, and F.V. Lenel, eds., Gordon and Breach, Science Publisher, New York, pp. 495-508.

Schröder, J.H.; and Artz, E.: Weak Beam Studies of Dislocation/Dispersoid Interaction in an ODS Superalloy. Scr. Metall., vol. 19, no. 9, Sept. 1985, pp. 1129-1134.

Selman, G.L.; Day, J.G.; and Bourne, A.A.: Dispersion Strengthened Platinum: Properties and Characteristics of a New High Temperature Material. Plat. Metals Rev., vol. 18, no. 2, Apr. 1974, pp. 46-56.

Sellars, C.M.; and Petkovic-Luton, R.A.: Creep of Dispersion-Strengthened Alloys. Mater. Sci. Eng., vol. 46, Nov. 1980, pp. 75-87.

Sherby, O.D.; Lytton, J.L.; and Dorn, J.E.: Activation Energy for Creep of High-Purity Aluminum. Acta Metall., vol. 5, no. 4, Apr. 1957, pp. 219-227.

Sherby, O.D.: Factors Affecting the High Temperature Strength of Polycrystalline Solids. Acta Metall., vol. 10, no. 2, Feb. 1962, pp. 135-147.

Sherby, O.D.; and Burke, P.M.: Mechanical Behavior of Crystalline Solids at Elevated Temperatures. Prog. Mater. Sci., vol. 13, no. 7, 1967, pp. 325-390.

Sherby, O.D.; Klundt, R.H.; and Miller, A.K.: Flow Stress, Subgrain Size, and Subgrain Stability at Elevated Temperatures. Metall. Trans. A, vol. 8, no. 6, June 1977, pp. 843-850.

Shewfelt, R.S.W.; and Brown, L.M.: High-Temperature Strength of Dispersion-Hardened Single Crystals-I. Experimental Results. Philos. Mag., vol. 30, no. 5, Nov. 1974, pp. 1135-1145.

Shewfelt, R.S.W.; and Brown, L.M.: High-Temperature Strength of Dispersion-Hardened Single Crystals-II. Theory. Philos. Mag., vol. 35, no. 4, Apr. 1977, pp. 945-962.

Singer, R.F.; Benn, R.C.; and Kang, S.K.: Creep Rupture Properties of Inconel Alloy MA 6000. Frontiers of High Temperature Materials II INCOMAP, J.S. Benjamin and R.C. Benn, eds., INCO Alloys International, New York, pp. 336-357.

Singer, R.F.; and Artz, E.: Structure, Processing, and Properties of ODS Superalloys. High Temperature Alloys for Gas Turbines and Other Applications, W. Betz et al., eds., D. Reidel Publishing, Company, Dordrecht, West Germany, 1986, pp. 98-126.

Sinha, R.K.; and Blachere, J.R.: On the Threshold Stress in Particle Inhibited Diffusive Creep. Scr. Metall., vol. 13, no. 1, Jan. 1979, pp. 41-44.

Snowden, K.U.: Some Creep and Fatigue Properties of Dispersed-Oxide-Strengthened Lead. J. Mater. Sci., vol. 2, no. 4, July 1967, pp. 324-331.

Springarn, J.R.; Barnett, D.M.; and Nix, W.D.: Theoretical Descriptions of Climb Controlled Steady State Creep at High and Intermediate Temperatures. Acta Metall., vol. 27, no. 9, Sept. 1979, pp. 1549-1561.

Srolovitz, D.; Petkovic-Luton, R.; and Luton, M.J.: On Dislocation-Incoherent Particle Interactions at High Temperatures. Scr. Metall., vol. 16, no. 12, Dec. 1982, pp. 1401-1406.

Srolovitz, D.J.; Petkovic-Luton, R.A.; and Luton, M.L.: Edge Dislcation-Circular Inclusion Interactions at Elevated Temperatures. Acta Metall., vol. 31, no. 12, Dec. 1983, pp. 2151-2159.

Srolovitz, D.J., et al.: Diffusionally Modified Dislocation-Particle Elastic Interactions. Acta Metall., vol. 32, no. 7, July 1984, pp. 1079-1088.

Stephens, J.J.; and Nix, W.D.: Creep and Fracture of Inconel MA 754 at Elevated Temperatures. Superalloys 1984, M. Gell, et al., ed, TMS-AIME, Warrendale, PA, 1984, pp. 327-334.

Stephens, J.J.; and Nix, W.D.: The Effect of Grain Morphology on Longitudinal Creep Properties of Inconel MA 754 at Elevated Temperatures. Metall. Trans. A, vol. 16, no. 7, July 1985, pp. 1307-1324.

Stephens, J.J.; and Nix, W.D.: Constrained Cavity Growth Models of Longitudinal Creep Deformation of Oxide Dispersion Strengthened Alloys. Metall. Trans. A, vol. 17, no. 2, Feb. 1986, pp. 281-293.

Takada, J., et al.: High Temperature Deformation of Internally Oxidized Fe-Cr Alloys. Jpn. Inst. Metals, vol. 39, no. 6, June 1975, pp. 615-620.

Takada, J.; Adachi, M.; and Tamura, I.: High Temperature Deformation of Single Crystals of Cu-Al_2O_3 and Cu-TiO_2 Alloys Prepared by Means of Internal Oxidation. Deformation of Mutli-Phase Particle Containing Materials, J.B. Bilde-Sørensen, et al., eds., Risø National Laboratory, Roskilde, Denmark, pp. 539-544.

Takeuchi, S.; and Argon, A.S.: Steady-State Creep of SIngle-Phase Crystalline Matter at High Temperature. J. Mater. Sci., vol. 11, no. 8, Aug. 1976, pp. 1542-1566.

Threadgill, P.L.; and Wilshire, B.: Mechanisms of Transient and Steady-State Creep in a γ'-Hardened Austenitic Steel. Creep Strength in Steel and High Temperature Alloys, The Metals Society, London, pp. 8-14.

Tomizuka, C.T.; and Sonder, E.: Self-Diffusion in Silver. Phys. Rev., vol. 103, no. 5, Sept. 1, 1956, pp. 1182-1184.

Vagarali, S.S.; and Langdon, T.G.: Deformation Mechanisms in H.C.P. Metals and Elevated Temperatures-I. Creep Behavior of Magnesium. Acta Metall., vol. 29, no. 12, Dec. 1981, pp. 1969-1982.

Weertman, J.: Dislocation Climb Theory of Steady-State Creep. Trans. ASM, vol. 61, 1968, pp. 681-694.

Whittenberger, J.D.: Diffusional Creep and Creep-Degardation in Dispersion-Strengthened Ni-Cr Base Alloys. Metall. Trans., vol. 4, no. 6, June 1973, pp. 1475-1483.

Whittenberger, J.D.: Creep and Tensile Properties of Several Oxide Dispersion Strengthened Nickel Base Alloys. Metall. Trans. A, vol. 8, no. 7, July 1977, pp. 1155-1163.

Whittenberger, J.D.: Effect of Strain Rate on the Fracture Behavior at 1366 K of the bcc Iron Base Oxide Dispersion Strengthened Alloy MA 956. Metall. Trans. A, vol. 10, no. 9, Sept. 1979, pp. 1285-1295.

Whittenberger, J.D.: Elevated Temperature Compressive Steady State Deformation and Failure in the Oxide Dispersion Strengthened Alloy MA 6000E. Metall. Trans. A, vol. 15, no. 9, Sept. 1984, pp. 1753-1762.

Whittenberger, J.D.: Diffusion and Diffusional Creep in Dispersion Strengthened Alloys. Handbook of Metallic Composites, S. Ochiai, ed., Marcel Dekker, New York, 1992, to be published.

Wilcox, B.A.; and Clauer, A.H.: Creep of Thoriated Nickel Above and Below 0.5 T_m. Trans. AIME, vol. 236.

Wilcox, B.A.; and Clauer, A.H.: Steady-State Creep of Dispersion-Strengthened Metals. NASA CR-54639, 1966, p. 14.

Wilcox, B.A.; Clauer, A.H.; and McCain, W.S.: Creep and Creep Fracture of Ni-20Cr-2ThO_2 Alloy. Trans. AIME, vol. 239, no. 11, Nov. 1967, pp. 1791-1796.

Wilcox, B.A.; and Clauer, A.H.: High Temperature Creep of Ni-ThO_2 Alloys. Oxide Dispersion Strengthening, G.S. Ansell, T.D. Cooper, and F.V. Lenel, eds., Gordon and Breach, Science Publishers, New York, pp. 323-355.

Wilcox, B.A.; and Clauer, A.H.: Creep of Dispersion-Strengthened Nickel-Chromum Alloys. Met. Sci. J., vol. 3, 1969, pp. 26-33.

Wilcox, B.A.; and Clauer, A.H.: The Role of Grain Size and Shape in Strengthening of Dispersion Hardened Nickel Alloys. Acta Metall., vol. 20, no. 5, May 1972, pp. 743-757.

Williams, K.R.; and Wilshire, B.: On the Stress- and Temperature-Dependence of Creep of Nimonic 80A. Met. Sci. J., vol. 7, Sept. 1973, pp. 176-179.

Wolf, S.; and Grant, N.J.: Structure-Property Relationships in Oxide-Dispersed Iron-Beryllia Alloys. Powder Metall. Int., vol. 9, May 1977, pp. 57-62, 64.

Wright, P.K.: The High Temperature Creep Behavior of Doped Tungsten Wire. Metall. Trans. A, vol. 9, no. 7, July 1978, pp. 955-963.

Yoshihara, M.; and McLellan, R.B.: Self-Diffusion in the Noble Metals. Acta Metall., vol. 29, no. 7, July 1981, pp. 1277-1283.

APPENDIX

A.1.0 A Compilation of the Creep Data for Several Dispersion-Strengthened Alloys

A compilation of the reported experimental data on several dispersion-strengthened materials is shown in Table A.1. The table also includes the material composition, the experimental conditions under which these results were obtained, and the reference sources. For convenience, the data are classified alphabetically according to the base metal composition, and the alloys are arranged in each category according to the degree of complexity. The commercial designations[14] for the alloys are also included in some cases. It should be noted that the experimental variables given in the table serve only as a guide, and they do not necessarily mean that the actual experiments were conducted over the entire range of stresses, temperatures, and microstructural and processing variables shown. The original references should be consulted for the exact experimental conditions employed in each investigation. In particular, a simple classification of the techniques used for processing each alloy proved to be difficult owing to the complex nature of these processes generally employed. Therefore, the information shown in the table generally indicates the last processing step or a combination of those which were likely to influence the mechanical properties. The codes used in this and other columns are explained in Sec. A.1.1.

The grain aspect ratio was estimated using $GAR = [L_1/(L_2L_3)^{1/2}]$, where L_1, L_2, and L_3 are the intercept lengths along the longitudinal, long transverse, and short transverse directions, respectively. In this case, d was assumed to be given by: $d = 0.85\ (L_1L_2L_3)^{1/3}$. Whenever possible, the volume fractions of the dispersoids are those given in the original reference, but in some cases, they have been estimated from the chemical composition of the alloy. The center to center interparticle spacing and the particle diameter are those reported in the original investigation.

The stress exponents and activation energies shown in the table are those reported in the original investigation except for ZGS Pt (Selman, Day, and Bourne, 1974), where these were estimated from the creep data presented by the authors. In some instances, the reported values of the activation energies include corrections for the temperature dependence of the elastic modulus according to the methods suggested by Barrett, Ardell, and Sherby (1964), Lund and Nix (1975), or Malu and Tien (1975), and these are indicated in the table. Finally, information on the microstructure and other factors reported in the original reference are included in the table for the sake of completeness.

[14]The designations MA 754, MA 956, and MA 6000 are the trademarks of the INCO Alloy Products Limited.

A.1.1 An Explanation of the Codes Used in Table A.1

A number of techniques are generally used in the processing of dispersion-strengthened alloys, and these can strongly influence the mechanical properties. Therefore, as much information as possible is included in Table A.1, especially since the microstructural characterization of the as-processed alloy is not often reported. As far as possible, an attempt has been made to indicate whether the final processing step consisted of a recrystallization heat treatment, since a recrystallized microstructure can significantly influence the creep properties of the alloy. Unfortunately, it was not always evident if the annealing treatment resulted in a recrystallized microstructure. In these instances, the heat treatment procedure has been designated as 'A'. An explanation of the processing codes are given below:

A = Annealing; HE = Hot extrusion; IO = Internally oxidized; MA = Mechanically alloyed; PM = Powder metallurgy; R = Recrystallization; RL = Rolled; SW = Swaging; VHP = Vacuum hot pressing; WD = Wire drawing; ZAP = Direction recrystallization.

The codes used to describe the testing procedure used are as follows:

CC = Constant stress compressive creep test; CL = Constant load compressive creep test; CSR = Constant strain rate test; HC = Helical coils; TC = Constant stress tensile creep test; TL = Constant load tensile creep test.

The shapes of the curves observed in a creep or a constant strain rate experiment are illustrated schematically in Fig. 2. The codes used to describe these are shown in the figure. Several types of microstructures have been reported in the literature and these are indicated in the remarks column in Table A.1. However, it should be noted that the deformation of these alloys is often localized and inhomogeneous. The codes used to describe these microstructures are as follows:

CE = Cells; DF = Dislocation free; DL = Dislocation loops; DMP = Deformation induced movement of particles; DP = Dislocation pinning; GS = Grain boundary sources; IS = Same as the initial microstructure; NE = Dislocation networks; SG = Subgrains; TA = Dislocation tangles.

A.1.2 The Estimation of the True Activation Energies for Creep

The activation energy data given in Table A.1 were corrected according to equation (6), and therefore the latter values may differ from those given in the original references, where the correction term included only the temperature dependence of the elastic modulus. The shear modulus at a particular temperature was calculated from

$$G = G_0 - (\partial G/\partial T)_P T \qquad (A1)$$

where G_0 is the shear modulus at 0 K, and $(\partial G/\partial T)_P$ is the rate of change in the shear modulus with temperature. The values of G_0, $(\partial G/\partial T)_P$, and Q_1 are

tabulated in Table A.2 for the matrix material. The shear modulii data were derived from the Young's modulus using $G = [E/2(1 + \nu)]$ for some materials, where ν is the Poisson's ratio.

The corrected activation energies for creep are tabulated in table A.3 and the classification scheme employed is similar to that shown in table A.1. Average values of n and T were used to make these corrections, and these are indicated in the table.

TABLE A.1. - DISLOCATION CREEP DATA FOR SEVERAL DISPERSION-STRENGTHENED ALLOYS

Experimental conditions										Experimental results				
Material	Processing[a]	d, μm	GAR	vol %	λ, μm	d_p, μm	σ, MPa	T, K	Test[a] mode	Creep[a] curve	n	Q_c, kJ mol^{-1}	Remarks[a]	References
Aluminum alloys														
$Al-Al_2O_3$	R	Large	-	-	0.05-1.5	0.03-0.3	0.7-35.0	673-873	TL	R	-	-	Erratic behavior	Ansell and Weertman (1959)
	HE	5	-	-	0.05-1.5	0.03-0.3	1.4-62.7	673-873	TL	R	exp (Bσ/G)	630	Quasi-steady state	Ansell and Weertman (1959)
	HE	-	-	10.3	-	-	0.75-51.7	813-1008	CC	N	-	1255;795	-	Meyers and Sherby (1961-62)
	RL	2.5	1	2.95-10.65	-	0.2-0.5	10.0-370.0	296-873	TC	N	exp (Bσ/G)	65-1045	T < 473 K; NE, DF T > 573 K; DF, IS	Milička *et al.* (1970)
	R	2000-3000	-	-	0.90	0.013-0.1	10.0-17.0	743-843	TL	-	4.1	155	DF, IS	Reynolds *et al.* (1971)
	MA,VHP	-	-	1.0	0.061	0.030	5.5-66.9	768-927	CSR	C	40	[b]2610	Threshold stress	Gilman (1979)
	MA,HE	-	-	2.2	0.05	0.014	37.0-200.0	523-803	CSR, CC	C	>25	[b]540	Threshold stress	Oliver and Nix (1982)
	HE,A	200-10000	1.5-40.0	0.19-0.92	0.74-0.18	0.027-0.047	2.0-115.0	77-873	CSR, TL	-	-	200-800	TA Threshold stress	Clauer and Hansen (1984)
$Al-Cu-Al_2O_3$	R	1000-2000	-	-	1.30-1.50	0.013-0.10	8.0-15.0	743-843	TL	-	3.9-4.1	120-140	DF, IS	Reynolds *et al.* (1971)
$Al-Mg-Al_2O_3$	R	1000-2000	-	-	1.23-1.41	0.013-0.10	8.0-20.0	743-843	TL	-	3.8-4.1	110-135	DF, IS	Reynolds *et al.* (1971)
Al-Mg-MgO	MA,HE	-	-	3.6	0.05	0.014	19.0-260.0	473-821	CSR, CC	A, B, C	15-20	[b]500	Threshold stress	Oliver and Nix (1982)
Copper alloys														
$Cu-Al_2O_3$	IO,VD	Single crystal <001>	-	0.21-0.82	0.485-0.815	0.031-0.064	19.5-40.0	823-923	CSR	B	7.5-9.3	[b]195	Stresses estimated from τ/G using $\sigma = 2\tau$	Takada *et al.* (1983)
$Cu-SiO_2$	IO	Single crystal	-	0.23-0.90	0.99-1.94	0.056-0.087	3.0-14.7	293-1323	CSR, TL	-	exp (Bσ/G) for T > 850 K	-	-	Shewfelt and Brown (1974)

[a]The abbreviations are explained in Sec. A.1.1.
[b]Modulus corrected.

TABLE A.1. - DISLOCATION CREEP DATA FOR SEVERAL DISPERSION-STRENGTHENED ALLOYS

Experimental conditions										Experimental results				
Material	Processing[a]	d, μm	GAR	vol %	λ, μm	d_p, μm	σ, MPa	T, K	Test[a] mode	Creep[a] curve	n	Q_c kJ mol^{-1}	Remarks[a]	References
Cu-TiO_2	IO,WD	Single crystal <001>	-	0.39	0.335	0.026	40-55	823-923	CSR	B	8.5	-	Stresses estimated from τ/G using $\sigma = 2\tau$	Takada *et al.* (1983)
Iron alloys														
Fe-Cr_2O_3	-	95-160	-	0.67-2.9	1.0-2.3	0.48-0.60	14.7-68.7	923-1123	CSR	-	3.8-8.6	215-260	-	Takada *et al.* (1975)
Fe-BeO-SiO_2	HE,SW	-	1.0-6.3	2.5	0.2-0.3	0.04-0.06	15.0-100.0	923-1088	TL	-	6.3-13.0	375-440	Q_c determined from stress rupture data	Wolf and Grant (1977)
Cr-Ni-Al_2O_3	PM,HE	-	-	10	-	0.03	110-165	923	TL	-	7.0	-	-	Sands *et al.* (1962)
Cr-Ni-TiO_2	PM,HE	-	-	10	-	0.026	165-250	923	TL	-	10.0	-	-	Sands *et al.* (1962)
MA 956	MA,HE,RL,R	Oriented grains	> 10	1.05	-	-	70.7-84.1	1366	CSR	D, E	100	-	-	Whittenberger (1979)
		15 mm	3.2	1.05	0.109	0.025	66.0-106.3	1323-1423	CSR, TL	-	5	370	IS, DP n and Q_c corrected for σ_{th}	Petkovic-Luton *et al.* (1983)
Nickel alloys														
Ni-Al_2O_3	R	10-15	-	2.5	1.0	0.042	13.8-137.9	733-1000	TC	-	4.0	85-275	-	Hancock *et al.* (1972)
Ni-ThO_2	SW	3.2-3.9	10.0-15.0	2.3	0.234	0.037	103-248	598-865 865-1373	TC	N,T N,T	- 40	190-240 795	DL DF,IS,GS	Wilcox and Clauer (1966a)
	R	-	-	1.0-4.40	0.18-0.53	0.022-0.055	13.8-103.4	973-1323	TC	N	7	270	NE	Clauer and Wilcox (1967)
	WD,SW	0.18-1.2	2.6	0.15	0.15	0.02	10.0-90.0	1376	CSR, TC	-	6.7-26.1	-	GAR increases creep strength	Wilcox and Clauer (1972)
	SW,RL,A	0.97-363.0	1.0-11.0	2.5	-	-	5.0-240.0	866-1589	CSR, TC	-	-	50 - 6980	DMP, GS	Petrovic and Ebert (1973)
	R	70.0	-	0.01-3.00	0.37-7.70	0.11	0.14	1198-1378	TC	-	3.5	[b]235	-	Durber and Davies (1974)
	A	3.5	19	1.80	-	-	48.2-75.8	1365	TL	N, T	13.5	-	Threshold stress	Whittenberger (1977)

[a]The abbreviations are explained in Sec. A.1.1.
[b]Modulus corrected.

TABLE A.1. - DISLOCATION CREEP DATA FOR SEVERAL DISPERSION-STRENGTHENED ALLOYS

Experimental conditions										Experimental results				
Material	Processing[a]	d, μm	GAR	vol %	λ, μm	d_p, μm	σ, MPa	T, K	Test[a] mode	Creep[a] curve	n	Q_c, kJ mol^{-1}	Remarks[a]	References
Ni-30% Co-Al_2O_3	R	10.0-15.0	-	2.5	1.0	0.042	13.8-137.9	733-1000	TC	-	4.0	185-275	-	Hancock *et al.* (1972)
Ni-67% Co-Al_2O_3	R	10.0-15.0	-	2.5	1.0	0.042	13.8-137.9	733-1000	TC	-	4.0	120-270	-	Hancock *et al.* (1972)
Ni-13.5% Cr-ThO_2	R	-	-	1.0	0.21	0.016	11.3-48.2	1073-1373	TC	N	6.3	270	-	Wilcox and Clauer (1969)
Ni-20% Cr-ThO_2	RL	-	-	2.2	0.132	0.0145	27.6-131.0	1089-1311	TL	N	9.7-24.3	385	-	Wilcox *et al.* (1967)
	WD,SW,A	0.3-4.0	1	1.70	0.160	0.018	7.0-40.0	1376	CSR, TC	-	7.1-8.4	-	-	Wilcox and Clauer (1972)
	RL,A	Single crystal <001>	-	2.0	-	-	80.0-115.0	1366	TC	N	18.5	[b]265-425	Q_c was stress dependent	Kane and Ebert (1976)
		3.7	2-4	2.0	-	-	10.5-16.5	1366	TC	N	6.0	[b]295	-	
		8.6	2-4	2.0	-	-	18.9-49.3	1366	TC	N	7.3	[b]315	-	
		190	2-4	2.0	-	-	38.9-80.0	1366	TC	N	7.3	[b]365-425	-	
	ZAP	Single crystal <100>	-	2.0	0.1	0.011	66.2-514.6	917-1572	TC	N	8.7-75.0	-	Threshold stress	Lund and Nix (1976)
	R	212	3	2.0	0.071	0.015	93.4-468.8	973-1373	CSR	D	-	-	Threshold stress	Hausselt and Nix (1977a)
	HE,A	Single crystal <100>	-	2.0	-	-	100.0-595.0	973-1373	CSR	A, C	6-25	-	Threshold stress	Hausselt and Nix (1977b)
	HE,A	Essentially single crystals		1.70	-	-	31.0-86.1	1365	TL	N, T	41.0	-	Threshold stress	Whittenberger (1977)
	RL	39.0	2.0	2.0	-	-	34.1-244.0	973-1573	CSR	D	8	[b]270	λ was estimated for coarse particles; Threshold stress	Lin and Sherby (1981)
	HE,A	147.0	3.0	2.0	1.0	0.095	97.2-238.0	973-1448	CSR	D	8-25	[b]285		
Ni-22.6% Cr-ThO_2	R	-	-	1.0	0.22	0.016	11.5-55.2	1088-1373	TC	N	6.3	310	-	Wilcox and Clauer (1969)

[a]The abbreviations are explained in Sec. A.1.1.
[b]Modulus corrected.

TABLE A.1. - DISLOCATION CREEP DATA FOR SEVERAL DISPERSION-STRENGTHENED ALLOYS

Experimental conditions										Experimental results				
Material	Processing[a]	d, μm	GAR	vol %	λ, μm	d_p, μm	σ, MPa	T, K	Test[a] mode	Creep[a] curve	n	Q_c kJ mol^{-1}	Remarks[a]	References
Ni-33.7% Cr-ThO_2	R	-	-	1.0	0.23	0.018	11.7-55.2	1073-1373	TC	-	6.7	325	-	Wilcox and Clauer (1969)
MA 754	-	250	0.73	1.0	-	-	13.8-34.5	1365	TL	N	16	-	Threshold stress; Long transverse direction	Whittenberger (1977)
	-	250	3.68	1.0	-	-	65.5-89.6	1365	TL	N	18	-	Threshold stress; Longitudinal direction	
	MA,HE,R	71.5	-	1.3	0.11	0.014	44.8-165.5	1033-1255	TL	-	-	-	Long transverse direction	Howson *et al.* (1980a)
		71.5	5.73	1.3	0.11	0.014	110.4-258.7	1033-1297	TL	-	19.8-33.4	[b]315-410	Longitudinal direction	
		104.9	10.72	1.3	0.11	0.014	93.2-241.4	1033-1366	TL	-	26.7-29.2	-	Longitudinal direction	
	MA,HE,R	163.0	7.2	1.3-1.5	0.175	0.0144	61.7-153.0	1273-1473	TC	-	40-46 (high stresses) 5-16 (low stresss)	[b]315	-	Stephens and Nix (1984, 1985)
		143.0	5.9	1.97	0.139	0.011	62.0-204.4	1273-1473	TC	-	30-36 (high stresses) 1.6-2.5 (low stresses)	[b]400-670	Duplex grain size	Stephens and Nix (1984, 1985)
Ni-16% Cr-4.2% Al-ThO_2	HE,A	235	2.37	1.59	-	-	41.3-75.8	1365	TL	N	23.0	-	Threshold stress	Whittenberger (1977)
Ni-16% Cr-4.2% Al-Y_2O_3	HE,R	1330	5.0	2.5-3.0	0.115	0.025	48.3-344.9	1019-1380	TL	N, T	7.8-29.8	525-1530	DP	McAlarney *et al.* (1982)
Ni-16% Cr-5.0% Al-ThO_2	HE,A	400	1.82	1.59	-	-	41.3-62.0	1365	TL	N	10.5	-	Threshold stress	Whittenberger (1977)
MA 6000	MA,HE,R	Several mm	high	-	-	0.025-0.040	158.7-565.8	1033-1366	TL	N, T	20, 40	670	-	Kim and Merrick (1979)
	MA,HE,R	3.0-4.5	> 10	2.5	0.149	0.028	161.5-557.4	1033-1366	TL	N	24.0, 47.7	620	-	Howson *et al.* (1980b)

[a]The abbreviations are explained in Sec. A.1.1.
[b]Modulus corrected.

TABLE A.1. - DISLOCATION CREEP DATA FOR SEVERAL DISPERSION-STRENGTHENED ALLOYS

Experimental conditions										Experimental results				
Material	Processing[a]	d, μm	GAR	vol %	λ, μm	d_p, μm	σ, MPa	T, K	Test[a] mode	Creep[a] curve	n	Q_c, kJ mol^{-1}	Remarks[a]	References
	MA,HE,R	-	-	2.5	0.15	0.03-1.0	160.0-600.0	1144-1366	CSR	D, E	13.1-20.0	800	Threshold stress	Whittenberger (1984)
Lead alloys														
Pb-PbO	HE	63.5	-	2.4-3.0	-	-	5.5-12.1	293	TL	R	6.0-27.0	-	Inhomogenous slip; Data show an exponential stress dependence	Snowden (1967)
	R	300-400	-	1.2	-	-	8.6-22.4	300	TL	-	5.0	-	-	Reynolds (1974)
Platinum alloys														
ZGS Pt	R	-	High	<0.5	-	0.02-0.1	10.3-24.1	1473-1673	TL	-	7.3-13.5	290-570	n and Q_c were estimated from creep data	Selman *et al.* (1974)
Silver alloys														
Ag-Ga_2O_3	R	420	-	1.6	0.16	0.045	0.69-6.90	923-1098	TC	N	1.0, 4.1	175	-	Lenel *et al.* (1971)
	PM,HE	10	-	1.6	0.19	0.057	0.69-6.90	923-1098	TC	N	12.6	920-1045	-	
Ag-MgO	IO,R	500	-	0.60	0.012	-	2.22-4.48	955-1073	TL	N	3.1	[b]185	-	Leverant *et al.* (1966)
		500	-	0.90	0.012	-	1.40-4.30	976-1143	TL	N	3.2	[b]170	-	
	IO,A	-	-	0.30	0.03	0.008	14.9-60.0	573-973	TC	N	10.0	[b]110	-	Nieh and Nix (1979)
Tungsten alloys														
AKS-W	PM,R	225 (wire diameter)	High	1.94	-	-	47.0-72.6	2723-3273	HC	N	8.4	545	-	Moon and Stickler (1971)
218	WD	-	-	-	-	-	69.0-89.7	3000	TL	N, T	25	-	Threshold stress	Pugh (1973)
	R	-	10	-	0.3	-	41.4-137.9	2500-3100	TL	-	similar to the above value	630-775	The values of Q_c are based on the stress rupture data	
	WD	350	> 15	0.2	0.3	0.01-0.03	30-50	2800	TL	N	4.9	-	DP	Gaal *et al.* (1983)
							25-60				1.0	-	-	

[a]The abbreviations are explained in Sec. A.1.1.
[b]Modulus corrected.

TABLE A.1. - DISLOCATION CREEP DATA FOR SEVERAL DISPERSION-STRENGTHENED ALLOYS

Experimental conditions										Experimental results				
Material	Processing[a]	d, μm	GAR	vol %	λ, μm	d_p, μm	σ, MPa	T, K	Test[a] mode	Creep[a] curve	n	Q_c, kJ mol^{-1}	Remarks[a]	References
W-ThO_2	PM,R	4	Equiaxed	1.94	-	0.2	2.0-69.7	2073-3023	HC	N	4.5	500	Values of n = 1 and Q_c = 340 kJ mol^{-1} were observed when T >2773 K and for σ < 9.8 MPa	Moon (1972)
		Large	High	1.94	-	0.2	42.7-69.7	2073	HC	N	15	-	-	
W-ZrO_2	PM,HE	6	-	1.7	2.0	0.2	25.0-150.0	1820-2160	TC	N	4.6	435	A value of n = 1 was observed when T = 1890 K and σ < 80 MPa	Blickensderfer (1974)

[a]The abbreviations are explained in Sec. A.1.1.
[b]Modulus corrected.

TABLE A.2. - THE VALUES OF G_o, $(\partial G/\partial T)_p$, AND Q_l USED IN TABLE A.3 FOR SEVERAL MATERIALS

Base material	$G_o(\times 10^{-4})$, MPa	$(\partial G/\partial T)_p$, MPa K^{-1}	Reference	Q_l, kJ mol^{-1}	Reference
Al Al-Mg Al-Cu	3.02	16.0	Mohamed and Langdon (1974b)	143	Mohamed and Langdon (1974b)
Ag	[a]3.64	[a]18.0	Yoshihara and McLellan (1981)	183	Tomizuka and Sonder (1956)
Ni	[a]6.41	[a]23.0	INCO (1977)	279	Hoffman *et al.* (1956)
Ni-Cr including MA 754	[a]10.34	[a]31.6	Lund and Nix (1976)	285	Lund and Nix (1976)
Ni-Cr-Al including MA 6000	[a]8.56	[a]23.2	Millan and Mays (1986)	[b]285	Lund and Nix (1976)

[a]These data were obtained from linear regression analysis of the published data. The Young's modulus, E, was converted to the shear modulus, G, using $G = E/[2(1 + \upsilon)G]$, where the Poisson's ratio, υ, was assumed to be 0.3.
[b]The value of Q_l for this alloy was assumed to be the same as that for Ni-Cr.

TABLE A.3. - TRUE ACTIVATION ENERGIES FOR CREEP OF SOME DISPERSION-STRENGTHENED ALLOYS

Alloy	Q_A, kJ mol^{-1}	n	T, K	$G(\times 10^{-4})$,[a] MPa	Q_c, kJ mol^{-1}	Q_c/Q_l	Reference
Aluminum alloys							
Al-Al_2O_3	-	-	296-873	-	[b]85-630	0.6-4.4	Milička *et al.* (1970)
	155	4.1	795	1.8	150	1.0	Reynolds *et al.* (1971)
	540	25.0	665	2.0	475	3.3	Oliver and Nix (1982)
Al-Mg-Al_2O_3	500	18.0	650	2.0	460	3.2	Oliver and Nix (1982)
Nickel alloys							
Ni-ThO_2	795	40.0	1100	3.9	570	2.1	Wilcox and Clauer (1966)
Ni-20%Cr-ThO_2	[c]390	8.7	1000	7.2	370	1.3	Lund and Nix (1976)
	[c]990	46.0	1373	6.0	630	2.2	
	400	8.0	1273	2.5	290	1.0	Lin and Sherby (1981)
Ni-22.6%Cr-ThO_2	310	7.2	1230	6.5	280	1.0	Wilcox and Clauer (1969)
Ni-33.7%Cr-ThO_2	325	6.7	1225	6.5	300	1.1	Wilcox and Clauer (1969)
MA 754	505	29.0	1033	7.1	400	1.4	Howson *et al.* (1980a)
	660	33.0	1255	6.4	460	1.6	
	315	43.0	1373	6.0	335	1.2	Stephens and Nix (1984, 1985)
	400-670	33.0	1373	6.0	420-690	1.5-2.4	
MA 6000	670	20.0	1060	6.1	610	2.1	Kim and Merrick (1979)
	620	24.0	1033	6.2	550	1.9	Howson *et al.* (1980b)
	800	16.6	1255	5.6	725	2.6	Whittenberger (1984)
Silver alloys							
Ag-Ga_2O_3	920-1045	12.6	1000	1.8	830-955	4.5-5.2	Lenel *et al.* (1971)

[a]These values were estimated from the data given in Table A.2.
[b]These values are based on Fig. 9 and Q_c decreased with increasing stress (Fig. 8).
[c]Estimated from the creep data for σ = 125 and 400 MPa, respectively.

NASA
National Aeronautics and Space Administration

Report Documentation Page

1. Report No.	2. Government Accession No.	3. Recipient's Catalog No.
NASA CR-185299		

4. Title and Subtitle	5. Report Date
Creep and Fracture of Dispersion-Strengthened Materials	June 1991
	6. Performing Organization Code

7. Author(s)	8. Performing Organization Report No.
Sai V. Raj	None (E-3612)
	10. Work Unit No.
	505-63-01

9. Performing Organization Name and Address	11. Contract or Grant No.
Cleveland State University Department of Chemical Engineering Cleveland, Ohio 44115	NCC3-72
	13. Type of Report and Period Covered
	Contractor Report Final

12. Sponsoring Agency Name and Address	14. Sponsoring Agency Code
National Aeronautics and Space Administration Lewis Research Center Cleveland, Ohio 44135-3191	

15. Supplementary Notes

Project Manager, Hugh R. Gray, Materials Division, NASA Lewis Research Center. Sai V. Raj, NASA Resident Research Associate at Lewis Research Center. This work will also be a chapter in the Handbook of Metallic Composites, S. Ochiai, editor; Marcel Dekker, New York, New York.

16. Abstract

The creep and fracture of dispersion-strengthened materials is reviewed. A compilation of creep data on several alloys showed that the reported values of the stress exponent for creep varied between 3.5 and 100. The activation energy for creep exceeded that for lattice self-diffusion in the matrix in the case of some materials and a threshold stress behavior was generally reported in these instances. The threshold stress is shown to be dependent on the interparticle spacing and it is significantly affected by the initial microstructure. The effect of particle size and the nature of the dispersoid on the threshold stress is not well understood at the present time. In general, most investigations indicate that the microstructure after creep is similar to that before testing and very few dislocations are usually observed. It is shown that the stress acting on a dispersoid due to a rapidly moving dislocation can exceed the particle yield strength of $G_P/1000$, where G_P is the shear modulus of the dispersoid. The case when the particle deforms is examined and it is suggested that the dislocation creep threshold stress of the alloy is equal to the yield strength of the dispersoid under these conditions. These results indicate the possibility that the dislocation creep threshold stress is determined by either the particle yield strength or the stress required to detach a dislocation from the dispersoid-matrix interface. The conditions under which the threshold stress is influenced by one or the other mechanism are discussed and it is shown that the particle yield strength is important until the extent of dislocation core relaxation at the dispersoid-matrix interface exceeds about 25% depending on the nature of the particle-matrix combination. Finally, the effect of grain boundaries and grain morophology on the creep and fracture behavior of dispersion-strengthened alloys is examined.

17. Key Words (Suggested by Author(s))	18. Distribution Statement
Creep; Creep fracture; Dispersion strengthened materials; Oxide dispersion strengthening	Unclassified—Unlimited Subject Categories 24 and 26

19. Security Classif. (of this report)	20. Security Classif. (of this page)	21. No. of pages	22. Price*
Unclassified	Unclassified	98	A05

NASA FORM 1626 OCT 86

*For sale by the National Technical Information Service, Springfield, Virginia 22161